pharmaceutics

MDPI

Article

Surface Modification of Titanate Nanotubes with a Carboxylic Arm for Further Functionalization Intended to Pharmaceutical Applications

Ranim Saker [1], Orsolya Jójárt-Laczkovich [1], Géza Regdon, Jr. [1], Tamás Takács [2], Imre Szenti [2], Noémi Bózsity-Faragó [3], István Zupkó [3] and Tamás Sovány [1,*]

[1] Institute of Pharmaceutical Technology and Regulatory Affairs, University of Szeged, Eötvös u 6., H-6720 Szeged, Hungary; rnmsaker@gmail.com (R.S.); jojartne.laczkovich.orsolya@szte.hu (O.J.-L.); geza.regdon@pharm.u-szeged.hu (G.R.J.)

[2] Department of Applied and Environmental Chemistry, University of Szeged, Rerrich Béla tér. 1., H-6720 Szeged, Hungary; takacstamas@chem.u-szeged.hu (T.T.); szentiimre@gmail.com (I.S.)

[3] Institute of Pharmacodynamics and Biopharmacy, University of Szeged, Eötvös u 6., H-6720 Szeged, Hungary; bozsity-farago.noemi@szte.hu (N.B.-F.); zupko.istvan@szte.hu (I.Z.)

* Correspondence: sovany.tamas@szte.hu; Tel.: +36-6254-5576

Abstract: Nanotechnology is playing a significant role in modern life with tremendous potential and promising results in almost every domain, especially the pharmaceutical one. The impressive performance of nanomaterials is shaping the future of science and revolutionizing the traditional concepts of industry and research. Titanate nanotubes (TNTs) are one of these novel entities that became an appropriate choice to apply in several platforms due to their remarkable properties such as preparation simplicity, high stability, good biocompatibility, affordability and low toxicity. Surface modification of these nanotubes is also promoting their superior characters and contributing more to the enhancement of their performance. In this research work, an attempt was made to functionalize the surface of titanate nanotubes with carboxylic groups to increase their surface reactivity and widen the possibility of bonding different molecules that could not be bonded directly. Three carboxylic acids were investigated (trichloroacetic acid, citric acid and acrylic acid), and the prepared composites were examined using FT-IR and Raman spectroscopy, scanning electron microscopy (SEM), transmission electron microscopy (TEM) and dynamic light scattering (DLS). The toxicity of these functionalized TNTs was also investigated using adherent cancer cell lines and fibroblasts to determine their safety profile and to draw the basic lines for their intended future application. Based on the experimental results, acrylic acid could be the suitable choice for permanent surface modification with multiple carboxylic groups due to its possibility to be polymerized, thus presenting the opportunity to link additional molecules of interest such as polyethylene glycol (PEG) and/or other molecules at the same time.

Keywords: titanate nanotubes; carboxylic acid; polyethylene glycol; functionalization; linkers

Citation: Saker, R.; Jójárt-Laczkovich, O.; Regdon, G., Jr.; Takács, T.; Szenti, I.; Bózsity-Faragó, N.; Zupkó, I.; Sovány, T. Surface Modification of Titanate Nanotubes with a Carboxylic Arm for Further Functionalization Intended to Pharmaceutical Applications. *Pharmaceutics* **2023**, *15*, 2780. https://doi.org/10.3390/pharmaceutics15122780

Academic Editor: Melgardt de Villiers

Received: 31 October 2023
Revised: 6 December 2023
Accepted: 12 December 2023
Published: 15 December 2023

1. Introduction

Nowadays, an accelerated transformation procedure from the use of traditional bulk materials into applying smart, predesigned nano ones is taking place in all aspects of modern life. All scientific disciplines should be keeping up with this tremendous evolution, and every single domain should explore the potential of investing in others' invented tools for its own benefit.

Titanate nanotubes (TNTs) are one of these newly invented materials that were introduced as efficient tools to serve in various fields aiming to achieve different purposes. Several research works demonstrated the effectiveness of TNTs in medical, industrial and chemical disciplines such as in dental implants and orthopedics [1,2], chemical catalysis,

biofuel synthesis, solar cells and water purification [3–6]. This outstanding performance in these multiple fields brings out an insistent question about the potential role they could play in the pharmaceutical domain.

For this reason, TNTs are attracting more and more attention in the pharmaceutical community as they could offer a novel platform and an appealing candidate for pharmaceutical uses, especially in the field of drug delivery. Their attractiveness arises from the preferable properties they could offer such as advantageous tubular geometry, large specific surface area compared to their spherical counterparts, hydrophilic nature, nano-size undetectable for the reticuloendothelial system, good biocompatibility and mechanical strength. This unique package of properties is of fundamental importance and is considered a key feature for their prospective use as drug carriers [1,7,8].

Unfortunately, only a few attempts have been made to bring these nanomaterials into therapeutic practice. For instance, promising results were successfully obtained in the field of oncology after using TNTs as antitumor carriers for doxorubicin and docetaxel to pancreatic and prostate tumors [9,10]. In fact, just depending on their photocatalytic activity, TNTs could induce the death of malignant cells upon UV irradiation [11]. This ability holds the potential of introducing a synergetic effect if combined with the loading of active pharmaceutical ingredients (APIs). In this context, TNTs were investigated as possible nanocarriers for various APIs such as ibuprofen, dexamethasone, curcumin, methotrexate and silibinin [12–15]. The use of TNTs as drug carriers would not just contribute to the effective therapeutic outcomes after the drug has been delivered to the site of action, but it would also have advantages on the technological and industrial levels. According to Sipos et al., the incorporation of APIs into TNTs could present superior processability in comparison to APIs alone, and this would shorten the time needed for preformulation studies, especially regarding the tableting process [16–18].

Although, the mentioned properties of TNTs are considered as advantages for several applications including medical and pharmaceutical ones. Nevertheless, surface modification could be an unavoidable step for further improvement of the existing properties, for adjustment of the unfavorable ones or even for providing them with new characteristics. The surface modification is considered as a recommended solution to overcome TNTs problems and upgrade their use to new scopes; for example, applying a hydrophobic cap for preventing the leaching of hydrophilic drugs to the surrounding environment and achieving a controllable release profile [19] or for enhancing the permeability of these hydrophilic nanotubes and facilitating their absorption/biological membrane bypassing [20]. Surface modification of TNTs was also conducted successfully as an approach to enhance the APIs loading, sustain/control the release rate and reduce toxicity using different molecules such as polyamidoamine dendrimers, P25 nanoparticles and chitosan [14,15,21,22].

However, it is worth mentioning that while there is a considerable number of scientific papers discussing surface functionalization of different nanomaterials, just a few of them focused on this type of modification with TNTs. This lack of research in this fundamental angle opens the door for further investigation in this unexplored subject.

This study aims to contribute to TNTs surface functionalization by creating an extended and flexible arm on their surface using carboxylic acids. This proposed approach could be an appropriate way to create functional nanomaterials, facilitating further functionalization with additional molecules, and would result in tailoring TNTs surface chemistry to enhance their characters or adapt them to fit well with the pharmaceutical requirements. Polyethylene glycol (PEG) was selected as the functionalizing agent that will be bonded to the carboxylic arm due to its well-known biological benefits such as resisting non-specific protein adsorption and thus the formation of protein corona [23–25], prolonging circulation time [26] and reducing cytotoxicity [27].

Creating a functional arm on the surface of TNTs for special purposes has been carried out before by Marques et al. to enhance TNTs adsorption capacity towards anionic materials in aqueous solutions. This purification technique could be achieved by linking amine groups to the originally negative-charged TNTs surface. These amine groups could turn

into positively charged groups after protonation in acidic media, leading to electrostatic interactions with negatively charged materials. Furthermore, the unfunctionalized sites of TNTs surface could continue to interact with cationic materials as these sites preserve their original negative charge. According to this strategy, TNTs could act as a bi-charged surface and interact with molecules that could not interact with TNTs in their original form [28].

A similar approach was suggested in this research article (Figure 1) which involves enriching TNTs surface with reactive carboxylic groups that could facilitate subsequent grafting of numerous molecules intended for shaping the surface properties or, furthermore, attaching biologically active substances that could not be directly linked to the original surface of TNTs. This proposed idea to create a functional carboxylic arm on the surface of TNTs is easily applicable with the organic counterpart through oxidation [29], which will provide carbon nanotubes (CNTs) with carboxylic groups, giving them the opportunity to be covalently functionalized [30]. However, with inorganic nanomaterials, this task is more challenging and more difficult to achieve. This study will also thoroughly discuss the type of the created interactions, as the desired one would differ according to the intended future implementation. To the best of our knowledge, this is the first paper to discuss the importance of tailoring the surface chemistry of nanotubes and create a connecting bridge with carboxylic groups that could serve as future linkers for additional molecules (APIs, markers, etc.) and then to investigate the toxicity of these modified samples in order to upgrade their use for safe therapeutic implementation.

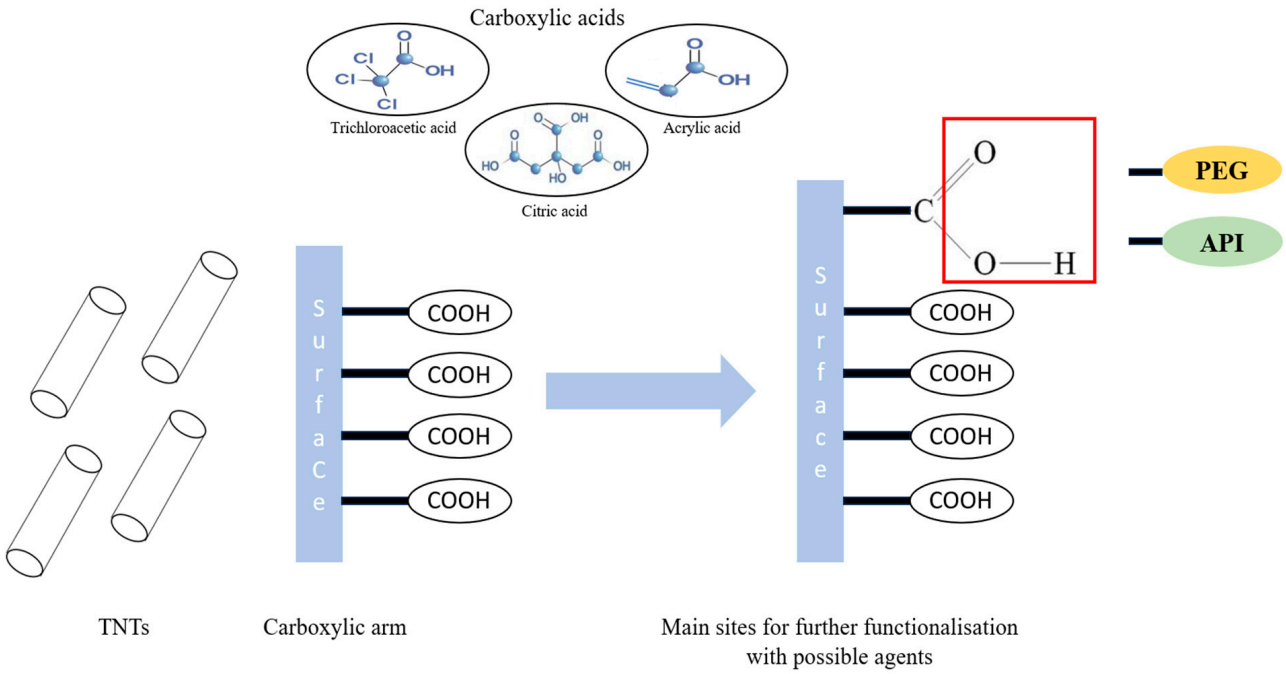

Figure 1. The suggested strategy for TNTs surface modification.

2. Materials and Methods

2.1. Materials

Three types of carboxylic acids, trichloroacetic acid (TCA), citric acid (CA) monohydrate (both from Molar, Chemicals Ltd., Budapest, Hungary) and acrylic acid (AA) (Sigma-Aldrich Ltd., Budapest, Hungary), in addition to two types of polyethylene glycol (PEG 600 and PEG 6000) (Fluka AG, Buchs, Switzerland), were used to functionalize the surface of TNTs. Sodium persulfate, sodium sulfite and sodium hypophosphite monohydrate reagents were also purchased from Sigma-Aldrich Ltd. (Budapest, Hungary).

2.2. Methods

2.2.1. Preparation of TNTs

TNTs were prepared at the Department of Applied and Environmental Chemistry, University of Szeged, according to Sipos et al. [18], using the hydrothermal treatment method. Briefly, 120 g of NaOH was added to 300 mL of distilled water during continuous mixing, then 75 g of TiO_2 was added and mixed for 15 min. This mixture was put in an autoclave at 185 °C for 24 h then cooled at room temperature for 2 h, followed by cooling with cold water. The TNTs were finally washed with distilled water under vacuum using filter No:4.

2.2.2. Preparation of Carboxylic Acid Functionalized TNTs

TCA functionalization of TNTs was performed by adding 3 g of TNTs to 90 mL of water in an ultrasonic bath for 1 h until a homogenous suspension was obtained. This suspension was heated at 80 °C in a condenser connected to nitrogen gas for 30 min, then TCA was added to the previous system and mixed for one day.

CA functionalized TNTs (CA-TNTs) were prepared by adding 0.5 g of TNTs to 15 mL of water containing citric acid on a magnetic stirrer. This mixture was stirred for 30 min to obtain a homogenous suspension then heated at 50 °C with continuous stirring for 24 h.

AA functionalized TNTs (AA-TNTs) were prepared by mixing 1 g of TNTs with 28.8 g of acrylic acid, 32 g of hexane and 8 g of water then placed for sonication in an ultrasonic bath for 20 min at room temperature. This mixture was stirred at room temperature in a magnetic stirrer for 2 days then separated by centrifugation at 12,000 rpm for 60 min at 8 °C.

2.2.3. Functionalization with PEG

CA-TNTs were further functionalized with PEG 600 by mixing CA-TNTs and PEG 600 at 130 °C in a silicon oil bath for 24 h in an inert atmosphere condition by bubbling nitrogen gas, then the mixture was cooled to room temperature and filtered.

AA/PEG 6000 functionalized TNTs were prepared by applying a two-step method, where first an AA-PEG copolymer was prepared according to Abo-shosha et al. [31] and Ibrahim et al. [32], followed by bonding the copolymer with TNTs. Briefly, the AA-PEG 6000 copolymer was prepared by a polymerization reaction in a thermostatic water bath at 40 °C under atmospheric oxygen. The polymerization medium of polyacrylic acid (PAA)/PEG was prepared by neutralizing 20% of AA (115.5 g) with the equivalent amount of an aqueous solution of 500 g/L of NaOH followed by dissolving 40 g of PEG 6000. After that, 3.3 mL of 40 g/L sodium sulfite (Na_2SO_3) solution and 12.2 mL of 330 g/L sodium persulfate ($Na_2S_2O_8$) solution were added with stirring. An exothermic polymerization reaction commenced after an induction period with the evolution of water vapor, followed by solidification of the polymerization medium. The latter was then cooled, disintegrated, oven dried at 105 °C for 2 h, cooled and kept over silica gel for at least 40 h before analysis. In the second step, this copolymer (50 g/L) was bonded with TNTs (5 g/L) after adding Na-hypophosphite (15 g/L) as a catalyst in this reaction.

All the prepared composites were subjected to a washing step to remove any residues adsorbed on the surface of TNTs and finally were dried in a drying oven (Memmert, Büchenbach, Germany).

2.2.4. Structural Investigations

The determination of the success of functionalization procedure and the nature of TNT–carboxylic acid interactions were evaluated using an Avatar 330 FT-IR spectrometer (Thermo Fisher Scientific Ltd., Waltham, MA, USA). FT-IR measurements were conducted with a transmission E.S.P. accessory by using 128 scans at a resolution of 4 cm^{-1} and applying H_2O and CO_2 corrections. Spectragryph 1.2.16.1 software (Friedrich Menges, Obersdorf, Germany) was used to evaluate the results.

A DXR Dispersive Raman spectrometer (Thermo Fisher Scientific Inc., Waltham, MA, USA) equipped with a CCD camera and a diode laser operating at a wavelength of 780 nm was applied to perform Raman measurements, which were carried out with a laser power of 12 and 24 mW at 25 μm slit aperture size. The data were collected in the spectral range of 200–3300 cm^{-1} using photobleaching to compensate fluorescence of titanate. OMNIC 8 software was used for data collection, averaging the total of 20 scans and making the spectral corrections. For the removal of cosmic rays, a convolution filter was applied on the original spectrum using Gaussian kernel.

2.2.5. Morphology

The morphology and size of bare and functionalized TNTs were investigated by scanning electron microscope (SEM) (Apreo C, Thermo Fisher Scientific Ltd., Waltham, MA, USA) and transmission electron microscope (TEM) (FEI Tecnai G2 20 X-TWIN, Hillsboro, OR, USA). SEM was instrumented with a cold field emission (CFE) cathode. The system was used under 10^{-7} Pa ultra-high vacuum, and the samples were maintained at room temperature and under 10^{-4} Pa vacuum during the characterization in the sample chamber. TEM images were taken at 200 kV of electron energy.

The hydrodynamic diameter and zeta potential measurements were taken using dynamic light scattering with a Nano ZS zetasizer system (Malvern Panalytical Ltd., Malvern, Worcestershire, UK), equipped with a 633 nm wavelength laser. The bare and functionalized TNT samples were prepared by dispersing them in different media (water, phosphate-buffered saline (PBS) and a PBS-based cell culture medium) with 30 min of ultrasonication, and then 1 mL of each dispersion was placed in folded capillary zeta cells.

2.2.6. Cell Viability Studies

The direct toxicity of the newly prepared TNTs was determined on two intact and three cancerous cell lines by standard MTT (3-(4,5-dimethylthiazol-2-yl)-2,5-diphenyltetrazolium bromide) method [33]. The TNTs were tested against non-cancerous human embryo fibroblast (MRC5) and mouse embryonic fibroblast cell lines (NIH/3T3), as well as on malignant human ovarian carcinoma (A2780) and two types of oropharyngeal squamous carcinoma cell lines (UPCI-SCC-131 and UPCI-SCC-154). The MRC5, NIH/3T3 and A 2780 cell lines were purchased from the European Collection of Cell Cultures (ECACC, Salisbury, UK), while the two oropharyngeal cell lines from the German Collection of Microorganisms and Cell Cultures GmbH (Braunschweig, Germany). Each cell line was maintained at 37 °C in a humidified atmosphere (containing 5% CO_2) in Eagle's Minimum Essential Medium (EMEM) supplemented with the appropriate amount of heat-inactivated fetal calf serum (FCS), non-essential amino acids and 1% antibiotic–antimycotic mixture (penicillin–streptomycin), according to the manufacturer's recommendations. All media and supplements were obtained from Lonza Group Ltd. (Basel, Switzerland).

For testing the action on cell growth, cells were seeded into 96-well plates at the density of 5000 cells/well, and after overnight standing, cells were treated with increasing concentrations of TNTs (1, 3, 10 and 30 μg/mL). After incubation for 72 h, 5 mg/mL MTT solution was added for another 4 h. The precipitated formazan crystals were solubilized in dimethyl sulfoxide, and the absorbance was measured at 545 nm using a microplate reader (SPECTROstarNano, BMG Labtech GmbH, Offenburg, Germany). Wells with untreated cells were utilized as control. The in vitro experiments were carried out twice with five parallels. TNTs were suspended in dimethylsulfoxide (DMSO), and the highest DMSO content of the medium (0.6%) did not substantially affect cell proliferation. Data were evaluated with GraphPad Prism version 10 for Windows software (GraphPad Software, San Diego, CA, USA), while statistical evaluation was performed with TIBCO Statistica v14.0.1.25 software (TIBCO Software Inc., Palo Alto, CA, USA).

3. Results and Discussion

Previous attempts to directly link PEG to TNTs were not successful. Although PEG was successfully linked to TNTs via H-bonds, the strength was not sufficient to hold the complex together after dispersion in aqueous medium, so the PEG was rapidly detached from the TNTs. Therefore, the main idea of creating a carboxylic arm on the surface of TNTs is to serve as a functional bridge and enable strong, covalent connecting of various molecules that could not be directly connected to TNTs hydroxylated surface.

In the first attempt, the same method which was previously used for functionalization of TNTs with trichloro-octyl-silane [20] was adopted to TCA. Nevertheless, the trial was not successful, as shown in Figure 2, as the characteristic peaks of TCA, mainly the C=O, C-O and C-Cl stretching vibration at 1751, 1262 and 679 cm^{-1}, respectively, are clearly absent in the spectrum of the corresponding composite, which suggests that it was removed during the washing procedure. This unsuccessful attempt could be attributed to the fact that TCA has only one carboxyl group, which was apparently not sufficient for creating a durable association with the surface of TNTs.

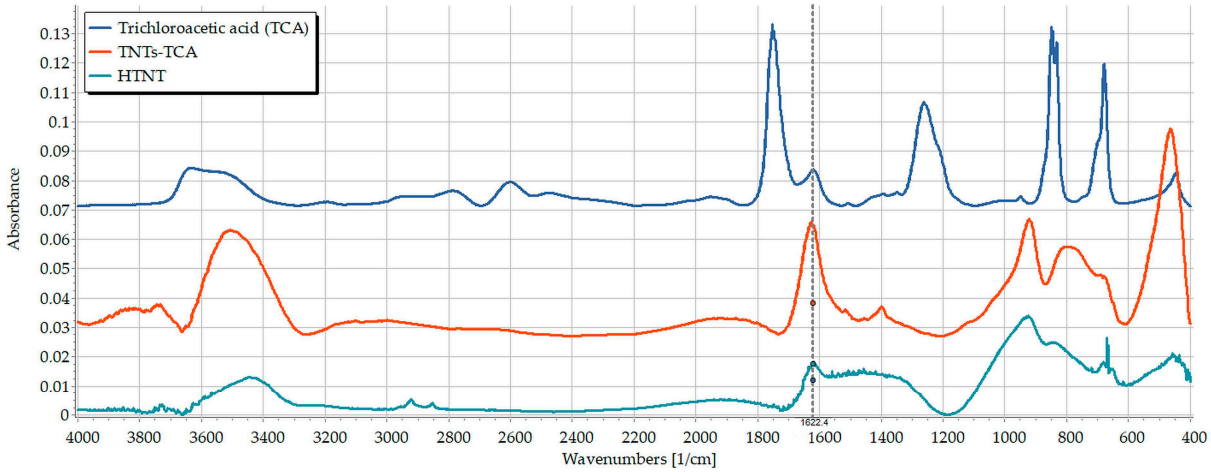

Figure 2. FT-IR spectra of TCA (blue), TNT (cyan) and the TCA-TNTs (red).

In contrast to the previous results, the functionalization experiments with citric acid appeared to be successful, and this was evidenced by the existence of its characteristic peaks (C=O stretching at 1728 cm^{-1} and C-O stretching with two peaks at 1233 cm^{-1} and 1213 cm^{-1}, belonging to CHOH and CH_2 attached carboxyl groups, respectively) in the spectra of CA-TNTs (Figure 3). However, the slight shift of the C=O stretching to 1717 cm^{-1} and the CH_2-C-O to 1200 cm^{-1} indicates a change in association due to the establishing of hydrogen bonds between the two entities, while the peak at 1233 cm^{-1} remained in an unchanged position. This suggests that the two primary COOH are attached to the surface of TNTs, while the third one is facing outwards in an unchanged form.

This would enable further functionalization trials with additional molecules intended to be connected to the free carboxylic arm. An esterification attempt between the carboxylated surface of CA-TNTs with PEG was made depending on the theory that titanate could serve as a heterogenous catalyst for such chemical esterification reactions [34,35]. For this reason, TNTs were used as a part of the reaction in addition to using them as a potential catalyst.

Unfortunately, in this study this theory did not work, and the planned esterification reaction failed, as was confirmed by the results of FT-IR examinations (Figure 4). The reaction outcome was purified with filtration. The spectrum of the filtered precipitate contained only the signals of the CA-TNTs. In addition, the unique peaks that are attributed to PEG structure, especially the C-H stretching vibration at 2868 cm^{-1} and the C-O stretching vibration at 1102 cm^{-1}, are absent, while the dried filtrate provided an identical spectrum of PEG. It could be concluded from the previous observations that PEG was not bonded

successfully to the carboxylated surface of TNTs as it was probably removed with water during the washing step.

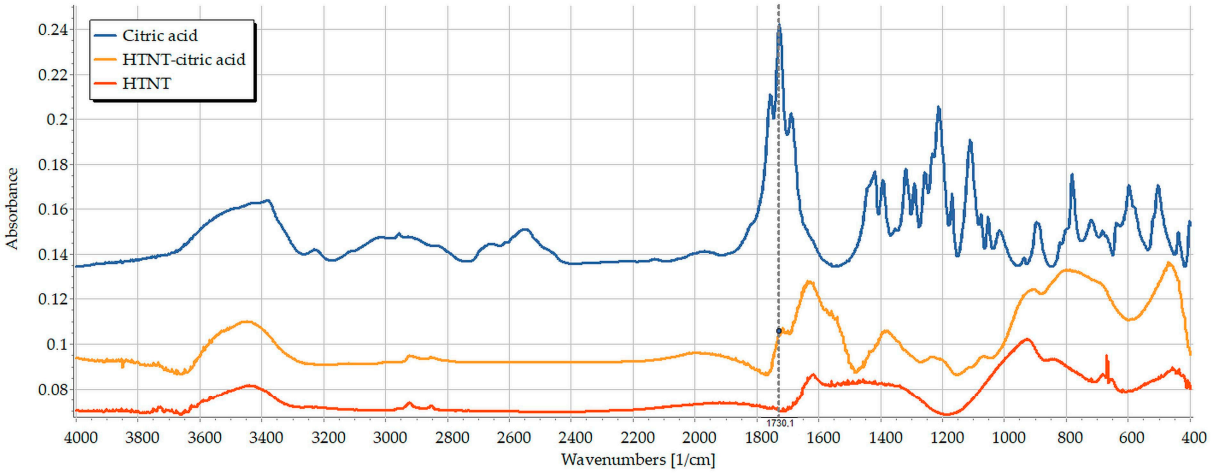

Figure 3. FT-IR spectra of citric acid (blue), TNTs (red) and CA-TNTs (yellow).

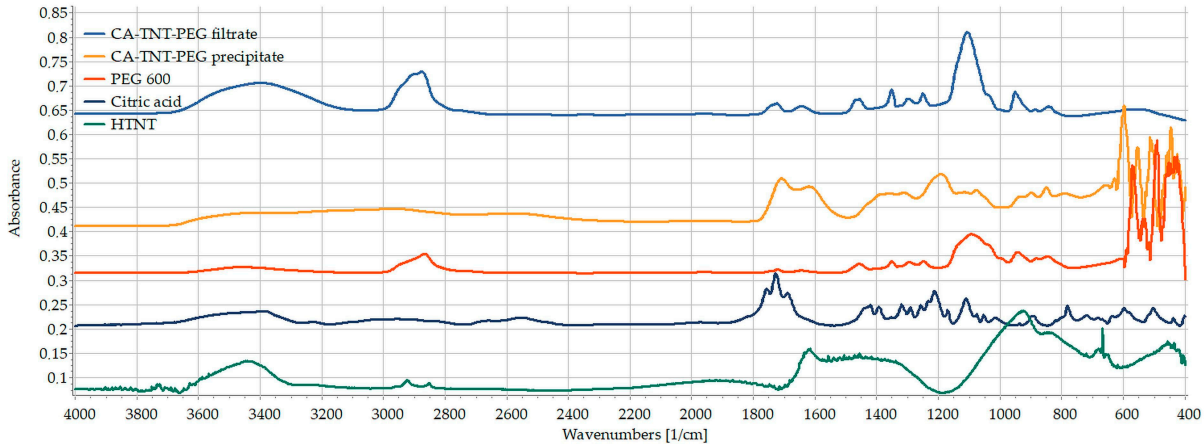

Figure 4. The spectra of PEG 600, esterification result and esterification filtrate.

According to these results, the choosing of multifunctional group carboxylic acid as citric acid is more favorable in terms of using one group to interact with TNTs surface and leaving the other one or two for further interactions with additional molecules. Nevertheless, it also could be concluded that creating a weak interaction/association between the surface of TNTs and the carboxylic acids is not sufficient to step further for additional functionalization, as the subsequent treatment could easily break this fragile association and result in bare TNTs after carboxylic acid is detached off the surface. This type of weak interaction, such as electrostatic attractions and hydrogen bonds, could be more favorable regarding TNTs loading with drugs so these drugs can be liberated later from this association and released to the biological medium. It is worth mentioning that these interactions could slow the release rate of the drug or change its kinetic if they were sufficiently intense [18,36]. On the other hand, stronger bonds are more favorable during functionalization/surface modification, so this surface adjustment could be permanent to provide the TNTs with special specifications intended for special purposes.

As the attempt for TNTs PEGylation via CA linker has failed, a third attempt using AA was applied where the hypothesis was to bond AA to TNTs by π-bonding via breaking up of its C=C bond. Although a weak interaction with the surface of TNTs was achieved similarly as the case with CA, the attempt was considered a failed experiment. Since the characteristic peaks of AA (C=O stretching vibration at 1722 cm^{-1}, the OH bending at

1410 cm^{-1}, and the C-O stretching at 1299 cm^{-1}) exhibited significant shifting (1630, 1440 and 1277 cm^{-1}, respectively) in the spectrum of the reaction result, the C=C stretching vibration at 1636 cm^{-1} was covered while =C-H bending vibration at 986 cm^{-1} remained in an unchanged position (Figure 5). These observations indicate that instead of the π-bonding with the C=C bond, the carboxylic group formed an H-bond with the TNTs. In this case, the carboxyl group of acrylic acid would be occupied and thus would not be available to act as an extended arm for further functionalization. Moreover, as it was previously mentioned, such a weak interaction as H-bonds with acrylic acid is not enough to step further and use this acid as a linker for additional molecules.

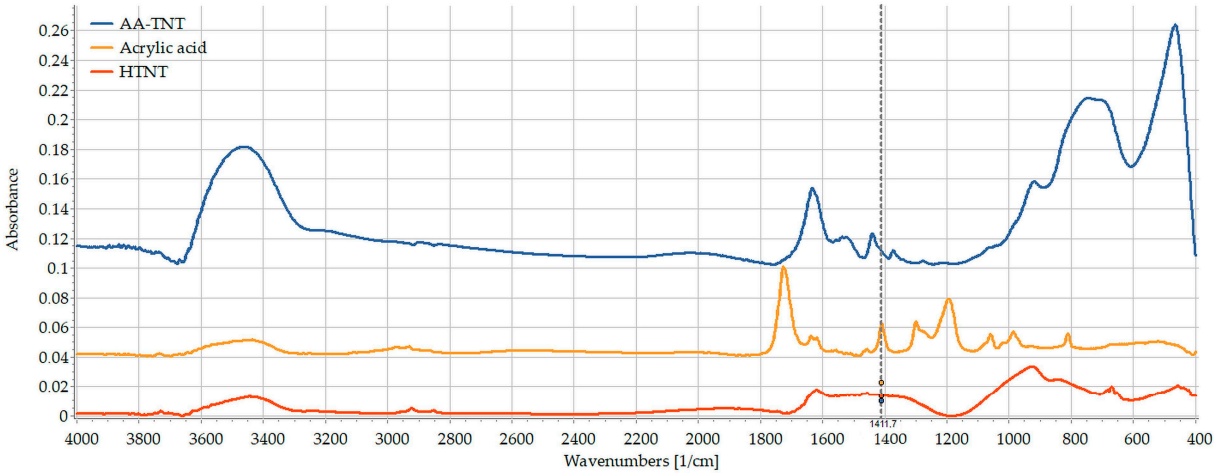

Figure 5. FT-IR spectra of acrylic acid (yellow), TNTs (red) and AA-TNTs (blue).

Based on the previous discussion, it is necessary to build a durable connection between the surface of TNTs and the carboxylic acid so it could tolerate the subsequent treatment for using it as a bridge connecting additional substances. For this reason, a reverse approach was conducted starting from bonding the acrylic acid with the molecule of interest (PEG) as the initial step depending on the carbon double bond as the main site of interaction. Then, this synthesized adduct could be linked to the hydroxylated surface of TNTs. Acrylic acid–PEG connection was carried out using free radical polymerization reaction, which will present a new copolymer (PAA–PEG) with multiple carboxylic groups. These groups could be utilized later to connect more molecules with the carboxylic arm of the pegylated TNTs such as drugs, markers or biological molecules.

Significant differences may be observed between the spectrum of the prepared copolymer and its precursors (PEG and AA) spectra (Figure 6). The disappearance of the peak assigned to the vibration of H in C=C-H at 986 cm^{-1} is clear evidence of the polymerization reaction. Furthermore, the absorption peak of C-H stretching of methylene groups is also visible at 2928 cm^{-1} in the spectrum of the prepared copolymer, and it also could be a sign for the saturation of C=C bond in acrylic acid during the polymerization process. Regarding the C=O stretching range between 1600 and 1750 cm^{-1}, there were two peaks visible in the spectrum of acrylic acid assigned to C=C and C=O vibrations which are at 1636 and 1727 cm^{-1}, respectively. In the newly synthesized material, the peak at 1727 cm^{-1} is separated to 1715 and 1737 cm^{-1}, indicating the presence of terminal and mid-chain carboxyl groups. The new peaks at 1558 and 1538 cm^{-1} may indicate that the carboxyl groups are presented in the form of carboxylate anions. The slight decrement of the O-H bending vibration of PEG at 1349 cm^{-1} and the increasement of C-O stretching at 1245 cm^{-1} in the copolymer indicate that PEG is attached to the end of the PAA chain through its terminal OH.

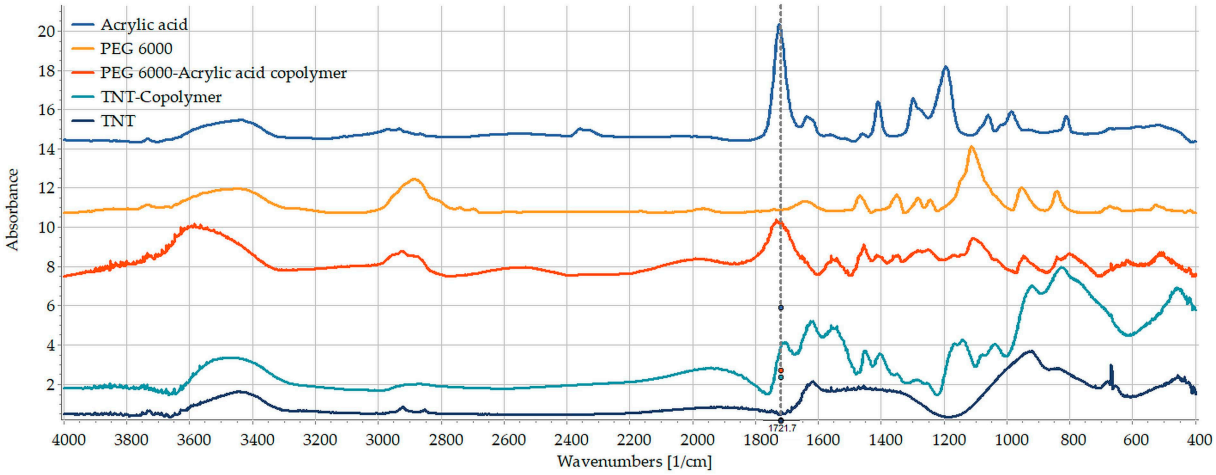

Figure 6. FT-IR spectra of acrylic acid (blue), PEG 6000 (yellow), AA/PEG copolymer (red), TNT (dark blue) and the AA/PEG functionalized TNT (light blue).

Regarding the spectrum of AA/PEG functionalized TNTs, the further shift of C=O stretching to 1706 cm^{-1}, and the multiple shifts of the peaks in the C-O stretching region at 1171, 1131 and 1038 cm^{-1}, indicate that the copolymer is strongly attached to the surface of TNTs. A similar slight but considerable shift may be observed in the carboxylate stretching to 1560 and 1540 cm^{-1}. According to Pouran et al. [37] and Liew et al. [38], this shift indicates a strong ionic bond between the carboxylate anion and Ti ions which might be irreversible.

The results were cross-confirmed by Raman spectroscopic investigations. It is well visible on Figure 7 that the intensive C=C stretching signal of AA at 1638 cm^{-1} has completely disappeared from the AA/PEG copolymer spectrum, confirming the successful free radical polymerization reaction. The other characteristic peaks at 1452 cm^{-1}, 1726 cm^{-1} and 2931 cm^{-1} may be attributed to the stretching of carboxylate anion, carbonyl groups and CH_2 groups, respectively. The peak at 2931 cm^{-1} may be clearly identified in the spectrum of AA/PEG functionalized TNTs in an unchanged position, but the other signals cannot be identified clearly due to the fluorescence of TNTs. However, a new peak with small intensity has appeared in the spectrum at 1970 cm^{-1}, which may also indicate the presence of intermolecular interactions that may be due to the conjugated Ti-O-C vibrations.

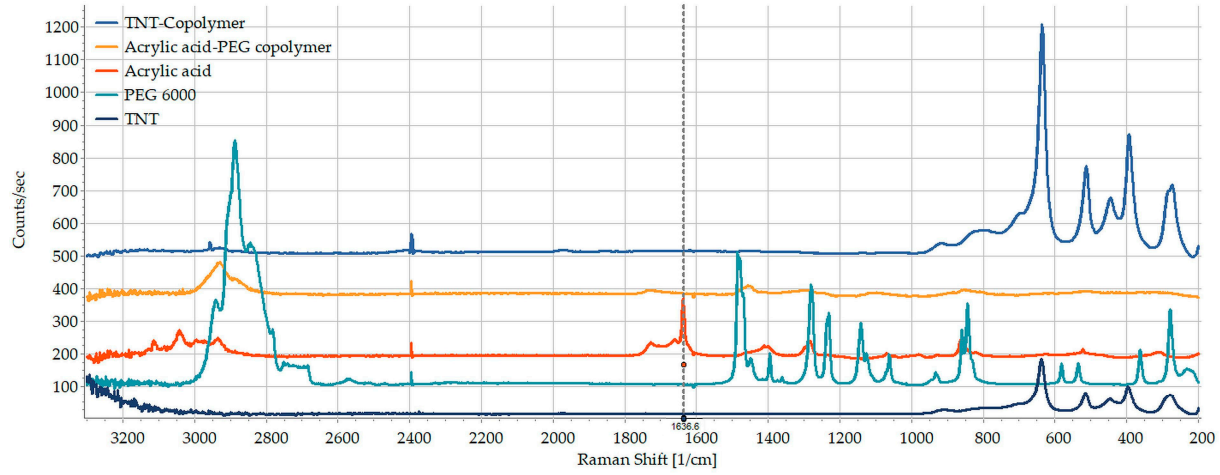

Figure 7. Raman spectra of acrylic acid (red), PEG 6000 (light blue), AA/PEG copolymer (yellow), TNT (dark blue) and the AA/PEG functionalized TNT (blue).

Morphological investigations have also been conducted on the bare and functionalized samples, with both scanning and transmission electron microscopy (Figure 8). No considerable difference was observed between the bare and functionalized TNTs except for some fragmentation, which may be due to the ultrasonication which was to aid the dispersion of TNTs before the functionalization reaction. The diameter was found to be 9.56 ± 1.56 nm vs. 10.42 ± 2.03 nm, while the length was found to be 128.27 ± 61.22 nm vs. 92.54 ± 20.97 nm for bare vs. functionalized TNTs, respectively, according to TEM pictures.

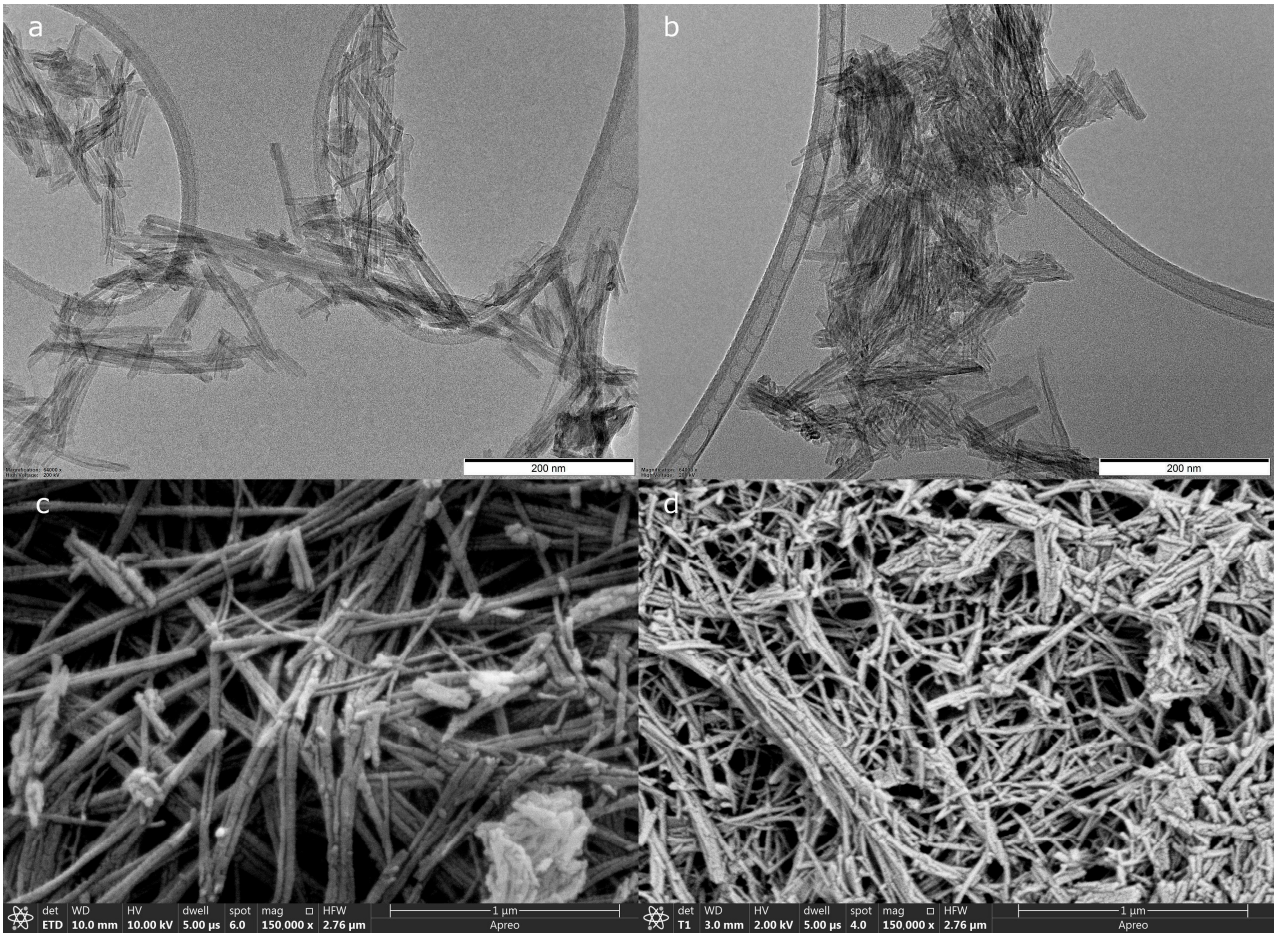

Figure 8. TEM picture of bare (**a**) and AA/PEG functionalized (**b**) TNTs, SEM pictures of bare (**c**) and AA/PEG functionalized (**d**) TNTs.

Nevertheless, these results show no correlation with those obtained with DLS measurements, where the hydrodynamic diameter in water was found to be 212.7 ± 0.2 nm vs. 417.2 ± 10.1 nm for bare and functionalized TNTs, respectively. The larger average particle size in water in comparison with that in the dried state can be attributed to the existence of a hydration layer that surrounds the hydrophilic nanotubes due to their hydroxylated surface, while the increased size of functionalized TNTs may be further proof of the successful functionalization, as the presence of AA/PEG copolymer on the surface of TNTs may lead to greater size and increased interaction with water molecules, probably due to their entrapment between its chains.

The hydroxylated surface of TNTs provides a stable negative zeta potential (−36.47 ± 0.35 mV), which corresponds well with the results of Bavykin et al. (−42.7 mV) [39] and of Papa et al., who reported a strongly negative zeta potential above the isoelectric point (pH 3.6) of TNTs [40], and indicated that although these nanotubes would be negatively charged at the physiological pH (−34.5 ± 4.3 mV), they can still interact well with the negatively charged cell surface, achieving good internalization supported by their tubular

morphology [41]. The functionalized TNTs exhibited the same stable negative zeta potential in purified water (−36.86 ± 0.41 mV).

However, there was a considerable difference in the behavior of bare and functionalized TNTs in PBS buffer where, despite the unchanged zeta potential (−33.96 ± 2.27 mV and −35.9 ± 2.01, respectively), the bare TNTs exhibited visible precipitation, which was in accordance with the size measurements that showed a size of 11,037 ± 7399 nm. According to our hypothesis, the PBS buffer induced a partial ion exchange on the surface of TNTs, which decreased the repulsion forces and induced the aggregation of nanotubes. In contrast, no similar effect was observed in the case of the functionalized TNTs, where only a slight increment was observed in the hydrodynamic diameter (570.43 ± 26.53 nm), so functionalization here has a positive impact by reducing agglomeration and enhancing dispersibility and stability of TNTs in this medium.

Similar observations were detected in the PBS-based cell culture medium, where 11,283 ± 6480 nm and 837.83 ± 18.48 nm size was detected for bare and functionalized TNTs, respectively. The increased size in the cell culture medium can be due to the decreased zeta potential (−3.14 ± 1.79 mV and −23.2 ± 0.95, for bare and functionalized TNTs, respectively) indicating strong TNT–cell interactions. However, another possible explanation is that the presence of cells probably interferes with the measurement and might influence the results. Nevertheless, the smaller change in zeta potential of the functionalized samples in cell culture medium compared to that of the bare TNTs also supports the stabilizing effect of functionalization, probably by sterically hindering the hydrophobic and electrostatic interactions with the cells, reducing their adsorption on the surface, and probably simulating what could happen with the plasma components [42]. However, decreasing the negative zeta potential would result in reducing the repulsion with cell membrane, thus leading to the enhancement of cell permeation, higher penetration but also higher potential of toxic effects [43].

The preliminary toxicity of the prepared TNTs has been investigated by a widely used viability assay against human adherent cancer cell lines and two different fibroblasts. The substances were applied in 1–30 μg/mL concentration range for 72 h. None of them exerted considerable cell growth inhibition as the growth inhibition values did not exceed 30% in any cases, so the investigated samples can be considered as safe (Figure 9). The statistical analysis revealed no significant ($p > 0.05$) difference between the tested samples. Regarding the sensitivity of various cell lines, the statistical evaluation confirmed that UPCI-SCC-154 oral squamous carcinoma cell line is the most sensitive cell line but in a non-concentration-dependent manner. Typical concentration-dependent effects were observed only against UPCI-SCC-131 cells where the 30 μg/mL concentration exhibited a significant increase in the growth inhibition in comparison with the 1 and 3 μg/mL concentrations ($p = 0.012$ and $p = 0.011$, respectively), but the inhibition did not exceed the 30% level even in this case. The proliferation of ovarian cancer cell line A2780 and fibroblasts were practically not influenced by the treatment with TNTs. There were no significant ($p > 0.05$) differences between human and murine fibroblasts (MRC5 and NIH/3T3, respectively) concerning the sensitivity toward the nanotubes. Though the presented cell-based viability results cannot substitute an appropriate toxicological study, they indicate that the tested substances have no relevant action on the cell growth, and, therefore, no outstanding toxicity can be expected from later in vivo experiments.

These results agreed with the findings of Papa et al., who reported no cytotoxicity of TNTs on Chinese hamster ovary cell lines (CHO) after 24 h of exposure in a concentration up to 10 μg/mL [40]. They were also in agreement with the findings of Fenyvesi et al. [44] and Wadha et al. [45], who demonstrated no cytotoxic effect of TNTs against Caco-2 cell lines in a concentration up to 5 mg/mL after short treatment (120 min) and against A549 epithelial cell lines in a concentration up to 1.1 mg/mL after long exposure (7 days), respectively. It is worth mentioning that these safety results were not limited to the bare TNTs, but the safety was also evidenced with different types of functionalization and with different chemical structures. For example, Ranjous et al. have reported the safety of silan-functionalized

TNTs up to 1 mg/mL and stearate-functionalized TNTs up to 2 mg/mL on Caco-2 cell lines using MTT assay for a short exposure (120 min) [20]. Papa et al. have also modified the surface of TNTs with polyethyleneimine (PEI) and then examined the toxicity with MTT assay on cardiomyocytes for 24 and 96 h. No significant toxicity was observed neither with TNTs nor with their functionalized samples in a concentration up to 10 μg/mL [41]. These studies, in addition to our research work, presented promising results to promote the future use of TNTs as safe nanocarriers and a novel platform for drug delivery.

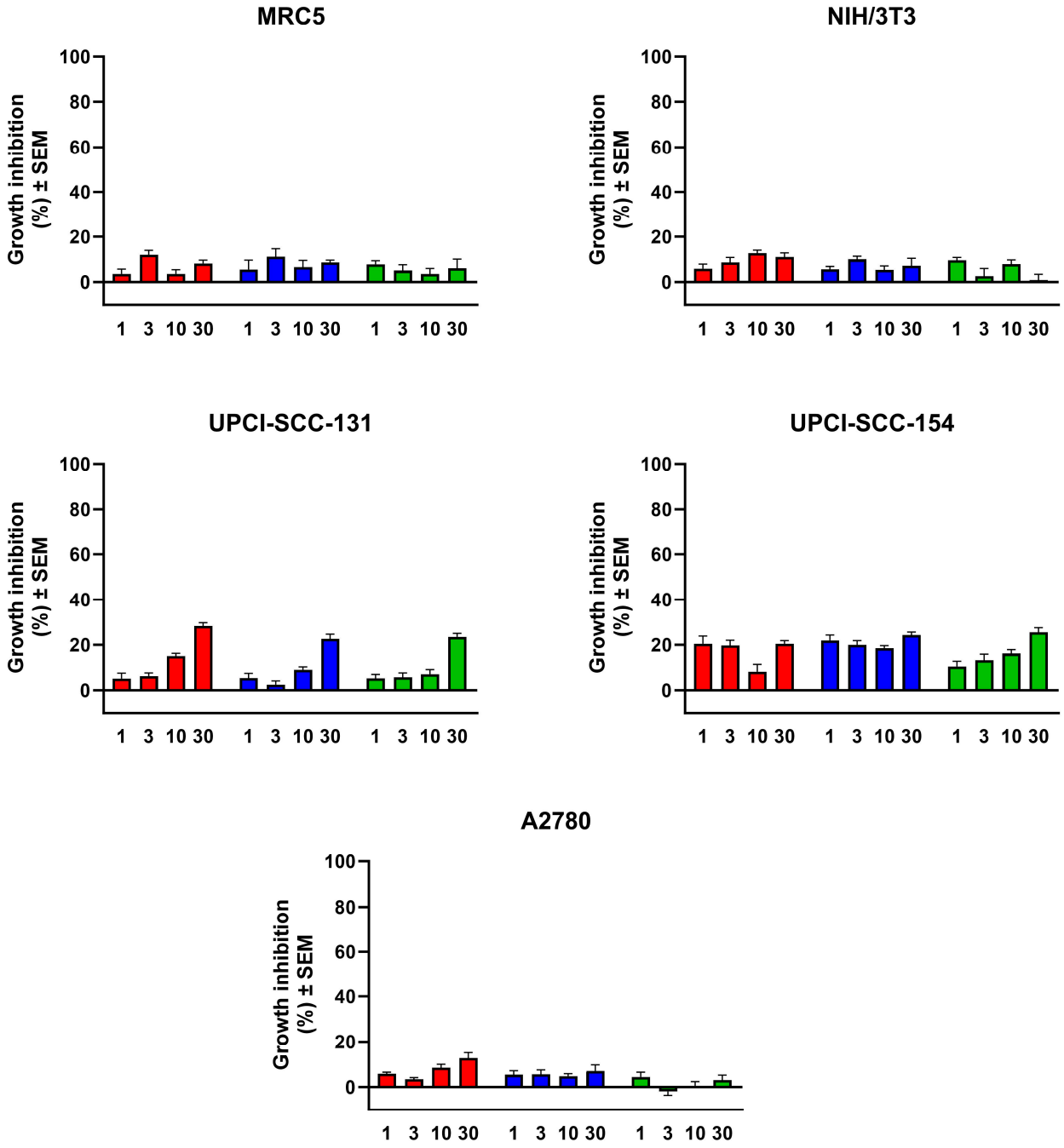

Figure 9. Effects of the prepared nanotubes on the growth of the utilized fibroblasts (MRC5, NIH/3T3) and cancer cells. Numbers on horizontal axes indicate final concentrations in μg/mL; red, blue and green columns mean TNT, AA/PEG copolymer and AA/PEG functionalized TNTs, respectively.

4. Conclusions

TNTs have been widely used in different disciplines since they first appeared in 1996 as a superior replacement for the organic carbon counterparts. They hold huge potential that could bring advantages to multiple platforms, including the pharmaceutical one. However, some of their characteristics which act as an obstacle hindering their successful use in health domains could be overcome by functionalizing their surface to shape their properties for suiting the pharmaceutical requirements.

Determining the type and the strength of the created interaction/association between TNTs and the functionalizing agent in the prepared composites is of crucial importance as it would highly affect the subsequent application of these synthesized composites. For instance, weak associations such as hydrogen bonds are not sufficient as the used agent would easily detach off the surface; thus, stronger interactions such as covalent or ionic bonds are more favorable as they are more stable and long-lasting ones.

The synthesized AA/PEG copolymer was successfully utilized for the durable functionalization of TNTs, and it has considerably increased the stability in aqueous environment. Furthermore, based on the results of the preliminary cell viability studies using multiple cell lines, TNTs could be a safe and promising candidate for drug delivery purposes.

Author Contributions: Conceptualization, T.S.; methodology, T.S. and R.S.; formal analysis, R.S., O.J.-L., T.T., I.S., N.B.-F. and I.Z.; investigation, R.S., O.J.-L., T.T., I.S., N.B.-F. and I.Z.; writing—original draft preparation, R.S.; writing—review and editing, T.S. and G.R.J.; visualization, T.S.; supervision, T.S. and G.R.J.; project administration, T.S.; funding acquisition, T.S. All authors have read and agreed to the published version of the manuscript.

Funding: This research was funded by Project No. TKP2021-EGA-32 and has been implemented with the support provided by the Ministry of Innovation and Technology of Hungary from the National Research, Development, and Innovation Fund, financed under the TKP2021-EGA funding scheme. The publication was supported by the Richter Centenáriumi foundation.

Institutional Review Board Statement: Not applicable.

Informed Consent Statement: Not applicable.

Data Availability Statement: Data are contained within the article.

Acknowledgments: The authors would like to thank Balázs Béniám for his valuable help in conducting DLS and XRPD measurements.

Conflicts of Interest: The authors declare no conflict of interest.

References

1. Wang, F.; Shi, L.; He, W.X.; Han, D.; Yan, Y.; Niu, Z.Y.; Shi, S.G. Bioinspired micro/nano fabrication on dental implant-bone interface. *Appl. Surf. Sci.* **2013**, *265*, 480–488. [CrossRef]
2. Popat, K.C.; Leoni, L.; Grimes, C.A.; Desai, T.A. Influence of engineered titania nanotubular surfaces on bone cells. *Biomaterials* **2007**, *28*, 3188–3197. [CrossRef] [PubMed]
3. Tsai, C.-C.; Teng, H. Regulation of the physical characteristics of titania nanotube aggregates synthesized from hydrothermal treatment. *Chem. Mater.* **2004**, *16*, 4352–4358. [CrossRef]
4. Adeleye, A.T.; John, K.I.; Adeleye, P.G.; Akande, A.A.; Banjoko, O.O. One-dimensional titanate nanotube materials: Heterogeneous solid catalysts for sustainable synthesis of biofuel precursors/value-added chemicals—A review. *J. Mater. Sci.* **2021**, *56*, 18391–18416. [CrossRef]
5. Wei, M.D.; Konishi, Y.; Zhou, H.S.; Sugihara, H.; Arakawa, H. Utilization of titanate nanotubes as an electrode material in dye-sensitized solar cells. *J. Electrochem. Soc.* **2006**, *153*, A1232–A1236. [CrossRef]
6. Hinojosa-Reyes, M.; Camposeco-Solis, R.; Ruiz, F. $H_2Ti_3O_7$ titanate nanotubes for highly effective adsorption of basic fuchsin dye for water purification. *Microporous Mesoporous Mater.* **2019**, *276*, 183–191. [CrossRef]
7. Camposeco, R.; Castillo, S.; Mejia-Centeno, I.; Navarrete, J.; Gomez, R. Effect of the Ti/Na molar ratio on the acidity and the structure of TiO_2 nanostructures: Nanotubes, nanofibers and nanowires. *Mater. Charact.* **2014**, *90*, 113–120. [CrossRef]
8. Ranjous, Y.; Regdon, G.; Pintye-Hodi, K.; Sovany, T. Standpoint on the priority of TNTs and CNTs as targeted drug delivery systems. *Drug Discov. Today* **2019**, *24*, 1704–1709. [CrossRef]
9. Wang, Y.; Yuan, L.; Yao, C.; Fang, J.; Wu, M. Cytotoxicity Evaluation of pH-Controlled Antitumor Drug Release System of Titanium Dioxide Nanotubes. *J. Nanosci. Nanotechnol.* **2015**, *15*, 4143–4148. [CrossRef]

10. Loiseau, A.; Boudon, J.; Oudot, A.; Moreau, M.; Boidot, R.; Chassagnon, R.; Said, N.M.; Roux, S.; Mirjolet, C.; Millot, N. Titanate Nanotubes Engineered with Gold Nanoparticles and Docetaxel to Enhance Radiotherapy on Xenografted Prostate Tumors. *Cancers* **2019**, *11*, 1962. [CrossRef]
11. Kalbacova, M.; Macak, J.; Schmidt-Stein, F.; Mierke, C.; Schmuki, P. TiO_2 nanotubes: Photocatalyst for cancer cell killing. *Phys. Status Solidi–Rapid Res. Lett.* **2008**, *2*, 194–196. [CrossRef]
12. Mandal, S.S.; Jose, D.; Bhattacharyya, A. Role of surface chemistry in modulating drug release kinetics in titania nanotubes. *Mater. Chem. Phys.* **2014**, *147*, 247–253. [CrossRef]
13. Khoshnood, N.; Zamanian, A.; Massoudi, A. Mussel-inspired surface modification of titania nanotubes as a novel drug delivery system. *Mater. Sci. Eng. C* **2017**, *77*, 748–754. [CrossRef] [PubMed]
14. Torres, C.C.; Campos, C.H.; Diáz, C.; Jiménez, V.A.; Vidal, F.; Guzmán, L.; Alderete, J.B. PAMAM-grafted TiO_2 nanotubes as novel versatile materials for drug delivery applications. *Mater. Sci. Eng. C* **2016**, *65*, 164–171. [CrossRef] [PubMed]
15. Wang, Z.; Xie, C.; Luo, F.; Li, P.; Xiao, X. P25 nanoparticles decorated on titania nanotubes arrays as effective drug delivery system for ibuprofen. *Appl. Surf. Sci.* **2015**, *324*, 621–626. [CrossRef]
16. Sipos, B.; Pintye-Hodi, K.; Regdon, G., Jr.; Konya, Z.; Viana, M.; Sovany, T. Investigation of the Compressibility and Compactibility of Titanate Nanotube-API Composites. *Materials* **2018**, *11*, 2582. [CrossRef]
17. Sipos, B.; Regdon, G.; Konya, Z.; Pintye-Hodi, K.; Sovany, T. Comparative study on the rheological properties and tablettability of various APIs and their composites with titanate nanotubes. *Powder Technol.* **2017**, *321*, 419–427. [CrossRef]
18. Sipos, B.; Pintye-Hodi, K.; Konya, Z.; Kelemen, A.; Regdon, G.; Sovany, T. Physicochemical characterisation and investigation of the bonding mechanisms of API-titanate nanotube composites as new drug carrier systems. *Int. J. Pharm.* **2017**, *518*, 119–129. [CrossRef]
19. Song, Y.Y.; Schmidt-Stein, F.; Bauer, S.; Schmuki, P. Amphiphilic TiO2 nanotube arrays: An actively controllable drug delivery system. *J. Am. Chem. Soc.* **2009**, *131*, 4230–4232. [CrossRef]
20. Ranjous, Y.; Kósa, D.; Ujhelyi, Z.; Regdon, G., Jr.; Nagy, K.A.; Szenti, I.; Kónya, Z.; Bácskay, I.; Sovány, T. Evaluation of the permeability and in vitro cytotoxicity of functionalized titanate nanotubes on Caco-2 cell line. *Acta Pharm. Hung.* **2021**, *91*, 31–39. [CrossRef]
21. Chen, X.; Cai, K.; Fang, J.; Lai, M.; Hou, Y.; Li, J.; Luo, Z.; Hu, Y.; Tang, L. Fabrication of selenium-deposited and chitosan-coated titania nanotubes with anticancer and antibacterial properties. *Colloids Surf. B Biointerfaces* **2013**, *103*, 149–157. [CrossRef] [PubMed]
22. Mohan, L.; Anandan, C.; Rajendran, N. Drug release characteristics of quercetin-loaded TiO_2 nanotubes coated with chitosan. *Int. J. Biol. Macromol.* **2016**, *93*, 1633–1638. [CrossRef] [PubMed]
23. Gombotz, W.R.; Wang, G.H.; Horbett, T.A.; Hoffman, A.S. Protein adsorption to poly(ethylene oxide) surfaces. *J. Biomed. Mater. Res.* **1991**, *25*, 1547–1562. [CrossRef] [PubMed]
24. Sharma, S.; Popat, K.C.; Desai, T.A. Controlling nonspecific protein interactions in silicon biomicrosystems with nanostructured poly(ethylene glycol) films. *Langmuir* **2002**, *18*, 8728–8731. [CrossRef]
25. Kingshott, P.; McArthur, S.; Thissen, H.; Castner, D.G.; Griesser, H.J. Ultrasensitive probing of the protein resistance of PEG surfaces by secondary ion mass spectrometry. *Biomaterials* **2002**, *23*, 4775–4785. [CrossRef] [PubMed]
26. Lipka, J.; Semmler-Behnke, M.; Sperling, R.A.; Wenk, A.; Takenaka, S.; Schleh, C.; Kissel, T.; Parak, W.J.; Kreyling, W.G. Biodistribution of PEG-modified gold nanoparticles following intratracheal instillation and intravenous injection. *Biomaterials* **2010**, *31*, 6574–6581. [CrossRef] [PubMed]
27. Mano, S.S.; Kanehira, K.; Sonezaki, S.; Taniguchi, A. Effect of Polyethylene Glycol Modification of TiO_2 Nanoparticles on Cytotoxicity and Gene Expressions in Human Cell Lines. *Int. J. Mol. Sci.* **2012**, *13*, 3703–3717. [CrossRef]
28. Marques, T.M.F.; Sales, D.A.; Silva, L.S.; Bezerra, R.D.S.; Silva, M.S.; Osajima, J.A.; Ferreira, O.P.; Ghosh, A.; Silva, E.C.; Viana, B.C.; et al. Amino-functionalized titanate nanotubes for highly efficient removal of anionic dye from aqueous solution. *Appl. Surf. Sci.* **2020**, *512*, 145659. [CrossRef]
29. Nagasawa, S.; Yudasaka, M.; Hirahara, K.; Ichihashi, T.; Iijima, S. Effect of oxidation on single-wall carbon nanotubes. *Chem. Phys. Lett.* **2000**, *328*, 374–380. [CrossRef]
30. Liu, Z.; Sun, X.; Nakayama-Ratchford, N.; Dai, H. Supramolecular chemistry on water-soluble carbon nanotubes for drug loading and delivery. *ACS Nano* **2007**, *1*, 50–56. [CrossRef]
31. Abo-Shosha, M.; El-Zairy, M.; Ibrahim, N. Preparation and rheology of new synthetic thickeners based on polyacrylic acid. *Dye. Pigment.* **1994**, *24*, 249–257. [CrossRef]
32. Ibrahim, N.A.; Amr, A.; Eid, B.M.; Mohamed, Z.E.; Fahmy, H.M. Poly(acrylic acid)/poly(ethylene glycol) adduct for attaining multifunctional cellulosic fabrics. *Carbohydr. Polym.* **2012**, *89*, 648–660. [CrossRef]
33. Mosmann, T. Rapid colorimetric assay for cellular growth and survival: Application to proliferation and cytotoxicity assays. *J. Immunol. Methods* **1983**, *65*, 55–63. [CrossRef]
34. Abdullah, F.Z.; Ma'amor, A.; Daud, N.A.; Abd Hamid, S.B. Selective Synthesis of Peg-Monoester Using Cesium Heteropoly Acid as Heterogeneous Catalyst. *Quim. Nova* **2017**, *40*, 506–512. [CrossRef]
35. Borges, M.E.; Diaz, L. Recent developments on heterogeneous catalysts for biodiesel production by oil esterification and transesterification reactions: A review. *Renew. Sust. Energ. Rev.* **2012**, *16*, 2839–2849. [CrossRef]

36. Ranjous, Y.; Regdon Jr, G.; Pintye-Hódi, K.; Varga, T.; Szenti, I.; Kónya, Z.; Sovány, T. Optimization of the Production Process and Product Quality of Titanate Nanotube–Drug Composites. *Nanomaterials* **2019**, *9*, 1406. [CrossRef] [PubMed]
37. Pouran, H.; Colodrero, R.P.; Wu, S.; Hix, G.; Zakharova, J.; Zhang, H. Assessment of ATR-FTIR spectroscopy with multivariate analysis to investigate the binding mechanisms of Ag and TiO_2 nanoparticles to Chelex®-100 or Metsorb™ for the DGT technique. *Anal. Methods* **2020**, *12*, 959. [CrossRef]
38. Liew, C.-M.; Ng, H.M.; Numan, A.; Ramesh, S. Poly(Acrylic acid)–Based Hybrid Inorganic–Organic Electrolytes Membrane for Electrical Double Layer Capacitors Application. *Polymers* **2016**, *8*, 179. [CrossRef] [PubMed]
39. Bavykin, D.V.; Friedrich, J.M.; Lapkin, A.A.; Walsh, F.C. Stability of aqueous suspensions of titanate nanotubes. *Chem. Mater.* **2006**, *18*, 1124–1129. [CrossRef]
40. Papa, A.-L.; Maurizi, L.; Vandroux, D.; Walker, P.; Millot, N. Synthesis of titanate nanotubes directly coated with USPIO in hydrothermal conditions: A new detectable nanocarrier. *J. Phys. Chem. C* **2011**, *115*, 19012–19017. [CrossRef]
41. Papa, A.L.; Dumont, L.; Vandroux, D.; Millot, N. Titanate nanotubes: Towards a novel and safer nanovector for cardiomyocytes. *Nanotoxicology* **2013**, *7*, 1131–1142. [CrossRef] [PubMed]
42. Cruje, C.; Chithrani, D.J.J.N.R. Polyethylene glycol density and length affects nanoparticle uptake by cancer cells. *J. Nanomed. Res.* **2014**, *1*, 8. [CrossRef]
43. Kamal, N.; Zaki, A.H.; El-Shahawy, A.A.; Sayed, O.M.; El-Dek, S.I. Changing the morphology of one-dimensional titanate nanostructures affects its tissue distribution and toxicity. *Toxicol. Ind. Health* **2020**, *36*, 272–286. [CrossRef] [PubMed]
44. Fenyvesi, F.; Konya, Z.; Razga, Z.; Vecsernyes, M.; Kasa, P., Jr.; Pintye-Hodi, K.; Bacskay, I. Investigation of the cytotoxic effects of titanate nanotubes on Caco-2 cells. *AAPS PharmSciTech* **2014**, *15*, 858–861. [CrossRef]
45. Wadhwa, S.; Rea, C.; O'Hare, P.; Mathur, A.; Roy, S.S.; Dunlop, P.S.; Byrne, J.A.; Burke, G.; Meenan, B.; McLaughlin, J.A. Comparative in vitro cytotoxicity study of carbon nanotubes and titania nanostructures on human lung epithelial cells. *J. Hazard. Mater.* **2011**, *191*, 56–61. [CrossRef]

pharmaceutics

MDPI

Review

An Overview of Hydrothermally Synthesized Titanate Nanotubes: The Factors Affecting Preparation and Their Promising Pharmaceutical Applications

Ranim Saker, Hadi Shammout, Géza Regdon, Jr. and Tamás Sovány *

Institute of Pharmaceutical Technology and Regulatory Affairs, University of Szeged, Eötvös u 6, H-6720 Szeged, Hungary; rnmsaker@gmail.com (R.S.); hadishammout2@gmail.com (H.S.); geza.regdon@pharm.u-szeged.hu (G.R.J.)

* Correspondence: sovany.tamas@szte.hu; Tel.: +36-62-545-576

Abstract: Recently, titanate nanotubes (TNTs) have been receiving more attention and becoming an attractive candidate for use in several disciplines. With their promising results and outstanding performance, they bring added value to any field using them, such as green chemistry, engineering, and medicine. Their good biocompatibility, high resistance, and special physicochemical properties also provide a wide spectrum of advantages that could be of crucial importance for investment in different platforms, especially medical and pharmaceutical ones. Hydrothermal treatment is one of the most popular methods for TNT preparation because it is a simple, cost-effective, and environmentally friendly water-based procedure. It is also considered as a strong candidate for large-scale production intended for biomedical application because of its high yield and the special properties of the resulting nanotubes, especially their small diameters, which are more appropriate for drug delivery and long circulation. TNTs' properties highly differ according to the preparation conditions, which would later affect their subsequent application field. The aim of this review is to discuss the factors that could possibly affect their synthesis and determine the transformations that could happen according to the variation of factors. To fulfil this aim, relevant scientific databases (Web of Science, Scopus, PubMed, etc.) were searched using the keywords titanate nanotubes, hydrothermal treatment, synthesis, temperature, time, alkaline medium, post treatment, acid washing, calcination, pharmaceutical applications, drug delivery, etc. The articles discussing TNTs preparation by hydrothermal synthesis were selected, and papers discussing other preparation methods were excluded; then, the results were evaluated based on a careful reading of the selected articles. This investigation and comprehensive review of different parameters could be the answer to several problems concerning establishing a producible method of TNTs production, and it might also help to optimize their characteristics and then extend their application limits to further domains that are not yet totally revealed, especially the pharmaceutical industry and drug delivery.

Keywords: TNTs; hydrothermal treatment; temperature; alkaline medium; post treatment; pharmaceutical applications

Citation: Saker, R.; Shammout, H.; Regdon, G., Jr.; Sovány, T. An Overview of Hydrothermally Synthesized Titanate Nanotubes: The Factors Affecting Preparation and Their Promising Pharmaceutical Applications. *Pharmaceutics* **2024**, *16*, 635. https://doi.org/10.3390/pharmaceutics16050635

Academic Editors: Jelena Djuris and Ivana Aleksić

Received: 7 April 2024
Revised: 1 May 2024
Accepted: 7 May 2024
Published: 9 May 2024

1. Introduction

Nowadays, nanoparticles have attracted huge attention in different domains of science and human life such as chemistry, energy, and medicine due to their special design and small size. Titanate nanotubes (TNTs) are one type of these novel materials, which was first prepared in 1996 by Hoyer [1] after organic carbon nanotubes were presented in 1991 with promising results in different areas. TNTs are described as a spiral-shaped type of inorganic nanoparticles which are originally derived from titanium dioxide (TiO_2) as a raw material [2]. Their diameter typically ranges between 10 and 100 nm according to the applied preparation method, but it might reach even 400 nm in some cases [2,3]. This nano-size combined with tubular structure are unique properties which differentiate

them from other types of nanoparticles (NPs), giving them higher surface area and cellular uptake [3,4]. Moreover, TNTs offer a distinguished profile of specifications that could be interesting in numerous fields, such as their hydrophilic nature, good wettability and biocompatibility [2,3,5], chemical stability [5], photocatalytic activity [5], excellent mechanical properties, and corrosion resistance [5,6], in addition to low toxicity [7–10]. Due to these remarkable specifications, TNTs have been successfully utilized in numerous fields with great outcomes and impressive performance (Figure 1) making them attractive candidates for investigation of their potentials in further disciplines [5,11–13]. Although some attempts have been made to investigate the possible application of these newly synthesized materials in biomedical research, few of them have focused on their application in the pharmaceutical field as drug carriers [5,14–17].

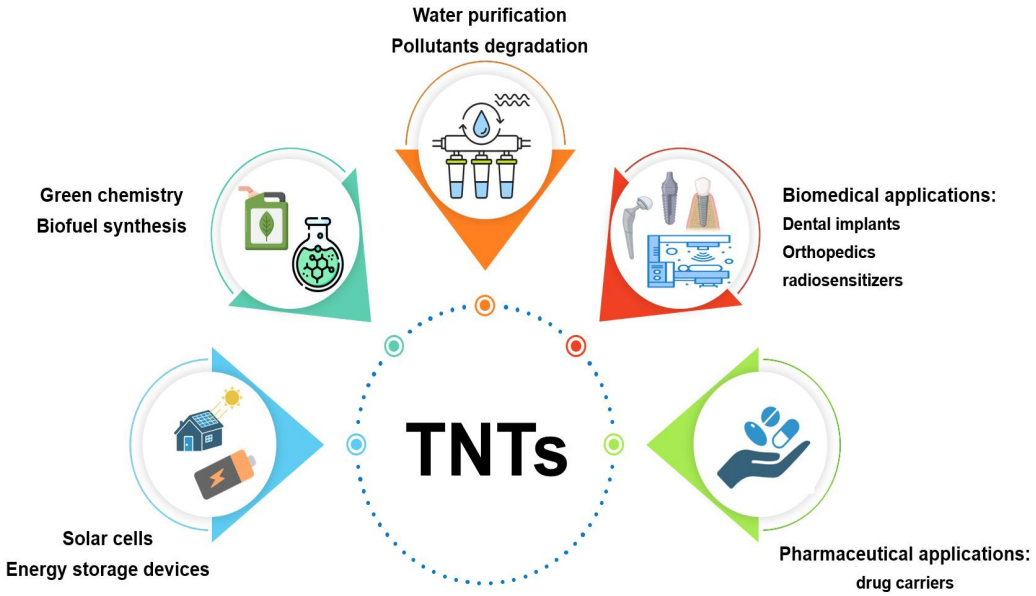

Figure 1. The applications of TNTs in different platforms.

Since their first appearance, many methods have been proposed for the proper preparation of TNTs, such as sol gel template, template-assisted synthesis, electrochemical treatment, and hydrothermal treatment [2,5]. Based on the literature data, it was clearly concluded that the final properties of the manufactured materials, especially their morphology, diameter, and crystal structure, are highly dependent on the method of preparation, which will subsequently affect their application field. For example, the diameter of nanotubes differs according to their preparation method, as electrochemical treatment would result in self-organized but large nanotubes (the typical diameter is >25 nm, often ≈100 nm). This large diameter is not convenient for biomedical uses because nanoparticles with this size will be easily cleared from the circulation by the reticuloendothelial system (RES). On the other hand, the use of the templating method is also limited in obtaining small-size nanotubes, due to the limitation of the pore size of the mold [3,5]. In contrast, hydrothermal treatment would result in a smaller diameter (10 nm) along with possibly hundreds of nanometers in length, making them possible candidates for medical and pharmaceutical use [2].

The small diameter and long circulation half-life of hydrothermally synthesized TNTs are not the only advantages that this method could offer, so it is becoming one of the most popular methods for the preparation of TNTs. It is a simple process that involves the crystallization of a starting material from a highly concentrated alkaline solution under a specific set of parameters (temperature, time, pressure). Moreover, as water is used as a reaction medium and no organic solvents are involved in any step of the process, it can be considered as an environmentally friendly and safe procedure to apply in laboratories and in larger scale production. Hydrothermal synthesis also provides high yields and mass

efficiency, which make it an attractive candidate for scaling up to industrial level [5,11,18]. However, although it is one of the most commonly used and discussed methods in the literature, it still generates controversies in the scientific community, as the published results are not totally in agreement. The differences in applied conditions/parameters during preparation makes the comparison of the results difficult, which could lead to conflicting results. Many theories have been proposed to explain TNTs formation. The most accepted one among authors using this method for the production of nanotubes involves several steps (Figure 2): breaking of Ti-O-Ti bonds after the dissolution of TiO_2 precursor in a strong alkaline medium, formation of Ti-O-Na bonds resulting in lamellar sheets, and rolling of the lamellar sheets into nanotubes [19]. According to Tsai et al., the starting TiO_2 precursor is converted into sheets through alkali treatment. These sheets mainly exist as an anatase phase that is more suitable for rolling to form nanotubes [20]. However, there is still a debate whether the formation of nanotubes occurs during the dynamic hydrothermal process [21–23] or only after exchanging sodium ions through acid treatment, which would lead to the scrolling of the precursor sheets [24–27]. The answer could highly depend on the reaction itself, as its conditions would significantly affect the resulting material, especially the properties/ratios of the starting precursors, sodium hydroxide (NaOH) concentration, reaction temperature, reaction time, mixing, and post treatment. Variations of these factors could affect the properties of the resulting nanotubes or even favor the formation of nanotubes with other nanomaterials such as nanosheets or nanoribbons. This could explain why it is always expected to have nanosheets that are not completely rolled up as byproducts of this preparation method [2,3].

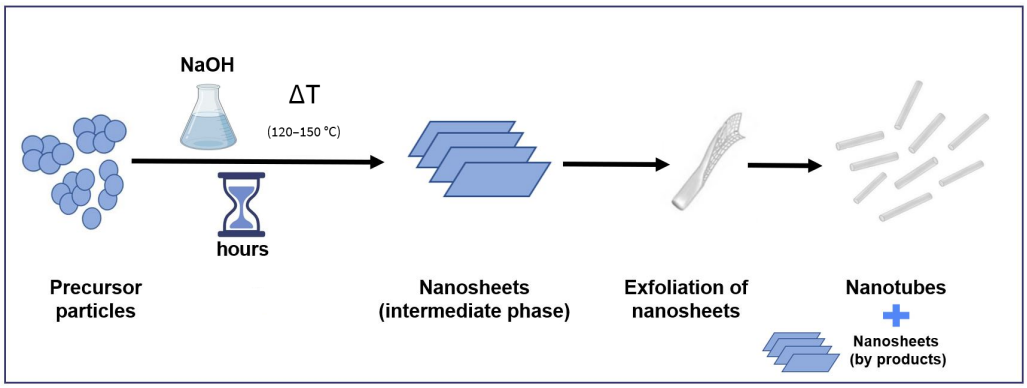

Figure 2. Schematic illustration of the mechanism of nanotubes formation during hydrothermal treatment method.

Based on the previous discussion, the specifications of the prepared nanotubes are closely related to the preparation method and strongly sensitive to the variation of its parameters. Hence, there is an urgent need to determine the appropriate range of preparation conditions under which nanotubes are produced in addition to precisely understanding the changes that could occur outside these ranges, such as changing morphology or crystal structure.

Therefore, this review highlights the importance of conducting an extensive screening and precise analysis of the different parameters involved in hydrothermal synthesis and their impact on the produced material, which could be the key to justifying the conflicted observations reported in the literature and to gaining a better understanding as to how to optimize this procedure to obtain the targeted nanotubes.

This investigation is of crucial importance in establishing a reproducible, robust, and scalable method for producing TNTs with controlled features as an initial step to later upgrading their use to the pharmaceutical domain.

The main parameters discussed in this review can be classified as thermal (reaction temperature, post-treatment calcination), chemical (concentrated alkaline medium, acid washing), or even mechanical (stirring, agitation). The variation of these parameters

could result in significant transformations, and controlling them will open the door for optimizing the production process and extending the applications of TNTs to new and innovative platforms.

This review also discusses the most important attempts that have been made in the last two decades regarding the utilization of TNTs for therapeutic purposes as drug carriers.

2. Hydrothermal Synthesis Conditions

2.1. Reaction Temperature

According to the literature, the temperature involved in the different stages of TNTs' preparation and post-preparation treatment highly affect their properties such as morphology, specific surface area (S.S.A.), and crystal structure, which would therefore affect their behavior and subsequent application, especially those related to their photocatalytic activity [28].

The utilization of a sufficient temperature (<130 °C) would lead to the formation of Ti-O-Na and Ti-OH bonds after breaking Ti-O-Ti bonds in the starting nanoparticles. This would subsequently lead to the formation of lamellar TiO_2 sheets because of the electrostatic repulsion of the charge on sodium. These lamellar sheets are considered an intermediate stage as they can scroll up to form the tubular structure. Treatment at higher temperatures results in granular particles rather than lamellar sheets. On the other hand, treatment at lower temperatures (<110 °C) results in thick plates which are not able to scroll and form nanotubes; thus, the extent of precursor conversion, the yield of the produced nanotubes, and the overall success of the procedure is determined by the treatment temperature [20].

Vu et al. suggested the same mechanism, as, at lower temperatures, the sphere-like particles and sheet-like structures will be dominant, but increasing the temperature would provide sufficient thermal energy to curl up nanosheets into tubular structures. This was first generated above 120 °C with the existence of some nanosheets that had completely transformed into tubes beyond 130 °C [21]. This was in agreement with the study of Sreekantan et al., who reported that temperature affects the morphology of the treated sample, as, at lower points (90 °C), the conversion of spherical particles to nanosheets will start, but the whole transformation would happen at higher temperatures (>110 °C) because, at this point, the additional thermal energy will lead to a sufficiently high surface energy to curl up the sheets [29]. In the same context, Ribbens et al. also reported that a low temperature (<110 °C) is not capable of forming nanotubes [30]. In addition, Viet et al. also demonstrated that a temperature lower than 115 °C is not enough for the formation of nanotubes. According to the study, the optimal range for successful preparation is between 115 and 180 °C, as a higher temperature could destroy the lamellar structure of TiO_2; therefore, nanotubes will not appear [27]. Yuan et al. also reported that the optimal range of hydrothermal temperature is 100–150 °C [31]. According to their findings and others, increasing the temperature within this range would increase the yield of nanotubes [31,32], their crystallinity, and outer diameter [32].

Increasing the reaction temperature would also increase the S.S.A. up to 150 °C, but, interestingly, a higher temperature would lead to opposite results (decreased S.S.A.) [33]. Lee et al. agreed, indicating that at a temperature greater than 160 °C, enormous decrease in surface area and pore volume will happen as a result of the formation of thick titanate nanorods [34]. Similar to the previous results, high temperature treatment led to the formation of different structures other than nanotubes in several studies, such as nanoribbons (>160 °C) [31,35], nanofibers or nanobelts (>170 °C) [36], and nanorods (180 °C) [32].

Bavykin et al. also studied the effect of temperature on diameter/morphology, concluding that increasing it in the range of 120–150 °C could increase the average diameter of the prepared nanotubes, but a subsequent increase could lead to morphological change presented as non-hollow nanofibers [37]. Although increasing temperature would generally increase the number and length of the formed nanotubes, it would also result in a decreased internal diameter. It is well known that S.S.A. normally increases with increased

temperature, but it is also in proportion to the internal diameter; therefore, the decreasing of internal diameter induces a decrease in the surface area of the produced nanotube [38].

2.2. Reaction Medium

As previously mentioned, the hydrothermal treatment method uses an alkaline medium which is mostly an aqueous solution of NaOH, and the concentration of this solution would affect the properties of the produced nanotubes, especially their morphology and surface area [39]. The full growth of nanotubes requires a highly concentrated solution of 10 M, as, below this limit, a large number of aggregates of unreacted powder, particles, and sheets will be observed. S.S.A. would also be affected and increases with increasing alkali concentration [21]. Too low (<5 mol/L) or too high (>15 mol/L) a concentration of NaOH will result limited formation of nanotubes. The optimal range for a high yield was found to be between 10 and 15 mol/L [31]. It was also found that NaOH concentration is the most important factor affecting morphology, and its effect is even stronger than that of temperature and reaction time. However, optimization of these three factors could be an effective tool to control/adjust the final shape [39]. In contrast, another study reported that, if a lower concentration of NaOH is utilized, a higher temperature could be used to fill this gap and obtain the desired tubular structure, suggesting that temperature could be the most critical factor affecting nanotubes formation [35].

In the same context, Guo et al. reported that NaOH concentration affects the scrolling of multi-layered nanosheets to form nanotubes, as low concentrations result in a weak driving force for scrolling, but extremely concentrated NaOH will interrupt the scrolling process [40].

Although NaOH is considered to be the most often used alkaline medium in hydrothermal treatment, other types of alkaline medium, such as potassium hydroxide, could also be applied. However, it was reported that using NaOH was more effective than potassium hydroxide in the enhancement of nanotube formation [41].

2.3. Reaction Time

The treatment time is a very important factor that gives the required time for nanomaterials to turn from a spherical shape into an intermediate phase (nanosheets) and finally into nanotubes. The complete transformation would require approx. 15 h [29]. It also highly affects the length of the resulting nanotubes, as a longer time would result in increased length [21]. Ma et al. reported that the optimal time period is about 24–72 h to obtain a high yield of TNTs, as a shorter duration would increase the ratio of unreacted TiO_2 particles [36], while Elsanousi et al. suggested a different opinion. Their results were in agreement with the study of Sreekantan et al. [29] that a short treatment (5–15 h) is enough to form pure nanotubes, as a longer duration would result in nanoribbon formation beside nanotubes, while pure nanoribbons are observed after very long treatments (48 and 72 h). However, the different applied temperature could be a reason for these conflicting results, as it is also deeply involved in this transformation. It is worth mentioning that nanotubes did not transform into nanoribbons at a low temperature, even if the duration of treatment was long, indicating that this transformation depends on several critical conditions in addition to the duration of the reaction, such as temperature and even pressure [42].

Guo et al. indicated that the thickness, width, and length of TNTs increase with the prolongation of process time [40]. Increasing the treatment duration leads to a growing amount of intermediate phase (nanosheets) through a dissolution–reprecipitation process and an increased tendency of curling and forming nanotubes. However, no further increase in their length was observed after 24 h of treatment [43]. In the same context, Ranjitha et al. indicated that the formation of lamellar fragments (the intermediate phase in TNTs preparation) would be the result of a short reaction time, and, as the reaction continues, the tubular structure will be obtained. They also highlighted the effect of reaction time on TNTs crystallinity and reported that the amount of rutile phase would increase with the

increasing reaction time [44]. Elsanousi et al. also indicated that the crystallinity of the final product might be improved by increasing the duration of the treatment [42].

According to the previously mentioned results, it is widely accepted that increasing the duration of heat treatment would improve crystallization, but at the same time it would negatively affect the surface area and therefore highly influence the related surface applications such as photocatalytic activity. From this point of view, if photocatalytic activity is the main target of the TNTs production, a compromise between surface area and crystallinity should be obtained to achieve their desired synergistic effect [45].

The optical properties would also be influenced by the duration of treatment. It was reported that the absorption edge of TNTs has a red shift (to a higher wavelength) with longer reaction time due to the modification of the TiO_2 band gap, concluding that increasing hydrothermal reaction time will decrease the band gap energy and increase the wavelength of the absorbed light [44].

2.4. Reaction Pressure

The effect of pressure on the formation of nanotubes was not intensively investigated. It was reported that the pressure in addition to the volume of solution inside the used autoclave will affect the crystallinity of the resulting nanotubes. This pressure is highly related to the filling fraction and to the thermal expansion of different volumes of the liquid. It was also reported that more pressure is needed in the case of nano powder to form crystalline nanotubes in comparison to micro powder [46]. Tsai et al. indicated that the pressure of saturated NaOH solution in the sealed autoclave would only impact the formation of TNTs at temperatures higher than 150 °C, as the differences between pressure values at temperatures lower than 150 °C would be minor [47]. Morgan et al. studied the effect of pressure on nanotube formation at a higher temperature range (up to 220 °C) and concluded that high pressure (accompanied with lower NaOH concentration) was not promoting nanotube formation as expected, so they excluded the pressure effect as an influencing factor [35].

2.5. Stirring, Agitation and Sonication

Mechanical forces should also be considered while listing the factors affecting the preparation of TNTs. For example, a stirring process could shorten the time needed for the transformation of TiO_2 into nanotubes as it would increase the contact between the precursor and NaOH, while, in a static condition without stirring, only a small amount of TiO_2 nanotubes would form. Thus, stirring clearly affects the production yield [21]. Agitation could also affect the morphology/surface area of the prepared TNTs, as it could accelerate the dissolution process of the precursor during preparation, thus affecting the subsequent nucleation after supersaturation [48].

Ma et al. indicated that the process of sonication and its power affect the morphology of nanomaterials during hydrothermal treatment. Sonication with enough power promotes the breaking of Ti-O-Ti bonds and sodium ions intercalating into the titania lattice; therefore, increasing the sonication time will result the transformation of the spherical particles into a rod configuration. These nanorods will continue to grow during hydrothermal treatment, extend their length, then form the tubular structure after washing with acid [49].

2.6. Starting Materials

It was previously reported that impurities and different sources/types of starting materials have no effect on nanotube formation [21]. Any type of TiO_2 could be used as a precursor for the preparation of TNTs. However, the properties of the used precursor would have a high impact on the resulting materials. For example, the particle size of the TiO_2 starting material could affect the morphology/surface area of the produced nanomaterials, as smaller TiO_2 starting particles will have a higher solubility in the preparation solution and this will result in a higher concentration of Ti ions, leading to a homogenous nucleation after the supersaturation is achieved. If a lower concentration of Ti ions is present due to

the larger particle size of the starting material, heterogenous nucleation is dominant [48]. Yuan et al. concluded that surface area would be influenced by the particle size of the raw materials, as finer particles will lead to a higher surface area, while yield is not significantly affected [31].

The smaller particle size of the starting material could also result in a faster formation of TNTs [41]. Ma et al. also reported the importance of the precursor's particle size, as smaller ones could effectively form TNTs during a combined sonication–hydrothermal process. However, precursors with larger particles would form sheets with rolled edges which cannot turn into the tubular shape, probably due to the steric hindrance of the larger particles [49].

In addition, the differences in TiO_2 precursor structure will also affect the formation of TNTs and their resulting properties. The type of the starting material would not highly affect the diameter and the thickness of the walls, but thermal stability would differ according to it. The anatase precursor presents TNTs with the highest thermal stability and preserves their tubular structure up to 400 °C, while an amorphous precursor presents TNTs with less thermal stability. This could be attributed to the defective sheets/foils formed from these precursors. Crystalline precursors originate fewer defective sheets compared to the ones originated from amorphous precursors. These defects make the occurrence of the rolling up process difficult, so more nanosheets were detected compared to the case of crystalline precursors [50]. Surprisingly, Yuan et al. reported that amorphous TiO_2 as a precursor did not lead to TNTs formation [31].

The crystalline phase of the used precursor will also affect the speed of TNTs formation, as anatase (a less stable phase with higher energy) reacts with NaOH faster than rutile during preparation [49]. Seo et al. also found that the anatase phase has a greater tendency for continuous elongation in a specific direction during preparation, which makes it more effective in TNTs formation than the rutile phase [38]. Moreover, the concentration of the starting material (TiO_2 precursor) is also a crucial factor to take into consideration, as increasing it apparently increases the length of the prepared nanotubes while the diameter is still the same. This systematic change in the aspect ratio reflects the increased density of the initial nucleation sites [51].

It could be concluded from the above-mentioned results that the morphology, surface area, phase transformation, thermal stability, and yield of TNTs highly differ according to the properties of starting materials, in addition to other parameters such as reaction time/temperature [41]. It should also be mentioned that titanium metal could also be used as a precursor for the preparation of TNTs in addition to crystalline and amorphous TiO_2 [40].

2.7. Molar Ratio

The molar ratio of starting materials (TiO_2 and alkali) will also affect the diameter and surface area of the resulting nanotubes. Increasing the TiO_2:NaOH molar ratio leads to a decrease in surface area and an increase in the average diameter of the nanotubes. A slow convection in the autoclave during preparation could be responsible for these differences in morphology [37]. The molar ratio will also play a significant role in gaining the desired morphology, as a higher NaOH:TiO_2 molar ratio means the existence of excess sodium ions that provide high surface energy, leading to the scrolling-up of the structure into nanotubes and a smaller outer diameter, while a lower molar ratio leads to the deposition of nanoparticles on the wall of the rods rather than the development into a tubular structure [29].

According to the literature, the chemical properties of prepared nanotubes would also be affected by the amount of NaOH and the Ti/Na ratio. Studies have shown that increasing the amount of NaOH will lead to a decreased number of Lewis acid sites on the surface. Furthermore, surface acidity of TNTs (Brönsted acid sites) also depends on the Ti/Na ratio, since increasing NaOH concentration to a sufficient quantity will enable the formation of Ti-O-Na, which transforms into Ti-O-H after washing with water. Basically, the surface of both anatase and rutile TiO_2 has only Lewis acid sites, but increasing the

Ti/Na ratio in addition to scrolling will generate more Brönsted acid sites due to exfoliation of the Ti-O planes. This surface acidity is nowadays a critical factor in several applications such as heterogeneous catalysis. To preserve this acidity in TiO_2 nanostructures, the best Ti/Na ratio is 7 [52]. The Ti/Na ratio also affects morphology, as different structures could be obtained by modifying it, such as nanofibers, nanotubes, and nanowires [52].

3. Post Treatment

3.1. Acid Treatment

As was previously mentioned, the various results have suggested that formation of TNTs and obtaining the tubular structure do not only depend on the alkaline synthesis but could be highly dependent on the washing step after it. Some reported results indicated that hydrothermal treatment is not enough to form the tubular structure, but an additional washing step with acid should be involved in the preparation procedure to transform the disordered intermediate phase into the desired geometry, due to a gradual Na^+/H^+ substitution [47]. This critical point of disagreement was further discussed by Nguyen et al., who concluded that hydrothermal treatment may not be sufficient alone to form the tubular structure for two reasons: first, the existence of a high sodium content if the washing process with water was not completed; second, washing with acid could serve as an assisted condition if the reaction condition was not sufficient for the formation of nanotubes [53].

In addition to the proposed theory that acid washing is necessary to obtain the desired tubular morphology, pH variation of the applied washing solution may cause crystal-structure transformation through simple rearrangement and could also lead to surface area variations. Nevertheless, it could also negatively affect morphology, as increasing the acidity of the washing solution would result in defective nanotubes caused by formation of anatase TiO_2 phase on some spots of the tubes. Also, extreme pH values could lead to coagulated particles or plates [47].

The previous results were in agreement with the study of Nguyen et al. who reported that the pH value of the washing solution will affect the morphology and thus the surface area of the produced TNTs. Decreasing pH from 9 to 2 resulted in more successful tube formation and, subsequently, a higher area, but when pH further decreased from 2 to 1 a decreased surface area could be noticed because of the low yield of nanotubes and appearance of nanosheets under this highly acidic condition. It is also worth mentioning that TNTs washed at pH = 0.5 were completely dissolved in the washing solution without any residual amount to be examined. In conclusion, TNTs washed at pH 1.6–4 showed the best appearance of tubes and the highest amount of tubular structures, while TNTs washed at pH = 2 showed the highest surface area, pore volume, and pore size [53].

According to other studies, acid treatment could also affect the size and crystallinity of the resulting nanotubes and result in a smaller average size and the appearance of crystalline rutile peaks. The untreated samples were only amorphous by examination [27].

It is of crucial importance to mention that the washing step mainly affects the sodium content of TNTs; therefore, increasing the number of washings could eliminate the sodium ions from the surface, although their presence is very important to preserve the regular structure. This could explain why washing with a high excess of liquid produces nanotubes with irregular shapes and thinner walls [24]. It also should be mentioned that the applied concentration of acid should be carefully determined in the post treatment, as some researchers have pointed out that highly concentrated acid (>0.01 M) could destroy the tubular structure, as it could break the Ti-O-Na bonds and lead to surface irregularity, confirming the previous result that the existence of sodium ions on the surface has a significant role in preserving the tubular structure of TNTs [54]. Nada et al. reported the same results, which confirm that only low-acid concentrations should be used during the washing step, otherwise a damaged structure could result [25].

However, Poudel et al. used a wider range of concentrations, suggesting that the optimal concentration of washing acid is between 0.5 and 1.5 M to obtain pure nanotubes

with a high yield. According to the study, concentrations below 0.5 M were not capable of removing sodium impurities, while concentrations above 2 M could damage nanotubular structure, leading to formation of clumps. The type of the applied acid was not significant, as treatment with nitric acid gave similar results [46]. This agreed with the findings of Turki et al., who also indicated that the use of a highly concentrated acid (above 2 M) would result in formation of clumps of irregular particles and damaged morphology. The complete removal of sodium ions by acid treatment did not significantly modify the morphology. However, some modifications can be noticed, such as fewer crystalline walls, a rough surface, larger pores, and a higher surface area [19].

Porosity also appeared to be affected by the concentration of acid. It would dramatically increase with higher concentrations up to 0.2 M. However, decreased porosity was detected with further increases, as fast elimination of electrostatic charges above 0.2 M would lead to sheets folding and transforming into granules. A decreased size of nanotubes could also be noticed. In conclusion, the products from a concentrated-HCl washing solution consist of granules rather than tubes [20].

Reducing the sodium content of TNTs by acid washing would also lead to a different response to temperature (different phase evolution), as TNTs with a lower Na content (the most effectively washed TNTs) would turn into the crystalline phase at a lower temperature. Furthermore, they would also lose their tubular structure due to sintering earlier compared to TNTs with high sodium content, confirming the theory that high sodium content provides higher thermal stability [23,55]. These findings are well correlated with those reported in the literature that the thermal stability of TNTs improves when washed under less acidic conditions [53]. Ribbens et al. reported that Na-TNTs exhibit higher thermal stability due to the stabilization effect of intercalated sodium ions, so no phase transformation can occur as a response to the extreme temperatures involved in many procedures such as calcination [30]. For example, Na-TNTs were found to preserve their tubular structure after calcination at 400 °C, but a higher temperature will lead to a partial or complete loss of structure (500 and 600 °C, respectively). In contrast to Na-TNT, H-TNTs completely lose their tubular structure at a calcination temperature starting from 500 °C. This result confirms the previous ones suggesting that better stability of nanotubes' morphology could be obtained with the presence of sodium ions, and this is only true at low temperatures; whereas, at higher temperatures, this effect was not detected [19].

There are also other differences reported in the surface properties of Na-TNTs and H-TNTs, as this is smooth in the case of Na-TNTs but obviously not in case of H-TNTs. The ion exchange during acidic post treatment leads to a smaller inter-layer distance as a result of replacing large sodium ions with small protons. It also leads to differences in the dimensions of nanotubes and the surface area [30]. Low sodium content was found to present a higher S.S.A. [23]. In the same context, Nakahira et al. reported that increasing the concentration of washing acid will increase the S.S.A. of the washed nanotubes [55]; thus, a higher specific area of the H-nanotubes means more active sites to react/bind, thus making it a more effective use in several applications [30].

It was also reported that sodium content also affects many functions of TNTs, as untreated samples (washed with water instead of acid) showed higher photocatalytic activity [41].

3.2. Thermal Treatment (Calcination)

According to the information reported in the literature, the temperature range (200–600 °C) is the range where the most important structural transformations probably happen. Annealing at high temperature (300 °C) is important to improve the crystallinity of TNTs and, thus, their performance in future applications such as photocatalysis. However, preserving the tubular structure during this treatment is highly important, as an extreme annealing temperature could lead to sintering (at 500 °C) or complete collapse of nanotubes and nanoparticles formation (at 600 °C) due to dehydration of inter-layered OH groups and reduction of the number of

hydrogen bonds. It could also cause an irregular shape (>600 °C) and a change of the anatase phase to rutile [29,56].

Similar findings were reported by Kiatkittipong et al. that calcination at moderate temperature (200 °C) is of crucial importance as it will lead to the appearance of an anatase phase and elimination of moisture that existed between titanate layers, but a high calcination temperature (500 °C) would lead to complete collapse of TNTs with elongated and irregular particles, which is confirmed by the decrease in S.S.A. and loss of pore volume [57]. This was in agreement with the study of Lee et al., who confirmed that an extremely high temperature used in calcination would negatively affect surface area and pore volume [34], and with the study of Yuan et al., who reported that nanotubes will be stable only at a calcination temperature lower than 400 °C, while they would be sintered and turned into nanorods after calcination at 540 °C [31]. Ma et al. also indicated that the tubular structure can remain intact at a calcination temperature below 450 °C, as a higher temperature would completely destroy the tubular structure [49].

Besides morphology/surface area changes, calcination would also affect the crystalline phase. It was reported that at a calcination temperature range of 200–800 °C the structure was primarily anatase, while rutile started to appear at 900 °C [58]. Another study suggested a similar discussion but at a relatively different temperature. Nanotubes mainly existed as an anatase phase below 650 °C, preserving their morphology. However, a rutile phase began to appear at a lower temperature (550 °C) compared to the previous study (900 °C). Further thermal treatment from 650 °C to 800 °C will accelerate the transformation to the rutile phase, and, therefore, the product mainly showed a rutile phase over 800 °C. However, at this high temperature, the tubes were destroyed and aggregated together to form rod-like particles [26]. In contrast, another study suggested that a temperature above 800 °C would turn nanotubes into aggregated nanoparticles but the anatase phase would be dominant [43].

In conclusion, this extreme thermal treatment would modify the characteristics of nanotubes such as morphology, surface area, and crystallinity and, consequently, the related application possibilities [29]. For this reason, the targeted application should be decided earlier to the production process so that the synthesis conditions can be adjusted to obtain the appropriate/balanced specifications for the requested application. For example, although S.S.A. is of crucial importance for photocatalytic activity, as discussed earlier, this still depends on the crystallinity of the prepared nanotubes [58]. An improvement in photocatalytic activity was observed after increasing the calcination temperature up to 400 °C, despite an approximately 30% decrease in surface area, which could be explained by the increase in the percentage amount of anatase. However, an extremely high temperature (above 500 °C) would lead to the loss of tubular structure and to a decrease in photoactivity irrespective of the improved crystallinity [57]. The factors influencing the properties of the nanotubes are summarized in Figure 3.

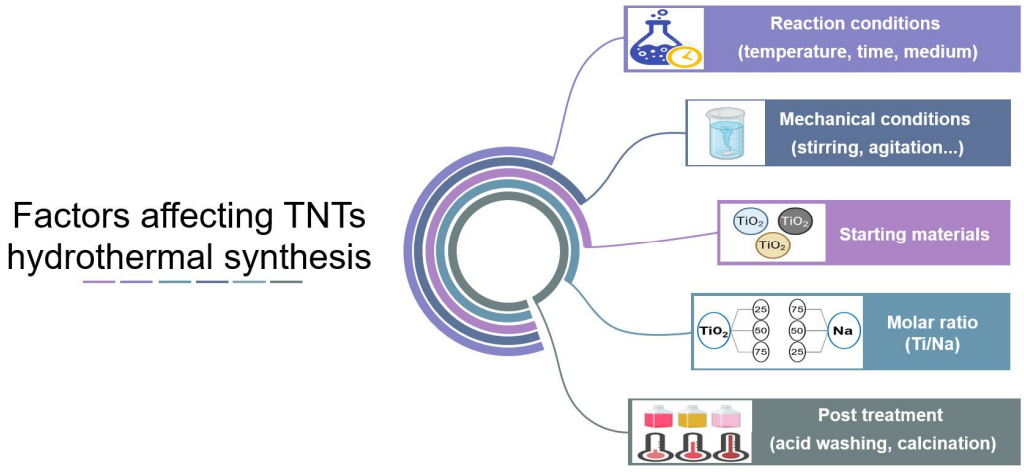

Figure 3. Factors affecting TNTs synthesis by hydrothermal treatment.

4. Stability of the Prepared Nanotubes

As TNTs have promising potential to be used in multiple applications, their fragile structure should be taken into consideration, as it could undergo numerous changes during handling/processing. For example, TNTs could be easily broken up due to mechanical forces such as stirring or ultrasonication, resulting in shorter nanotubes [10,37]. Also, extremely high-temperature treatments used in many procedures could result in changing the surface chemistry and reducing the number of OH groups on it. Later, this could negatively affect their reactivity [59], photocatalytic activity, and other possible surface modifications, as a result of decreased Brönsted/Lewis acid sites and diminished surface OH-groups, which are the main sites of reaction [30,52]. In addition to that, pH could affect the stability of TNTs as they are not stable under acidic conditions. It was reported that treatment with 0.1 mol/L H_2SO_4 for 5 days at room temperature led to a deformation of TNTs, evidenced by thinner walls and corroded surfaces. Two months later, the tubular structure had completely disappeared, while, in pure water and basic solution, minimal morphological changes were observed, indicating the stability of TNTs in these media. This was explained by favoring the layered sodium titanate phase with high pH and high sodium ion levels, which stabilize the multi-layered wall TNTs [59]. On the other hand, the explanation of TNTs transformation in acidic media includes partial dissolution of nanotubes, releasing Ti, which is then crystallized to nanoparticles. This procedure depends on the acid type and decreases in the order $H_2SO_4 > HNO_3 \approx HCl$, as a higher release of Ti during dissolution resulted in faster transformation [59].

5. Applications in the Pharmaceutical Field

As previously mentioned, TNTs present a wide range of specifications that could have great importance on their usefulness in different applications. For example, their hydrophilic properties and good wettability, due to their partially hydroxylated surface, make them suitable candidates to use in the biomedical field, such as in dental implants, orthopedics, and cardiovascular stents [14–17]. However, agglomeration could appear as a result of the presence of hydroxyl groups on their surface [2], and this should be taken into consideration during the preparation process.

TNTs also have a higher S.S.A. compared to the traditional type of TiO_2 [52]. This vast surface created by the hydrothermal alkali treatment provides higher activity compared to precursor nanoparticles and could be an advantage for various uses such as catalysis in chemical reactions [20]. It is also an available option to tailor the surface chemistry by functionalizing it with different molecules or replacing Na^+/H^+ ions on it with other ions such as Cu^{2+}/Ni^{2+} and Mg^{2+}. This would help to control/adjust TNTs properties and provide them with secondary characteristics and new behaviors other than the original ones, which could be the key to overcome some of their problems and extend their application to further disciplines [60–63].

These impressive characteristics are gradually being used in the biomedical field and even in the field of animal treatment. The highly specific area of TNTs was considered as an advantage in preparing drug delivery systems specified for animals for the first time. This was performed by physical absorption of enrofloxacin hydrochloride, and controlled drug release was successfully obtained [64]. In addition, Papa et al. reported that the tubular shape and nano-size of TNTs facilitate their cell uptake and present them as promising agents for DNA transfections in the cardiovascular field [9]. Table 1 contains more examples of the possible uses of TNTs in pharmaceutical field.

Table 1. Some of the reported biomedical/pharmaceutical application of TNTs prepared by several methods other than hydrothermal treatment.

Synthesis Method	Diameters (nm)	Loaded Agent	Application	Ref.
anodization	80	Bovine serum albumin/lysozyme	Controlled drug release in orthopedics and dental implants	[65]

Table 1. *Cont.*

Synthesis Method	Diameters (nm)	Loaded Agent	Application	Ref.
anodization	80	Gentamicin	- Local delivery of antibiotics at the site of implantation - Minimize initial bacterial adhesion - Enhance osteoblast differentiation	[66]
anodization	60	Penicillin Streptomycin Dexamethasone	Prolonged drug release up to 3 days (nanotubes were coated with drugs)	[67]
anodization	-	Violet-blue fluorescent marker	Magnetically guided nanotubes for site-specific photoinduced drug release	[68]
anodization	100–300	Albumin Sirolimus Paclitaxel	Small and large molecules for controlled delivery	[69]
Sol gel/ anodization	130	Transcriptional factors	Protein delivery	[70]
anodization	110	Coumarin6 Indomethacin	Implantable extended drug delivery for poorly water-soluble drug	[71]
anodization	-	Indomethacin Itraconazole Gentamicin sulfate	Multi-drug delivery system with immediate, delayed and sustained therapeutic action possibility in bone implant	[72]
anodization	25–100	Silver NPs	Anti-bacterial activity against *E. coli*	[73]
anodization	180	Silver NPs	Anti-bacterial activity against *E. coli* and *S. aureus*	[74]
anodization	80	Silver NPs	Anti-bacterial activity	[75]
anodization	70–90	cefuroxime	reservoir on the orthopedic implant for local delivery	[76]
anodization	-	Gentamicin coated with biopolymers (PLGA and chitosan)	- Sustained release (3–4 weeks) - excellent osteoblastic adhesion - effective antibacterial properties	[77]
anodization	70	alendronate	titanium-based implant with local anti-osteoporosis property	[78]
Sol-gel	10–38	5-Fluorouracil	anticancer sustained drug delivery system	[79]

According to the previously mentioned specifications and uses, TNTs have proven to be an efficient tool in several fields. However, no serious attempts have been made to use them as novel carriers of therapeutic molecules. Their pharmacokinetics in the human body have not yet been totally revealed, which could be one of the major reasons for not fully exploring their potentials in pharmaceutical applications. Furthermore, their safety/toxicity studies still present conflicting results. Some studies have reported their safe use without showing any toxic effects [7,10,80]. Others even displayed positive outcomes such as increased cell viability [8], enhanced proliferation, and bone cell adhesion [81], probably due to their porous structure allowing the flow of nutrients and blood [82], while other studies reported their toxic effects and classified them as more toxic than other nanomaterials such as nanorods, nanoribbons, and nanowires [83,84]. However, the potential utilization of TNTs in health-related applications is supported by the promising results obtained by numerous studies which investigated their cytotoxicity using different cell lines (intact and cancerous) with different concentrations (range from 1 µg/mL to 5 mg/mL) and different times of exposure (from short treatment of 120 min to long exposure of 7 days) [7,8,10,85]. Even surface-modified TNTs with several molecules (silane, stearate, polyethyleneimine,

acrylic acid-polyethylene glycol copolymer) have presented similar results which could promote the shifting of TNTs (bare and surface-modified) to the health domain [9,10,61].

Based on these results, researchers have started to give more attention to TNTs and to consider them as possible carriers for drugs/biological molecules. For example, Ray et al. prepared nano-conjugates using HTNTs with cytochrome C. These conjugates displayed enhanced peroxidase enzymatic activity and could be of great importance for cancer treatment in the future, as they could work as caspase activators and apoptosis initiators [86]. Moreover, TNTs have proven to be a promising tool to apply in oncology. Hydrothermally synthesized TNTs have been investigated for their possible use as radiosensitizers in radiotherapy. They appeared to increase the accumulation of cells at the G2/M checkpoint and decrease DNA repair efficiency, making cancer cells more sensitive to radiotherapy [87]. Similar findings were reported with TNTs prepared by anodization, as they were able to reduce the number of vital cancerous cells upon a low dose of UV irradiation [88]. These results were reported with bare TNTs without being loaded with any therapeutic agents; therefore, researchers expect to have a stronger effect if the combination with antitumor drugs is successfully accomplished. In this context, Wang et al. reported the possibility of using TNTs as an antitumor delivery system for doxorubicin to pancreatic cancer cells. This was achieved by loading the drug onto the surface of these nanotubes [89]. Furthermore, TNTs present a versatile method of carrying docetaxel on their surface after grafting, and they were able to deliver it locally to prostate tumors in addition to enhancing the response to irradiation by delaying tumor growth [90]. TNTs have also been investigated for their ability to graft optical imaging probes (OI) for diagnostic purposes and photodynamic therapy (PDT) [91].

TNTs were also used as carriers for other drugs such as ibuprofen and dexamethasone, and it was found that the release rate of these drugs could be regulated through modifying surface chemistry, with molecules having different properties such as a different polarity [92,93]. Modifying surface chemistry could also play a significant role improving drug loading with several drugs (curcumin, methotrexate, silibinin, ibuprofen), decreasing toxicity and achieving sustained release [94,95].

However, until now, few attempts have been made to incorporate those newly synthesized materials into API-composites and then into final dosage forms. For example, Sipos et al. investigated the impact of TNTs' incorporation with different drugs, diltiazem hydrochloride, diclofenac sodium, atenolol, and hydrochlorothiazide, indicating that TNTs–drug composites appeared to have superior processability compared to pure active pharmaceutical ingredients (APIs), such as better flowability, compactibility, compressibility, and even post-compressional properties of the composite-containing tablets (greater hardness and tensile strength). In the same context, it is of crucial importance to mention that these advantages are closely related to the success of the incorporation process and the type of the created interaction between both entities, which strongly depends on the drug characteristics [6,96,97]. Accordingly, TNTs could be implemented to modify drug release from their composites based on the strength of the created drug–TNTs association [97,98].

It is also worth mentioning that successful incorporation could be a useful tool to shorten preformulation studies regarding the tableting process, as the unique properties of those novel carriers will be predominant, so the composites will behave similarly regardless of the used APIs [6].

6. Future Perspectives, Concerns, and Challenges

Hydrothermal synthesis may be the best choice to produce TNTs for pharmaceutical applications due to its numerous advantages over other techniques, mainly the long circulation half-life due to their small diameters being undetected by RES [2]. However, this intended shifting is not an easy mission to accomplish due to several problems TNTs are facing. For example, their hydrophilic nature is supposed to reduce their accumulation in tissues, but it is also expected to hinder their absorption through the gastrointestinal tract (GIT) [61]. Moreover, their tubular morphology is considered as an advantage boosting their

cell internalization [2], but this could also increase their cytotoxicity [83]. Based on this, their properties should be carefully balanced to utilize their benefits and avoid their drawbacks. In this context, functionalization appeared as a golden choice to adapt TNTs characteristics and shape their features to suit the intended application. Ranjous et al. have modified the surface of TNTs with hydrophobic moieties (trichloro(octyl) silane and magnesium stearate) to enhance their GIT absorption after oral administration [61]. Saker et al. have also highlighted the importance of surface modification by fixing a carboxylic arm on the surface of TNTs to serve as a connecting bridge for several molecules. This approach could be useful for optimizing the surface properties to achieve multiple targets, such as reducing toxicity, enhancing water dispersibility, etc., or for loading therapeutic/diagnostic agents (APIs, biomarkers, probes) [10]. However, even though several studies have reported the safety of TNTs and their modified versions [7–10,61,85], a deeper toxicity assessment should be initiated at diverse levels (cytotoxicity, genotoxicity, carcinogenicity, etc.) to assure a smooth transformation of titanate nanotubes into therapeutic practice, and to provide a guarantee for patients/markets that these nanocarriers are as safe as possible.

In a nutshell, we believe that the optimization of hydrothermal synthesis of TNTs and their surface modification present a wide window for future research to improve their properties and avoid their obstacles (enhancing pharmacokinetics and assuring safety). This would promote their pioneering application as a drug carrier and write a new chapter in the field of nano-based drug delivery systems.

7. Conclusions

TNTs are emerging as an attractive candidate to apply in health-related applications after proving their impressive performance in numerous disciplines. Therefore, this review attempts to highlight the importance of establishing a reproducible method for the preparation of TNTs with predesigned specifications that could fit the strict pharmaceutical requirements. This cannot be achieved without a comprehensive understanding of the factors affecting their preparation and the impact of its variation on the resulting nanotubes.

During hydrothermal treatment, several factors could be responsible for the final result. Temperature is one of the most important factors among them, as it is involved in the preparation and post-preparation treatment to provide sufficient thermal energy for rolling up and controlling the crystalline structure, respectively. This would not be possible without the use of a highly concentrated alkaline medium in addition to a sufficient time for the reaction to be completed. It is also worth mentioning that the properties/quantities of the starting materials also have a huge impact on the reaction pathway and its final product. Washing with acid as a post treatment step also has significant importance, but its role is still generating arguments and is considered as a point of disagreement. Based on the available data, the determination of the impact of preparation conditions on the resulting nanotubes is still considered to be challenging. This is crucially important as these operational conditions closely affect the properties of the produced nanotubes and therefore their subsequent applications.

Once the exact mechanism of TNTs production and the effect of the preparation parameters on their formation are clearly understood, a reproducible fabrication procedure could be generated and scaled up to create controlled features of TNTs that could fit their intended future implementation in therapeutic systems as drug carriers.

Author Contributions: Conceptualization, R.S., T.S. and G.R.J.; methodology, R.S., H.S. and T.S.; formal analysis, R.S. and H.S.; investigation, R.S. and H.S.; writing—original draft preparation, R.S.; writing—review and editing, T.S. and G.R.J.; supervision, T.S. and G.R.J.; project administration, T.S.; funding acquisition, T.S. All authors have read and agreed to the published version of the manuscript.

Funding: Project no. TKP2021-EGA-32 has been implemented with the support provided by the Ministry of Culture and Innovation of Hungary from the National Research, Development and Innovation Fund, financed under the TKP2021-EGA funding scheme.

Institutional Review Board Statement: Not applicable.

Informed Consent Statement: Not applicable.

Data Availability Statement: The data used in the current review are available in public databases.

Conflicts of Interest: The authors declare no conflicts of interest.

References

1. Hoyer, P. Semiconductor nanotube formation by a two-step template process. *Adv. Mater.* **1996**, *8*, 857–859. [CrossRef]
2. Boudon, J.; Papa, A.-L.; Paris, J.; Millot, N. Titanate nanotubes as a versatile platform for nanomedicine. In *Nanomedicine*; One Central Press (OCP): Sydney, Australia, 2014; pp. 403–428.
3. Ranjous, Y.; Regdon, G., Jr.; Pintye-Hodi, K.; Sovany, T. Standpoint on the priority of TNTs and CNTs as targeted drug delivery systems. *Drug Discov. Today* **2019**, *24*, 1704–1709. [CrossRef] [PubMed]
4. Kasuga, T.; Hiramatsu, M.; Hoson, A.; Sekino, T.; Niihara, K. Formation of titanium oxide nanotube. *Langmuir* **1998**, *14*, 3160–3163. [CrossRef]
5. Batool, S.A.; Maqbool, M.S.S.; Javed, M.A.; Niaz, A.; Rehman, M.A.U. A Review on the Fabrication and Characterization of Titania Nanotubes Obtained via Electrochemical Anodization. *Surfaces* **2022**, *5*, 456–480. [CrossRef]
6. Sipos, B.; Pintye-Hodi, K.; Regdon, G., Jr.; Konya, Z.; Viana, M.; Sovany, T. Investigation of the Compressibility and Compactibility of Titanate Nanotube-API Composites. *Materials* **2018**, *11*, 2582. [CrossRef]
7. Fenyvesi, F.; Konya, Z.; Razga, Z.; Vecsernyes, M.; Kasa, P., Jr.; Pintye-Hodi, K.; Bacskay, I. Investigation of the cytotoxic effects of titanate nanotubes on Caco-2 cells. *AAPS PharmSciTech* **2014**, *15*, 858–861. [CrossRef]
8. Wadhwa, S.; Rea, C.; O'Hare, P.; Mathur, A.; Roy, S.S.; Dunlop, P.S.; Byrne, J.A.; Burke, G.; Meenan, B.; McLaughlin, J.A. Comparative in vitro cytotoxicity study of carbon nanotubes and titania nanostructures on human lung epithelial cells. *J. Hazard. Mater.* **2011**, *191*, 56–61. [CrossRef] [PubMed]
9. Papa, A.L.; Dumont, L.; Vandroux, D.; Millot, N. Titanate nanotubes: Towards a novel and safer nanovector for cardiomyocytes. *Nanotoxicology* **2013**, *7*, 1131–1142. [CrossRef]
10. Saker, R.; Jojárt-Laczkovich, O.; Regdon, G.J.r.; Takács, T.; Szenti, I.; Bózsity-Faragó, N.; Zupkó, I.; Sovány, T. Surface Modification of Titanate Nanotubes with a Carboxylic Arm for Further Functionalization Intended to Pharmaceutical Applications. *Pharmaceutics* **2023**, *15*, 2780. [CrossRef] [PubMed]
11. Adeleye, A.T.; John, K.I.; Adeleye, P.G.; Akande, A.A.; Banjoko, O.O. One-dimensional titanate nanotube materials: Heterogeneous solid catalysts for sustainable synthesis of biofuel precursors/value-added chemicals-a review. *J. Mater. Sci.* **2021**, *56*, 18391–18416. [CrossRef]
12. Hossen, M.A.; Solayman, H.; Leong, K.H.; Sim, L.C.; Yaacof, N.; Abd Aziz, A.; Lihua, W.; Monir, M.U. A comprehensive review on advances in TiO_2 nanotube (TNT)-based photocatalytic CO2 reduction to value-added products. *Energies* **2022**, *15*, 8751. [CrossRef]
13. Zakir, O.; Ait-Karra, A.; Idouhli, R.; Khadiri, M.; Dikici, B.; Aityoub, A.; Abouelfida, A.; Outzourhit, A. A review on TiO_2 nanotubes: Synthesis strategies, modifications, and applications. *J. Solid State Electrochem.* **2023**, *27*, 2289–2307. [CrossRef]
14. Wang, F.; Shi, L.; He, W.X.; Han, D.; Yan, Y.; Niu, Z.Y.; Shi, S.G. Bioinspired micro/nano fabrication on dental implant-bone interface. *Appl. Surf. Sci.* **2013**, *265*, 480–488. [CrossRef]
15. Yao, C.; Webster, T.J. Prolonged antibiotic delivery from anodized nanotubular titanium using a co-precipitation drug loading method. *J. Biomed. Mater. Res. B Appl. Biomater.* **2009**, *91*, 587–595. [CrossRef]
16. Junkar, I.; Kulkarni, M.; Bencina, M.; Kovac, J.; Mrak-Poljsak, K.; Lakota, K.; Sodin-Semrl, S.; Mozetic, M.; Iglic, A. Titanium Dioxide Nanotube Arrays for Cardiovascular Stent Applications. *ACS Omega* **2020**, *5*, 7280–7289. [CrossRef]
17. Zhang, Y.; Gulati, K.; Li, Z.; Di, P.; Liu, Y. Dental Implant Nano-Engineering: Advances, Limitations and Future Directions. *Nanomaterials* **2021**, *11*, 2489. [CrossRef]
18. Abdullah, M.; Kamarudin, S.K. Titanium dioxide nanotubes (TNT) in energy and environmental applications: An overview. *Renew. Sustain. Energy Rev.* **2017**, *76*, 212–225. [CrossRef]
19. Turki, A.; Kochkar, H.; Guillard, C.; Berhault, G.; Ghorbel, A. Effect of Na content and thermal treatment of titanate nanotubes on the photocatalytic degradation of formic acid. *Appl. Catal. B Environ.* **2013**, *138*, 401–415. [CrossRef]
20. Tsai, C.C.; Teng, H.S. Regulation of the physical characteristics of Titania nanotube aggregates synthesized from hydrothermal treatment. *Chem. Mater.* **2004**, *16*, 4352–4358. [CrossRef]
21. Vu, T.H.T.; Au, H.T.; Tran, L.T.; Nguyen, T.M.T.; Tran, T.T.T.; Pham, M.T.; Do, M.H.; Nguyen, D.L. Synthesis of titanium dioxide nanotubes via one-step dynamic hydrothermal process. *J. Mater. Sci.* **2014**, *49*, 5617–5625. [CrossRef]
22. Yang, J.; Jin, Z.; Wang, X.; Li, W.; Zhang, J.; Zhang, S.; Guo, X.; Zhang, Z. Study on composition, structure and formation process of nanotube $Na_2Ti_2O_4(OH)_2$. *Dalton Trans.* **2003**, *20*, 3898–3901. [CrossRef]
23. Morgado, E.; de Abreu, M.A.S.; Pravia, O.R.C.; Marinkovic, B.A.; Jardim, P.M.; Rizzo, F.C.; Araújo, A.S. A study on the structure and thermal stability of titanate nanotubes as a function of sodium content. *Solid State Sci.* **2006**, *8*, 888–900. [CrossRef]
24. Arruda, L.B.; Santos, C.M.; Orlandi, M.O.; Schreiner, W.H.; Lisboa, P.N. Formation and evolution of TiO_2 nanotubes in alkaline synthesis. *Ceram. Int.* **2015**, *41*, 2884–2891. [CrossRef]
25. Nada, A.; Moustafa, Y.; Hamdy, A. Improvement of titanium dioxide nanotubes through study washing effect on hydrothermal. *Br. J. Environ. Sci.* **2014**, *2*, 29–40. [CrossRef]

26. Li, W.J.; Fu, T.; Xie, F.; Yu, S.F.; He, S.L. The multi-staged formation process of titanium oxide nanotubes and its thermal stability. *Mater. Lett.* **2007**, *61*, 730–735. [CrossRef]
27. Viet, P.V.; Phan, B.T.; Van Hieu, L.; Thi, C.M. The Effect of Acid Treatment and Reactive Temperature on the Formation of TiO_2 Nanotubes. *J. Nanosci. Nanotechnol.* **2015**, *15*, 5202–5206. [CrossRef] [PubMed]
28. Vuong, D.; Tram, D.; Pho, P.; Chien, N. Hydrothermal synthesis and photocatalytic properties of TiO_2 nanotubes. In *Physics and Engineering of New Materials*; Springer Proceedings in Physics (SPPHY, volume 127); Springer: Berlin/Heidelberg, Germany, 2009; pp. 95–101. [CrossRef]
29. Sreekantan, S.; Wei, L.C. Study on the formation and photocatalytic activity of titanate nanotubes synthesized via hydrothermal method. *J. Alloys Compd.* **2010**, *490*, 436–442. [CrossRef]
30. Ribbens, S.; Meynen, V.; Van Tendeloo, G.; Ke, X.; Mertens, M.; Maes, B.U.W.; Cool, P.; Vansant, E.F. Development of photocatalytic efficient Ti-based nanotubes and nanoribbons by conventional and microwave assisted synthesis strategies. *Microporous Mesoporous Mater.* **2008**, *114*, 401–409. [CrossRef]
31. Yuan, Z.Y.; Su, B.L. Titanium oxide nanotubes, nanofibers and nanowires. *Colloid Surf. A* **2004**, *241*, 173–183. [CrossRef]
32. Lan, Y.; Gao, X.P.; Zhu, H.Y.; Zheng, Z.F.; Yan, T.Y.; Wu, F.; Ringer, S.P.; Song, D.Y. Titanate nanotubes and nanorods prepared from rutile powder. *Adv. Funct. Mater.* **2005**, *15*, 1310–1318. [CrossRef]
33. Lee, D.S.; Lee, S.Y.; Rhee, K.Y.; Park, S.J. Effect of hydrothermal temperature on photocatalytic properties of TiO_2 nanotubes. *Curr. Appl. Phys.* **2014**, *14*, 415–420. [CrossRef]
34. Lee, C.K.; Lyu, M.D.; Liu, S.S.; Chen, H.C. The synthetic parameters for the preparation of nanotubular titanate with highly photocatalytic activity. *J. Taiwan Inst. Chem. Eng.* **2009**, *40*, 463–470. [CrossRef]
35. Morgan, D.L.; Zhu, H.Y.; Frost, R.L.; Waclawik, E.R. Determination of a morphological phase diagram of titania/titanate nanostructures from alkaline hydrothermal treatment of Degussa P25. *Chem. Mater.* **2008**, *20*, 3800–3802. [CrossRef]
36. Ma, R.; Fukuda, K.; Sasaki, T.; Osada, M.; Bando, Y. Structural features of titanate nanotubes/nanobelts revealed by Raman, X-ray absorption fine structure and electron diffraction characterizations. *J. Phys. Chem. B* **2005**, *109*, 6210–6214. [CrossRef] [PubMed]
37. Bavykin, D.V.; Parmon, V.N.; Lapkin, A.A.; Walsh, F.C. The effect of hydrothermal conditions on the mesoporous structure of TiO_2 nanotubes. *J. Mater. Chem.* **2004**, *14*, 3370–3377. [CrossRef]
38. Seo, D.S.; Lee, J.K.; Kim, H. Preparation of nanotube-shaped TiO_2 powder. *J. Cryst. Growth* **2001**, *229*, 428–432. [CrossRef]
39. Cho, S.H.; Nguyen, H.H.; Gyawali, G.; Son, J.E.; Sekino, T.; Joshi, B.; Kim, S.H.; Jo, Y.H.; Kim, T.H.; Lee, S.W. Effect of microwave-assisted hydrothermal process parameters on formation of different TiO_2 nanostructures. *Catal. Today* **2016**, *266*, 46–52. [CrossRef]
40. Guo, Y.; Lee, N.H.; Oh, H.J.; Yoon, C.R.; Park, K.S.; Lee, H.G.; Lee, K.S.; Kim, S.J. Structure-tunable synthesis of titanate nanotube thin films via a simple hydrothermal process. *Nanotechnology* **2007**, *18*, 295608. [CrossRef]
41. Nakahira, A.; Kato, W.; Tamai, M.; Isshiki, T.; Nishio, K.; Aritani, H. Synthesis of nanotube from a layered $H_2Ti_4O_9{\cdot}H_2O$ in a hydrothermal treatment using various titania sources. *J. Mater. Sci.* **2004**, *39*, 4239–4245. [CrossRef]
42. Elsanousi, A.; Elssfah, E.M.; Zhang, J.; Lin, J.; Song, H.S.; Tang, C.C. Hydrothermal treatment duration effect on the transformation of titanate nanotubes into nanoribbons. *J. Phys. Chem. C* **2007**, *111*, 14353–14357. [CrossRef]
43. Weng, L.Q.; Song, S.H.; Hodgson, S.; Baker, A.; Yu, J. Synthesis and characterisation of nanotubular titanates and titania. *J. Eur. Ceram. Soc.* **2006**, *26*, 1405–1409. [CrossRef]
44. Ranjitha, A.; Muthukumarasamy, N.; Thambidurai, M.; Velauthapillai, D.; Agilan, S.; Balasundaraprabhu, R. Effect of reaction time on the formation of TiO_2 nanotubes prepared by hydrothermal method. *Optik* **2015**, *126*, 2491–2494. [CrossRef]
45. Qamar, M.; Zaidi, S.A.; Rafatullah, M.; Qutob, M.; Kim, S.J.; Drmosh, Q.A. Role of Post-Hydrothermal Treatment on the Microstructures and Photocatalytic Activity of TiO_2-Based Nanotubes. *Catalysts* **2022**, *12*, 702. [CrossRef]
46. Poudel, B.; Wang, W.Z.; Dames, C.; Huang, J.Y.; Kunwar, S.; Wang, D.Z.; Banerjee, D.; Chen, G.; Ren, Z.F. Formation of crystallized titania nanotubes and their transformation into nanowires. *Nanotechnology* **2005**, *16*, 1935–1940. [CrossRef]
47. Tsai, C.C.; Teng, H.S. Structural features of nanotubes synthesized from NaOH treatment on TiO_2 with different post-treatments. *Chem. Mater.* **2006**, *18*, 367–373. [CrossRef]
48. Safaei, M.; Sarraf-Mamoory, R.; Rashidzadeh, M. The interactive effect of agitation condition and titania particle size in hydrothermal synthesis of titanate nanostructures. *J. Nanoparticle Res.* **2010**, *12*, 2723–2728. [CrossRef]
49. Ma, Y.T.; Lin, Y.; Xiao, X.R.; Zhou, X.W.; Li, X.P. Sonication-hydrothermal combination technique for the synthesis of titanate nanotubes from commercially available precursors. *Mater. Res. Bull.* **2006**, *41*, 237–243. [CrossRef]
50. Preda, S.; Teodorescu, V.S.; Musuc, A.M.; Andronescu, C.; Zaharescu, M. Influence of the TiO_2 precursors on the thermal and structural stability of titanate-based nanotubes. *J. Mater. Res.* **2013**, *28*, 294–303. [CrossRef]
51. Saponjic, Z.V.; Dimitrijevic, N.M.; Tiede, D.M.; Goshe, A.J.; Zuo, X.; Chen, L.X.; Barnard, A.S.; Zapol, P.; Curtiss, L.; Rajh, T. Shaping Nanometer-Scale Architecture Through Surface Chemistry. *Adv. Mater.* **2005**, *17*, 965–971. [CrossRef]
52. Camposeco, R.; Castillo, S.; Mejia-Centeno, I.; Navarrete, J.; Gomez, R. Effect of the Ti/Na molar ratio on the acidity and the structure of TiO_2 nanostructures: Nanotubes, nanofibers and nanowires. *Mater. Charact.* **2014**, *90*, 113–120. [CrossRef]
53. Nguyen, N.H.; Bai, H. Effect of washing pH on the properties of titanate nanotubes and its activity for photocatalytic oxidation of NO and NO_2. *Appl. Surf. Sci.* **2015**, *355*, 672–680. [CrossRef]
54. Lee, C.-K.; Wang, C.-C.; Juang, L.-C.; Lyu, M.-D.; Hung, S.-H.; Liu, S.-S. Effects of sodium content on the microstructures and basic dye cation exchange of titanate nanotubes. *Colloids Surf. A Physicochem. Eng. Asp.* **2008**, *317*, 164–173. [CrossRef]

55. Nakahira, A.; Kubo, T.; Numako, C. TiO_2-derived titanate nanotubes by hydrothermal process with acid treatments and their microstructural evaluation. *ACS Appl. Mater. Interfaces* **2010**, *2*, 2611–2616. [CrossRef] [PubMed]
56. Lopez Zavala, M.A.; Lozano Morales, S.A.; Avila-Santos, M. Synthesis of stable TiO_2 nanotubes: Effect of hydrothermal treatment, acid washing and annealing temperature. *Heliyon* **2017**, *3*, e00456. [CrossRef]
57. Kiatkittipong, K.; Scott, J.; Amal, R. Hydrothermally synthesized titanate nanostructures: Impact of heat treatment on particle characteristics and photocatalytic properties. *ACS Appl. Mater. Interfaces* **2011**, *3*, 3988–3996. [CrossRef]
58. Aphairaj, D.; Wirunmongkol, T.; Niyomwas, S.; Pavasupree, S.; Limsuwan, P. Synthesis of anatase TiO2 nanotubes derived from a natural leucoxene mineral by the hydrothermal method. *Ceram. Int.* **2014**, *40*, 9241–9247. [CrossRef]
59. Bavykin, D.V.; Friedrich, J.M.; Lapkin, A.A.; Walsh, F.C. Stability of aqueous suspensions of titanate nanotubes. *Chem. Mater.* **2006**, *18*, 1124–1129. [CrossRef]
60. Nian, J.N.; Chen, S.A.; Tsai, C.C.; Teng, H. Structural feature and catalytic performance of Cu species distributed over TiO_2 nanotubes. *J. Phys. Chem. B* **2006**, *110*, 25817–25824. [CrossRef]
61. Ranjous, Y.; Kósa, D.; Ujhelyi, Z.; Regdon, G.; Nagy, K.A.; Szenti, I.; Kónya, Z.; Bácskay, I.; Sovány, T. Evaluation of the permeability and in vitro cytotoxicity of functionalized titanate nanotubes on Caco-2 cell line. *Acta Pharm. Hung.* **2021**, *91*, 31–39. [CrossRef]
62. Peng, S.Q.; Zeng, X.P.; Li, Y.X. Titanate nanotube modified with different nickel precursors for enhanced Eosin Y-sensitized photocatalytic hydrogen evolution. *Int. J. Hydrogen Energy* **2015**, *40*, 6038–6049. [CrossRef]
63. Vasilev, K.; Poh, Z.; Kant, K.; Chan, J.; Michelmore, A.; Losic, D. Tailoring the surface functionalities of titania nanotube arrays. *Biomaterials* **2010**, *31*, 532–540. [CrossRef]
64. Lai, S.; Zhang, W.; Liu, F.; Wu, C.; Zeng, D.; Sun, Y.; Xu, Y.; Fang, Y.; Zhou, W. TiO_2 nanotubes as animal drug delivery system and in vitro controlled release. *J. Nanosci. Nanotechnol.* **2013**, *13*, 91–97. [CrossRef]
65. Popat, K.C.; Eltgroth, M.; LaTempa, T.J.; Grimes, C.A.; Desai, T.A. Titania nanotubes: A novel platform for drug-eluting coatings for medical implants? *Small* **2007**, *3*, 1878–1881. [CrossRef] [PubMed]
66. Popat, K.C.; Eltgroth, M.; Latempa, T.J.; Grimes, C.A.; Desai, T.A. Decreased Staphylococcus epidermis adhesion and increased osteoblast functionality on antibiotic-loaded titania nanotubes. *Biomaterials* **2007**, *28*, 4880–4888. [CrossRef]
67. Aninwene, G.E.; Yao, C.; Webster, T.J. Enhanced osteoblast adhesion to drug-coated anodized nanotubular titanium surfaces. *Int. J. Nanomed.* **2008**, *3*, 257–264. [CrossRef]
68. Shrestha, N.K.; Macak, J.M.; Schmidt-Stein, F.; Hahn, R.; Mierke, C.T.; Fabry, B.; Schmuki, P. Magnetically guided titania nanotubes for site-selective photocatalysis and drug release. *Angew. Chem. Int. Ed. Engl.* **2009**, *48*, 969–972. [CrossRef] [PubMed]
69. Peng, L.; Mendelsohn, A.D.; LaTempa, T.J.; Yoriya, S.; Grimes, C.A.; Desai, T.A. Long-term small molecule and protein elution from TiO_2 nanotubes. *Nano Lett.* **2009**, *9*, 1932–1936. [CrossRef] [PubMed]
70. Cho, S.J.; Kim, H.J.; Lee, J.H.; Choi, H.W.; Kim, H.G.; Chung, H.M.; Do, J.T. Silica coated titania nanotubes for drug delivery system. *Mater. Lett.* **2010**, *64*, 1664–1667. [CrossRef]
71. Aw, M.S.; Simovic, S.; Addai-Mensah, J.; Losic, D. Polymeric micelles in porous and nanotubular implants as a new system for extended delivery of poorly soluble drugs. *J. Mater. Chem.* **2011**, *21*, 7082–7089. [CrossRef]
72. Aw, M.S.; Addai-Mensah, J.; Losic, D. A multi-drug delivery system with sequential release using titania nanotube arrays. *Chem. Commun.* **2012**, *48*, 3348–3350. [CrossRef]
73. Li, H.R.; Cui, Q.; Feng, B.; Wang, J.X.; Lu, X.; Weng, J. Antibacterial activity of TiO_2 nanotubes: Influence of crystal phase, morphology and Ag deposition. *Appl. Surf. Sci.* **2013**, *284*, 179–183. [CrossRef]
74. Guo, Z.J.; Chen, C.; Gao, Q.; Li, Y.B.; Zhang, L. Fabrication of silver-incorporated TiO_2 nanotubes and evaluation on its antibacterial activity. *Mater. Lett.* **2014**, *137*, 464–467. [CrossRef]
75. Mei, S.; Wang, H.; Wang, W.; Tong, L.; Pan, H.; Ruan, C.; Ma, Q.; Liu, M.; Yang, H.; Zhang, L.; et al. Antibacterial effects and biocompatibility of titanium surfaces with graded silver incorporation in titania nanotubes. *Biomaterials* **2014**, *35*, 4255–4265. [CrossRef] [PubMed]
76. Chennell, P.; Feschet-Chassot, E.; Devers, T.; Awitor, K.O.; Descamps, S.; Sautou, V. In vitro evaluation of TiO_2 nanotubes as cefuroxime carriers on orthopaedic implants for the prevention of periprosthetic joint infections. *Int. J. Pharm.* **2013**, *455*, 298–305. [CrossRef] [PubMed]
77. Kumeria, T.; Mon, H.; Aw, M.S.; Gulati, K.; Santos, A.; Griesser, H.J.; Losic, D. Advanced biopolymer-coated drug-releasing titania nanotubes (TNTs) implats with simultaneously enhanced osteoblast adhesion and antibacterial properties. *Colloids Surf. B Biointerfaces* **2015**, *130*, 255–263. [CrossRef] [PubMed]
78. Shen, X.; Ma, P.; Hu, Y.; Xu, G.; Xu, K.; Chen, W.; Ran, Q.; Dai, L.; Yu, Y.; Mu, C. Alendronate-loaded hydroxyapatite-TiO_2 nanotubes for improved bone formation in osteoporotic rabbits. *J. Mater. Chem. B* **2016**, *4*, 1423–1436. [CrossRef] [PubMed]
79. Faria, H.A.; de Queiroz, A.A. A novel drug delivery of 5-fluorouracil device based on TiO_2/ZnS nanotubes. *Mater. Sci. Eng. C Mater. Biol. Appl.* **2015**, *56*, 260–268. [CrossRef] [PubMed]
80. Feschet-Chassot, E.; Raspal, V.; Sibaud, Y.; Awitor, O.K.; Bonnemoy, F.; Bonnet, J.L.; Bohatier, J. Tunable functionality and toxicity studies of titanium dioxide nanotube layers. *Thin Solid Film.* **2011**, *519*, 2564–2568. [CrossRef]
81. Popat, K.C.; Leoni, L.; Grimes, C.A.; Desai, T.A. Influence of engineered titania nanotubular surfaces on bone cells. *Biomaterials* **2007**, *28*, 3188–3197. [CrossRef]
82. Bjursten, L.M.; Rasmusson, L.; Oh, S.; Smith, G.C.; Brammer, K.S.; Jin, S. Titanium dioxide nanotubes enhance bone bonding in vivo. *J. Biomed. Mater. Res. A* **2010**, *92*, 1218–1224. [CrossRef]

83. Kamal, N.; Zaki, A.H.; El-Shahawy, A.A.; Sayed, O.M.; El-Dek, S.I. Changing the morphology of one-dimensional titanate nanostructures affects its tissue distribution and toxicity. *Toxicol. Ind. Health* **2020**, *36*, 272–286. [CrossRef]
84. Magrez, A.; Horvath, L.; Smajda, R.; Salicio, V.; Pasquier, N.; Forro, L.; Schwaller, B. Cellular toxicity of TiO_2-based nanofilaments. *ACS Nano* **2009**, *3*, 2274–2280. [CrossRef]
85. Papa, A.-L.; Maurizi, L.; Vandroux, D.; Walker, P.; Millot, N. Synthesis of titanate nanotubes directly coated with USPIO in hydrothermal conditions: A new detectable nanocarrier. *J. Phys. Chem. C* **2011**, *115*, 19012–19017. [CrossRef]
86. Ray, M.; Chatterjee, S.; Das, T.; Bhattacharyya, S.; Ayyub, P.; Mazumdar, S. Conjugation of cytochrome c with hydrogen titanate nanotubes: Novel conformational state with implications for apoptosis. *Nanotechnology* **2011**, *22*, 415705. [CrossRef]
87. Mirjolet, C.; Papa, A.; Créhange, G.; Raguin, O.; Seignez, C.; Paul, C.; Truc, G.; Maingon, P.; Millot, N. The radiosensitization effect of titanate nanotubes as a new tool in radiation therapy for glioblastoma: A proof-of-concept. *Radiother. Oncol.* **2013**, *108*, 136–142. [CrossRef] [PubMed]
88. Kalbacova, M.; Macak, J.; Schmidt-Stein, F.; Mierke, C.; Schmuki, P. TiO_2 nanotubes: Photocatalyst for cancer cell killing. *Phys. Status Solidi–Rapid Res. Lett.* **2008**, *2*, 194–196. [CrossRef]
89. Wang, Y.; Yuan, L.; Yao, C.; Fang, J.; Wu, M. Cytotoxicity Evaluation of pH-Controlled Antitumor Drug Release System of Titanium Dioxide Nanotubes. *J. Nanosci. Nanotechnol.* **2015**, *15*, 4143–4148. [CrossRef]
90. Loiseau, A.; Boudon, J.; Oudot, A.; Moreau, M.; Boidot, R.; Chassagnon, R.; Said, N.M.; Roux, S.; Mirjolet, C.; Millot, N. Titanate Nanotubes Engineered with Gold Nanoparticles and Docetaxel to Enhance Radiotherapy on Xenografted Prostate Tumors. *Cancers* **2019**, *11*, 1962. [CrossRef]
91. Paris, J.; Bernhard, Y.; Boudon, J.; Heintz, O.; Millot, N.; Decréau, R.A. Phthalocyanine–titanate nanotubes: A promising nanocarrier detectable by optical imaging in the so-called imaging window. *RSC Adv.* **2015**, *5*, 6315–6322. [CrossRef]
92. Mandal, S.S.; Jose, D.; Bhattacharyya, A.J. Role of surface chemistry in modulating drug release kinetics in titania nanotubes. *Mater. Chem. Phys.* **2014**, *147*, 247–253. [CrossRef]
93. Khoshnood, N.; Zamanian, A.; Massoudi, A. Mussel-inspired surface modification of titania nanotubes as a novel drug delivery system. *Mater. Sci. Eng. C Mater. Biol. Appl.* **2017**, *77*, 748–754. [CrossRef]
94. Torres, C.C.; Campos, C.H.; Diaz, C.; Jimenez, V.A.; Vidal, F.; Guzman, L.; Alderete, J.B. PAMAM-grafted TiO_2 nanotubes as novel versatile materials for drug delivery applications. *Mater. Sci. Eng. C Mater. Biol. Appl.* **2016**, *65*, 164–171. [CrossRef] [PubMed]
95. Wang, Z.; Xie, C.L.; Luo, F.; Li, P.; Xiao, X.F. P25 nanoparticles decorated on titania nanotubes arrays as effective drug delivery system for ibuprofen. *Appl. Surf. Sci.* **2015**, *324*, 621–626. [CrossRef]
96. Sipos, B.; Regdon, G.; Konya, Z.; Pintye-Hodi, K.; Sovany, T. Comparative study on the rheological properties and tablettability of various APIs and their composites with titanate nanotubes. *Powder Technol.* **2017**, *321*, 419–427. [CrossRef]
97. Sipos, B.; Pintye-Hodi, K.; Konya, Z.; Kelemen, A.; Regdon, G., Jr.; Sovany, T. Physicochemical characterisation and investigation of the bonding mechanisms of API-titanate nanotube composites as new drug carrier systems. *Int. J. Pharm.* **2017**, *518*, 119–129. [CrossRef]
98. Ranjous, Y.; Regdon, G., Jr.; Pintye-Hodi, K.; Varga, T.; Szenti, I.; Konya, Z.; Sovany, T. Optimization of the Production Process and Product Quality of Titanate Nanotube-Drug Composites. *Nanomaterials* **2019**, *9*, 1406. [CrossRef]

Journal of Drug Delivery Science and Technology 99 (2024) 105979

Contents lists available at ScienceDirect

Journal of Drug Delivery Science and Technology

journal homepage: www.elsevier.com/locate/jddst

Review article

Pharmacokinetics and toxicity of inorganic nanoparticles and the physicochemical properties/factors affecting them

Ranim Saker, Géza Regdon jr., Tamás Sovány *

University of Szeged, Institute of Pharmaceutical Technology and Regulatory Affairs, Eötvös U 6., H-6720, Szeged, Hungary

ARTICLE INFO

Keywords:
Inorganic nanoparticles
Pharmacokinetics
Physicochemical properties
Toxicity

ABSTRACT

Nowadays, inorganic nanoparticles have been widely incorporated into broad disciplines such as medicinal, chemical, and electronical ones. Their special characteristics and distinct design provide tremendous potential to be employed in several applications. This emerging popularity makes these modern nanomaterials extensively existing around us, almost impossible to avoid. A question regarding their safety/toxicity assessment has been arisen due to their widespread use and increasing exposure. To clarify this uncertainty, this review summarizes the current knowledge and the recent findings regarding toxicity effects of inorganic nanoparticles that are most discussed in literature and appeared to be common to all of them, and investigates the important mechanisms behind their toxicity which are not totally revealed yet. It also highlights the main factors/parameters affecting toxicity which are strongly based on their physicochemical properties and declares the necessity for unified methods and further exploration in the future to build safer nano-based drug delivery systems. Additionally, this review will present an overview of pharmacokinetics of inorganic nanoparticles which have a huge impact on their toxicity therefore should be investigated in more detail. This investigation will help to provide a comprehensive profile and will contribute to optimizing NPs design ensuring safety and presenting minimal toxicity.

1. Introduction

Since the introduction of "nanotechnology" concept for the first time in 1959 by the American Nobel Prize laureate Richard Feynman, this field of research has gradually attracted attention of many researchers from different fields of science, and now it is one of the fastest growing domain in modern life [1]. Nanomaterials are defined by the European Union (EU) as "manufactured material containing particles, in an unbound state or as an aggregate or as an agglomerate and where, for 50 % or more of the particles in the number size distribution, one or more external dimensions in the size range of 1 nm–100 nm" [2]. These nanoparticles (NPs) could be classified according to several criteria among them chemical structure is one of the most used one. According to it, they could be divided into two main categories (Fig. 1): organic NPs such as liposomes, dendrimers, micelles, polymeric NPs, etc, and inorganic NPs which would be the main focus of this review [3,4]. Inorganic NPs can be categorized into three main classes: metal-based NPs such as gold (Au), silver (Ag), iron (Fe), copper (Cu), zinc (Zn), cadmium (Cd), etc., and metal oxide-based NPs (MONPs) such as iron oxide NPs (IONPs), titanium dioxide NPs (TiO_2 NPs), zinc oxide NPs (ZnO NPs), silicon dioxide NPs (SiO_2 NPs), aluminum oxide NPs (Al_2O_3 NPs), cerium oxide (CeO_2 NPs), zirconium dioxide (ZrO_2 NPs) etc., which were developed to enhance the efficacy and reactivity of their metallic counterparts. The third class is quantum dots (QDs) which would be further discussed in section 3.3 [5–7].

As the traditional type of dosage forms are not capable of meeting the requirements of health-care providers and fulfilling the increasing needs of patients, the investment of nanotechnology and its products in medical and pharmaceutical domain has emerged as a key solution to overcome the drawbacks of conventional drugs and surpass their limitations. Therefore, recent research has introduced a new generation of drug-nanocarriers (both organic and inorganic) which could present several advantages such as improving stability and biocompatibility, increasing water solubility and bioavailability, crossing biological barriers, achieving targeted delivery, reducing side effects and toxicity. These advantages in general would lead to the improvement of effectiveness and patient compliance [3,4].

Organic NPs have been extensively used in biomedical applications

* Corresponding author.
E-mail address: sovany.tamas@szte.hu (T. Sovány).

https://doi.org/10.1016/j.jddst.2024.105979
Received 19 March 2024; Received in revised form 2 July 2024; Accepted 14 July 2024
Available online 15 July 2024

due to their preferred specifications such as good biocompatibility, biodegradability and low toxicity, for both diagnostic and therapeutic purposes such as biosensing, bioimaging, targeted drug delivery, fluorescence guided surgery, cosmetics, etc [8–11]. Also, because of their huge potentials, they are continuously being investigated for novel applications, for example, the treatment of central nervous system (CNS) disorders by enhancing brain-targeting through intranasal administration (nose to brain delivery) overcoming one of the biggest limitations of conventional methods [12,13]. On the other hand, it is true that inorganic NPs have been basically used for diagnostic and imaging purposes [4,6]. Nevertheless, their implementation in therapeutic field came into focus in recent years due to their higher stability and drug loading capacity in addition to unique physicochemical (optical, thermal, mechanical, catalytic and magnetic) properties. This could present an added value to the treatment when combined with additional therapeutic agents [6]. For example, photocatalytic activity and radio sensitizing effect of titanate nanotubes (TNTs) can be combined with the ability to be loaded with drugs resulted in synergistic effect of great importance, especially in the field of oncology [4,14–17]. Similarly, cerium oxide nanoparticles have also shown potential to act as radiosensitizers by increasing the production of reactive oxygen species (ROS) [18] and activation of Jun terminal kinase (JNK) apoptotic pathway in pancreatic cancer cells in vitro and in vivo [19]. In the same context, some types of inorganic NPs such as gold nanorods (GNRs) have been successfully utilized in tumor targeting treatment depending on photothermal therapy (PTT) [20].

Moreover, certain types of inorganic NPs may themselves act as therapeutic agents in some inflammatory diseases. For instance, researchers have reported the efficacy of selenium nanoparticles (SeNPs) in acute rheumatoid arthritis initiated in Wistar albino rats and indicated their ability to increase mRNA expression of catalase (CAT), glutathione peroxidase (GPx1), and cyclooxygenase (COX-2) levels depending on their antioxidant property, and confirmed their findings by histological changes of angle joints in the treated animals [21].

Other beneficial effects could be obtained by specific types of inorganic NPs such as silver nanoparticles (AgNPs) which presented antibacterial, anti-inflammatory and antioxidant activity according to recent studies [22,23]. These properties are considered as fundamental advantages allowing the usage of AgNPs in wound healing with promising outcomes [24]. ZnO NPs have also shown similar properties (antibacterial and anti-inflammatory effect) which give them a distinctive role among other NPs regarding preventing infections and wound-dressing [6].

Researchers have also reported that the use of specific types of NPs (for example, TNTs) would not only contribute to the therapeutic procedure by delivering drugs [25] but would also impact the manufacturing process on technological aspects (hardness, tensile strength, flowability, compressibility, compactibility) which would positively affect the scale-up procedure and industrial production [26–28].

Based on the previous discussion and depending on the fact that inorganic NPs could exert multiple effects due to their unique composition, improved performance could be achieved by combining these NPs with appropriate active pharmaceutical ingredients (APIs) to achieve specific purposes or treat specific medical conditions. This combination will have a positive impact on therapeutic outcomes as nanocomposites may be more potent than the bare NPs or the free drugs (For example, TNTs with antitumor drugs or AuNPs with antibiotic drugs) [14,29].

Fig. 2 shows some of the most used applications of inorganic NPs in biomedical-related fields.

It is also worth to mention that the pharmaceutical use of inorganic NPs has increasing popularity as they can flexibly integrated as drug carriers in multiple dosage forms, thus providing multiple options for manufacturers to incorporate them (tablets, hydrogels, transdermal films, contact lenses, inhalable dry powder, etc.) for different administration routes (oral, dermal, ophthalmic, pulmonary, etc.) and for systemic or local effect [24,30–33]. Hence, they are not limited to laboratory experiments or for research purposes, but they have succeeded to reach the global market specifically in oncology and cancer treatment (chemotherapy, thermal therapy and radiotherapy) in addition to wound-dressing applications [6,34–37]. Tables 1 and 2 show examples of inorganic NPs being used as drug carriers and in different biomedical applications (in their original form or after being surface-modified or combined with different molecules).

Although the utilization of inorganic NPs in health-related applications is accelerating in a regular base with impressive outcomes supported by their outstanding specifications, it is also bringing possible

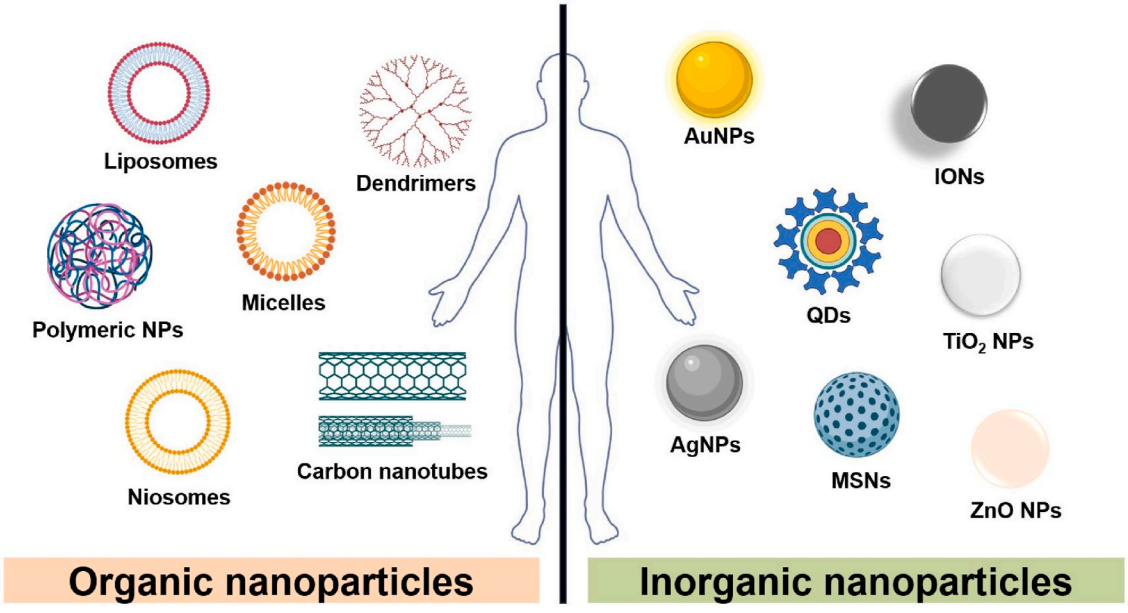

Fig. 1. Different types of organic and inorganic nanoparticles.
This figure represents different types of organic nanoparticles such as liposomes, dendrimers, polymeric NPs, micelles, niosomes and carbon nanotubes, in addition to the most used types of inorganic nanoparticles in biomedical applications and consumer products such as AuNPs, AgNPs, QDs, TiO_2 NPs, MSNs and ZnO NPs.

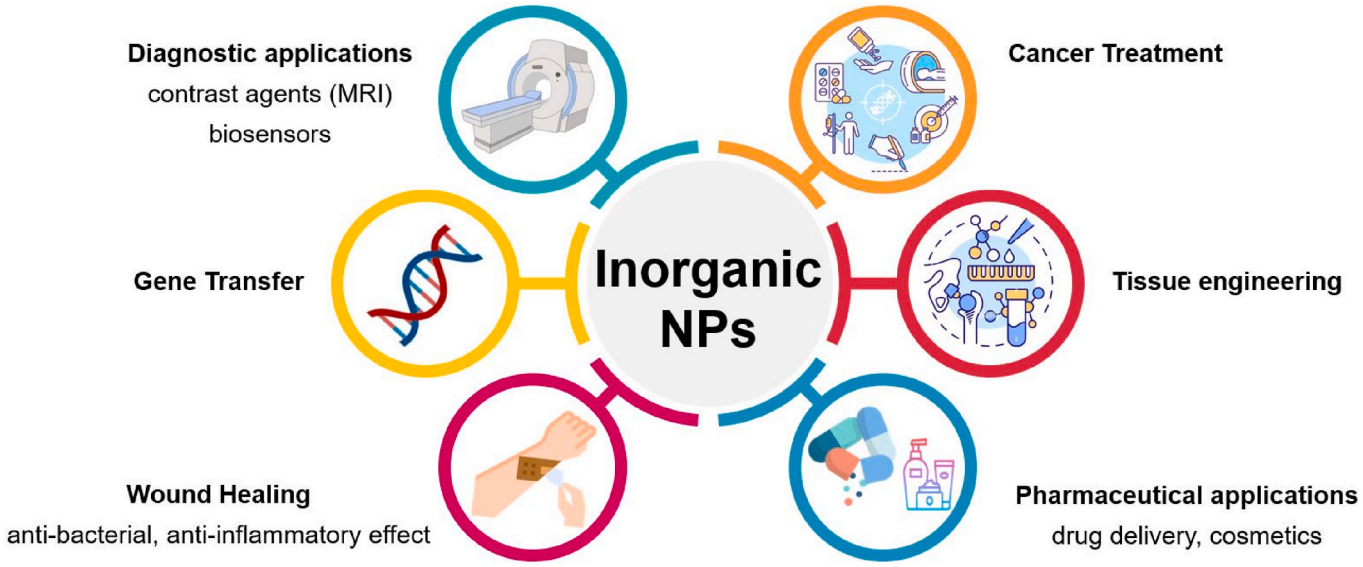

Fig. 2. Biomedical applications of inorganic nanoparticles.
This figure represents the most popular uses of inorganic NPs in biomedical applications such as drug carriers in pharmaceutical applications and cosmetics, contrast agents in magnetic resonance imaging (MRI) and biosensors for diagnostic purposes, anti-bacterial and anti-inflammatory agents in wound dressings, cancer treatment as radiosensitizers/anti-tumor carriers and photothermal agents in addition to gen transfer and tissue engineering applications.

Table 1
Pharmaceutical application of inorganic nanoparticles as drug carriers.

Type	Drug	Ref
TNTs	ibuprofen, dexamethasone, curcumin, methotrexate, silibinin	[38–41]
AuNPs	varlitinib, cisplatin, levofloxacin, cefotaxime, ceftriaxone and ciprofloxacin	[29,42, 43]
$CaCO_3$ NPs	doxorubicin	[44]
Mesoporous silica nanoparticles (MSNs)	doxorubicin	[45,46]
AgNPs	donepezil	[30]

Table 2
Examples of biomedical applications of different types of inorganic nanoparticles.

Type	application	Ref
TNTs	radiosensitizer	[15]
SeNPs	anti-inflammatory agent	[21]
GNRs	photothermal NPs in PTT	[20]
CeO_2 NPs	radiosensitizer	[18,19]
AgNPs	anti-bacterial, anti-inflammatory, antioxidant agent	[22,23]
IONPs	contrast agents in magnetic resonance imaging (MRI)	[47]
TiO_2 NPs	UV absorption in sunscreens	[48]
ZnO NPs	UV absorption in sunscreens	[49]

hazards to public health/environment (controversial results on biocompatibility/biodegradability and hence safety) which should be closely monitored and controlled [5,6]. This task is challenging due to the huge diversity of inorganic NPs (in their chemical structure, size, shape, etc.) as their behavior is significantly varying based on these diverse properties. For instance, the fact that even a single type of these NPs could exist in several sizes and shapes (nanotubes, nanorods, nanowires, nanoribbons, nanobelts, etc.) complicates the prediction of its behavior as possible drug carrier especially regarding biopharmaceutical and toxicological aspects. Therefore, a separate assessment should be carried out for each type of these NPs, taking into consideration its entire physicochemical properties as they hugely affects its pharmacokinetics (PK) and safety profile, and the concluded judgement on this specific type could not be generalized to others.

Therefore, the main aim of this review is to provide a solid background on the progress made so far in the toxicological assessment of inorganic NPs most commonly used in biomedical applications and consumer products in daily life, with particular attention on the impact of their physicochemical properties, the key players in this critical assessment. The toxicological assessment and safety profile of inorganic NPs could not be completed without the accurate evaluation of their pharmacokinetics: the administration route (dermal, gastrointestinal, pulmonary, etc.), the absorption mechanism, the migration route from the initial site of exposure, their accumulation, the metabolization and excretion routes [5,50]. For this reason, this review would also discuss the pharmacokinetics of inorganic NPs in living organism as its better understanding will lead to further improvement in their efficacy and safety profile.

2. The fate of nanoparticles in living organisms

2.1. Absorption

The exposure to inorganic NPs especially with their widespread use in numerous products (cosmetics, food products, paints, detergents, disinfectants, textiles, biosensors, probes, etc.) is not limited to a specific route as they could access the living organism through several pathways (ingestion, injection, inhalation, skin penetration, etc.) [5,50]. The precise investigation of the next step after exposure is crucial as it would determine whether these NPs would be absorbed to the systemic circulation thus translocated to distal organs, or they would be restricted to the primary site of exposure. This critical point regarding absorption still represents a critical issue and considered controversial due to the huge diversity of the affecting factors which further complicates its study and related research.

2.1.1. Dermal route

The absorption of NPs through the skin or the stratum corneum (SC) is one of the most interesting fields to researchers because of the common use of for example, TiO_2 NPs or ZnO NPs in some daily products, such as sunscreens and cosmetics, not just in medical ones. Dermal penetration has been investigated using different types of NPs such as TiO_2 NPs which were found to be not able to permeate through the intact skin [48,51], or even the damaged one [52]. However, their penetration

through the damaged skin still controversial as Vaudagna et al. reported the existence of small amount of TiO_2 NPs inside hair follicles as a result of shaving the particular skin area of the treated animals to prepare it for the application of the cream, hence they suggested not to use NPs-containing products on harmed or newly shaved skin to prevent NPs permeation [48]. Similarly to TiO_2 NPs, ZnO NPs used as physical sunscreen were detected only on the surface of the skin (in the uppermost stratum corneum regions) and no important permeation toward the underlying keratinocytes was observed [53].

Another study on penetration of SiO_2 NPs into the skin showed that dermal absorption is size-dependent. 42 nm particles were observed to be associated with epidermal cells while SiO_2 NPs of above 75 nm in size have been blocked even after mild skin barrier disruption [54].

In this context, many attempts have been made to enhance the dermal absorption of NPs by applying new methods of pharmaceutical formulation like oily dispersions which provide better penetration than the aqueous ones, probably via sebum lipids of hair follicles [55]. Surface functionalization could also be used to improve dermal penetration [54].

2.1.2. Gastrointestinal route

Enormous efforts have been made to investigate NPs absorption through gastrointestinal tracts (GIT) aiming to create new carriers that would improve the oral uptake of drugs. Many authors demonstrated the translocation of TiO_2 NPs to distal organs like liver, spleen, lung, and peritoneal tissues after oral intake through GIT [56].

This absorption could be governed by numerous factors, for example Schleh et al. used gold nanoparticles of different sizes (1.4–200 nm) to study the effect of surface charge/size on absorption after oral administration. They concluded that the small/negatively charged particles tend to be absorbed across intestinal barriers more readily than larger/positively charged ones [57]. Similar to the dermal route, oral absorption of inorganic NPs could be improved by surface functionalization with hydrophobic molecules such as trichloro (octyl)silane and magnesium stearate [58].

2.1.3. Respiratory route

Studies related to NPs absorption after inhalation in humans are scarce. After Lung instillation of near-infrared (NIR) fluorescent nanoparticles, different in their physicochemical properties (size, shape, surface charge and chemical composition), Choi et al. concluded that non-cationic NPs (hydrodynamic diameter <34 nm) distributed from the lung to mediastinal lymph nodes whereas NPs of hydrodynamic diameter <6 nm translocated rapidly to lymph nodes and the systemic circulation, then successively excreted through urine [59]. Other results also suggest that intra-nasally instilled TiO_2 NPs can directly distribute to CNS through the olfactory bulb [60] which poses safety concerns regarding developing neurodegenerative diseases [61], but also could be used to offer an innovative method to bypass the blood-brain barrier (BBB) using nano-carriers in direct nose to brain delivery systems [12, 62].

2.2. Interacting with biological fluids and protein corona formation

After absorption of NPs and reaching the systemic circulation, they can be distributed/accumulated or excreted out of the body. It is worth to mention that assessing biocompatibility, therapeutic outcome, and toxicity of inorganic NPs could not be conducted without determining their biodistribution and excretion profiles. For instance, easy clearance demonstrates a smaller overall cumulative toxicity.

The interaction between the biological fluid and NPs after reaching the blood will lead to a so-called protein corona which arises from the binding of serum proteins on the surface of the NPs [63] and has a significant impact on the behavior of these nanoparticles in the body including fostering cellular uptake or increasing toxicity [64].

Regarding this aspect, the amount of adsorbed proteins on the surface of Au nanorods was evaluated by Qiu et al. using reducing sodium dodecyl sulphate–polyacrylamide gel electrophoresis (SDS-PAGE). They suggested that there is a positive relationship between the cellular uptake efficiency and the amount of adsorbed proteins. Adsorbed proteins could expose ligands which could be recognized by the membrane receptors thus facilitating cellular uptake. This theory was confirmed by noticing that the most favored NPs in cellular uptake are the ones who adsorbed the greatest amount of proteins [65]. In contrast to these findings, Lesniak et al. reported greater cell internalization efficiency of SiO_2 NPs in the absence of serum in comparison to NPs which had a protein corona on their surface due to the presence of serum [66]. Another study by the same group investigated the influence of protein corona formation on cellular uptake and declared the effect of serum heat inactivation on this property. This study supported the previous findings, and concluded that cellular internalization was found to be different when nanoparticles were dispersed in a heat-inactivated serum as medium and lower NPs internalization was observed with a more protein-rich corona NPs [67]. These discrepancies could be explained by the differences in the mechanism of cellular uptake whether it is mediated by membrane-receptors or not. Many attempts have been made to reduce this interaction between NPs and the surrounding biological environment and hence the formation of protein corona and the subsequent detection by the immune system, and among them surface functionalization seems to be the most promising.

Several studies investigated the impact of surface functionalization on protein corona formation and the subsequent cellular uptake. For example, Cruje et al. evaluated the effect of polyethylene glycol (PEG) grafting density using gold NPs (50 nm), and concluded that higher grafting densities minimize protein adsorption and thus NPs uptake by all tested cell lines while lower grafting densities resulted in greater nonspecific protein adsorption and higher cellular uptake [68]. Chalot et al. also reported that the uptake of SiO_2 NPs (50 nm) enhanced in the absence of PEG as PEGylation decreased the formation of protein corona [69]. However, the current information regarding the formation of protein corona and its impact on pharmacokinetics in vivo is still insufficient. Simberg et al. indicated that the attached proteins will not affect the clearance of IONPs by spleen and liver macrophages as they did not mask their entire surface [70]. Another study demonstrated the importance of PEGylation to extend the blood circulation time of AuNPs where 10 kDa PEG-AuNPs showed prolonged retention time in systemic circulation while non-PEGylated and 750 Da PEG-AuNPs distributed mainly to spleen and liver [71].

2.3. Distribution and accumulation

The distribution, accumulation and excretion routes are summarized in Fig. 3. The distribution of intravenously injected TiO_2 NPs (<100 nm) in rats (5 mg/kg) was investigated and found to be in its highest level in liver, followed by spleen. No detectable levels of TiO_2 NPs were found in blood, lymph nodes or plasma which could be attributed to the fast clearance of these NPs from blood to other organs mainly liver and spleen where TiO_2 NPs have found to be accumulated, but with no signs of inflammation or organs toxicity [72]. In contrast, another study found the highest accumulation level of the crystalline TiO_2 NPs (80–110 nm) in the spleen, causing serious spleen lesion and additional toxic effects to other organs (hepatic fibrosis, thrombosis in the pulmonary vascular system, hepatocellular necrosis and apoptosis) after intraperitoneal injection in mice [73]. The presence of reticuloendothelial system in liver and spleen is responsible of this high uptake while the low distribution inside the heart is due to the limited time of the cardiac cycle and the existence of dense cardiac tissue hindering retention NPs [74].

Biodistribution studies of SiO_2 NPs in nude mice found that 75 % of their total number were accumulated in liver, spleen, and stomach [75]. Moreover, MSNs and their PEGylated versions translocated in the same way, mainly to spleen and liver after tail-vein injection in mice [76]. In case of AgNPs, they showed extensive distribution to several

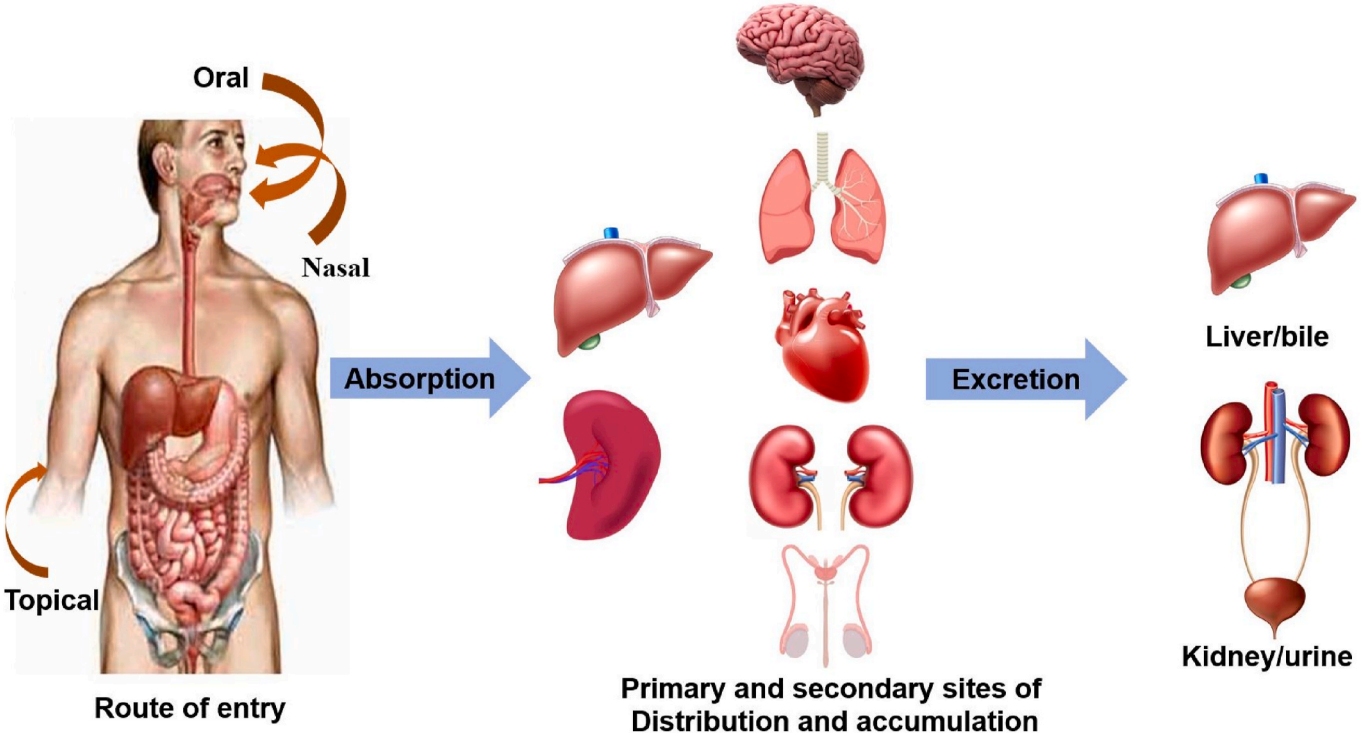

Fig. 3. Route of entry of inorganic nanoparticles, the main sites of accumulation and pathways of excretion
This figure represents the major routes of entry for NPs which are oral route by ingestion, nasal route by inhalation and dermal route by skin penetration. It also shows the primary and secondary sites of accumulation (liver, spleen, brain, lungs, heart, kidneys, testes) in addition to elimination pathway through urine or feces.

destinations in the body, but mainly to spleen followed by liver, lungs, and kidneys after intravenously injected in mice [77]. Dziendzikowska et al. indicated that the distribution of AgNPs was size/time-dependent after intravenously injected to male Wistar rats at a dose of 5 mg/kg where NPs with smaller size (20 nm) were detected in several tissues with higher concentration in comparison to the larger ones (200 nm). The highest translocation was also changing from one organ to another upon time. For example, the greatest concentration of silver was detected in the liver after 24 h of exposure and in brain/kidneys after 28 days [78].

20 nm AuNPs accumulated in lungs and brain after IV injection in mice, whereas their accumulation in other organs such as pancreas, stomach, and heart was relatively low [79]. According to De Jong et al. their distribution was also size-dependent (similar to AgNPs) with the smallest nanoparticles displaying widespread organ translocation in rats after IV injection [80]. Similar results were obtained by Sonavane et al. who demonstrated that AuNPs of all sizes were mainly accumulated in organs like liver, lung, spleen, and kidneys after intravenous injection (1 g/kg) in mice with the smallest size (15 nm) showing the highest amount of gold in all tissues [81]. This distribution-size relationship was not limited to AgNPs or AuNPs but was further confirmed with ZnO NPs as they were absorbed within 30 min after oral administration, then translocated to liver, spleen, and kidney, exhibiting much higher absorptivity and biodistribution compared to ZnO microparticles [82]. In some cases, this size could be influenced by the dose being administered and this would have reflection on the subsequent uptake and accumulation. De et al. reported higher accumulation of Al_2O_3 NPs at 30 mg/kg dose than that of the 60 mg/kg dose which was attributed to the agglomeration occurred at high concentrations which increased the size of NPs and hindered their uptake [83]. Surprisingly, in contrast to the previous popular belief, 18-nm AuNPs accumulated in the brain and heart of mice after oral administration in a higher amount compared to the smaller 1.4-nm ones without any proposed explanation [57]. Based on these results, the prediction of NPs biodistribution, accumulation and toxicity could not be accomplished based on the determination of size range (or other properties) but comprehensive experiments should be done to confirm our prediction.

2.4. Excretion

After reaching the bloodstream, inorganic nanoparticles could be eliminated through two routes: excretion into the urine by renal filtration, or into the bile/feces by hepatobiliary processing. According to the International Program on Chemical Safety for TiO_2, most of the ingested TiO_2 is excreted unabsorbed, probably with urine [84].

The clearance studies of SiO_2 NPs (20–25 nm) in vivo suggested hepatobiliary excretion without causing any abnormal effect [75] while another study has observed that 36 % of the injected SiO_2 NPs (150 nm) were excreted with urine and the remaining particles were accumulated in lungs and kidneys [85].

Regarding QDs, Tang et al. indicated that AgSe QDs are transformed into Ag and Se, which are excreted from the body through feces/urine without obvious toxic effects although Se appeared to be harder to eliminate [86]. Moreover, Choi et al. used intravenously injected QDs in rodents to study the requirements and limits for urinary excretion of inorganic nanoparticles and concluded that the size of NPs plays a significant role in the elimination process with QDs smaller than 5.5 nm being excreted into urine, and efficiently eliminated from the human body in contrast to larger ones (>15 nm) [87]. Dziendzikowska et al. also confirmed that the excretion of AgNPs was size/time-dependent through kidney/urine or liver/feces [78]. On the other hand, according to Lee et al. size was not a determining factor with orally administered AgNPs in Sprague–Dawley rats. Ag concentrations gradually decreased (during the examination period) to control levels in most tissues except in testes and brain indicating difficult elimination of AgNPs across some biological barriers such as BBB and blood-testis barriers [88]. Furthermore, the elimination procedure could be influenced by several properties other than size such as surface charge and

route of exposure. Regarding these aspects, Wang et al. reported that gold nanoclusters (Au NCs) with negative charge showed lower excretion and longer retention time in liver and spleen compared to neutral ones [89] while Li et al. demonstrated faster clearance of orally administered ZnO NPs in comparison to intraperitoneally injected ones, resulted in transient histopathological lesions in liver [82].

2.5. Crossing the protective biological borders

Many studies discussed the ability of NPs to bypass the biological protective barriers such as blood-brain barrier, placenta, and blood-testis barrier. Regarding this fundamental issue, Li et al. suggested that TiO_2 NPs might induce brain injury when passing through BBB after intratracheal instillation [90].

In the same context, Au NPs (15 and 50 nm) crossed BBB after intravenous injection (1 g/kg) in mice [81] and PEGylated SiO_2 NPs could also cross BBB in vivo and in vitro using an in vitro BBB model. This transportation was significantly dependent on size [91].

De et al. also suggested that the exposure to Al_2O_3 NPs (10–55 nm) might produce increased permeability of BBB in Swiss albino mice after oral administration thus leading to Al_2O_3 NPs accumulation in brain causing histopathological changes including neurofibrillary tangles which are commonly associated with neurodegenerative diseases [83]. This result was correlated well with the study of Chen et al. who reported decreased expression of tight junction proteins (occludin and claudin-5) caused by nano-alumina thus disturbing BBB permeability [92].

Morishita et al. studied the testicular distribution of SiO_2 NPs in mice after systemic administration and suggested that they can cross the blood-testis barrier in addition to the nuclear membranes of spermatocytes but without causing any testicular injury [93]. De et al. observed the same ability of Al_2O_3 NPs (10–55 nm) in bypassing the blood-testis barrier in mice causing abnormalities in sperm head morphology after oral administration (30 and 60 mg/kg) [83].

In case of AgNPs (14 nm) that were intravenously injected (1 mg/kg) in male CD1 mice, the results revealed significant changes in the size of Leydig cells with no important decrease in the weight of testis or the concentrations and motility of sperms. However, increasement of testicular and serum testosterone levels were reported [94].

Furthermore, by using the *ex vivo* human placental perfusion model, fluorescent polystyrene NPs (up to 240 nm) were capable of penetrating the placental barrier [95]. This ability might affect the offspring especially the development of their reproductive and nervous system [96]. The same result was obtained with SiO_2 NPs (70 nm) and TiO_2 NPs (35 nm) which were detected in the placenta, fetal brain and fetal liver after being injected intravenously into pregnant mice causing pregnancy complications while larger particles did not [97].

3. Toxicity of inorganic nanoparticles

Many attempts have been made to investigate the possible harmful effects of inorganic NPs (for example TiO_2 NPs) on the environment and human health indicating no toxic effect, starting from experiments on some simple living organisms like Ciliated Tetrahymena pyriformis which reported no in vitro toxicity effect of tested TiO_2 nanotubes [98]. This was in agreement with the findings of Ammendolia et al. that TiO_2 nanoparticles were not cytotoxic to human colorectal adeno carcinoma HT-29 cell line at all tested concentrations (1.8, 4.5, 9, 36 μg/ml) even though they were able to penetrate the intestinal cells and cause a gender-specific effect at male rats after oral administration (increased length of intestinal villi and increased testosterone serum levels) [99], and the finding of Fenyvesi et al. who reported that TNTs (length 50–150 nm, diameter 6–10 nm, specific surface area S·S.A 185 m^2/g) were not cytotoxic to Caco-2 cells, and not capable to penetrate the intestinal cell layers even though they were used in higher concentrations compared to the previous study (up to 5 mg/ml) [100].

These promising results were also confirmed regarding the crucial genotoxicological aspect. Brandao et al. reported efficient cellular uptake of TiO_2 NPs but without disturbing chromosomal integrity or lead to any genotoxic effect which was investigated by Micronuclei analysis using flow cytometry. This was explained by the probable distribution of TiO_2 NPs in cytoplasmic compartments rather than nucleus which minimized their direct interaction with DNA [101]. Another study attributed this non-genotoxic effect to the activation of DNA repair pathway which repaired the occurred damage in its early stage [102].

Some studies even displayed positive outcomes of TiO_2 anatase nanostructures (30 % nanotubes + 70 % nanorods) with diameter of 8–10 nm and S·S.A of 265 m^2/g like increased A549 cell viability compared to control [103], improved bone cell adhesion and proliferation without triggering any chronic inflammation or fibrosis in vivo [104] which could be attributed to their porous channeled structure permitting continuous flow of blood and nutrients [105].

On the other hand, many studies revealed negative results after using TiO_2 NPs like decreased viability and apoptosis of Microglia N9 cells, the resident macrophages in CNS, even with low concentrations (16 μg/ml) [106]. In another study, physiologically relevant doses of TiO_2 NPs (30 nm) decreased the intestinal barrier function and caused an increase in the production of ROS and proinflammatory signals in addition to a decrease in zinc, iron, and fatty acid transport. They also altered nutrient transporter protein gene expression and disturbed cells which work to regulate the transport mechanisms [107]. Moreover, due to their worldwide use in sunscreens, the effect of TiO_2 NPs upon irradiation was evaluated in vitro (prokaryotic and eukaryotic cells) and in vivo (in adult male Wistar rats), and significant toxicity was reported evidenced by the elevation of ROS production leading to macromolecular oxidation (proteins and cell membrane lipids), in addition to damaged integrity of SC [48]. These conflicted results impose an urgent need to establish a new discipline that combines toxicology and nanotechnology, deals with the interaction of nanoparticles with biological molecules/organisms, and aims to determine the possible adverse effects of these NPs. This discipline is called nanotoxicology which evaluates the toxicity of these novel nanomaterials as it cannot be predicted from the toxicity profile of the same bulk materials.

Toxicity studies of inorganic nanoparticles revealed a dependence on their physicochemical properties such as shape, size, surface properties, crystal structure, chemical composition. Therefore, in this review some of these most important physicochemical properties will be highlighted. The discussed properties could differ between different groups of inorganic nanoparticles (metal oxides NPs, metallic NPs and QDs) due to their unique structures/composition or simply due to the lack of available research discussing every single factor. It is also worth to mention that these toxicity studies could be conducted in vivo or in vitro. In vivo studies depend basically on histopathological examination of sacrificed animals (rats, mice, etc.) to detect any signs of abnormalities, changes or dysfunction in addition to the sites of NPs accumulation [74,83] while in vitro studies are more diverse ranging from simple assays investigating viability and/or oxidative stress to more complicated ones investigating genotoxicity as shown in Table 3.

3.1. Metal oxide nanoparticles

3.1.1. Morphology

Using 3 shapes of TiO_2 NPs (nanotubes, nanorods and nano ribbons) to study the impact of morphology on distribution and toxicity in male albino rats after intravenous tail injection (5 mg/kg), Kamal et al. indicated the importance of 3 factors related to morphology that affect cellular uptake which are aspect ratio, surface charge and surface area. An increase in surface area, decrease in negative zeta potential and aspect ratio would enhance cell penetration thus TiO_2 nanotubes with their lowest zeta potential and largest surface area achieved the highest uptake, were the most harmful nanomaterials and caused the strongest inflammations among the three tested shapes. Pathological findings

Table 3
Some of the most used methods/assays to investigate the toxicity signs of inorganic nanoparticles.

Toxicity Indicator	Name of the method/assay	References
Viability	MTT assay	[100,103, 108–112]
	Lactate dehydrogenase (LDH) assay (cell membrane integrity)	[69,111, 113–115]
	Neutral Red (NR) Uptake Assay	[116]
	Live/dead cell assay	[117–119]
	Cell Counting Kit-8 (CCK-8)	[65,115,120,121]
	Annexin V/PI Staining (early marker of cell death)	[120,122]
	Propidium iodide (PI) exclusion	[120]
	Cellular proliferation colorimetric assay	[123]
	WST-1 assay	[124]
Oxidative stress	Intracellular ROS measurement	[65,69,111–113, 117,118]
	Quantification of Reduced Glutathione	[111,113,114]
	Mitochondrial potential	[65,117,120]
	MitoSOX Assay (measurement of superoxide production)	[120]
	Measurement of enzymatic antioxidants activity (CAT- SOD)	[83,113]
	Measurement of Membrane lipid peroxidation (LPO)	[83]
Pro-inflammatory effect	Production of TNF-a	[69,114]
	Cytokine quantification	[114,124]
Genotoxicity	Comet assay	[83]
Apoptosis/ Necrosis	Annexin V-FITC Kit	[65,112,123]

showed hepatic fibrosis around the central vein, cells with apoptotic bodies, necrotic cells, cells with condensed nuclear, spleen lesions and inflammation, thrombosis in the pulmonary vascular system and dilatation of the cardiac blood vessels [74]. Another study also reported the importance of geometry in toxicity assessment confirming the previous results, with the thinner nanotubes being slightly more toxic than the corresponding nanowires [125]. In the same context, Al_2O_3 NPs (two shapes: nanorods and nanoflakes) caused an increase in the concentrations of ROS and inflammatory cytokines in addition to disturbing several metabolic pathways, such as those related to oxidative stress and nucleic acids damage and repair. Morphology also has a great impact on their cytotoxicity with nanorods (width 20–30 nm/length 100–200 nm) causing greater cytotoxicity (greater ROS generation, apoptosis, and more affected metabolic pathways) than nanoflakes (width 20–30 nm/length 20–30 nm) when applied with the same concentration [112].

3.1.2. *Surface properties (chemistry, coating, charge)*

In addition to the previous findings concerning the impact of morphology, Magrez et al. highlighted the importance of surface properties of TiO_2-based nanofilaments on affecting cell proliferation/activity and concluded that nanowires/nanotubes in H form (with protons on their surface) were more toxic than in Na form as this ion exchange can cause damage within the structure. These structural damages increased toxicity because they acted as chemically active sites. The observed morphological changes in H596 Human Lung tumor cells included disturbed cell-cell contacts and apoptotic cells in addition to the presence of apoptotic cells with no signs of NPs accumulation which is an obvious indicator of indirect toxic effect caused by the released cytokines from dying cells [125].

In the same context, Ranjous et al. noticed an important decrease in cell viability after replacing Na^+ ions with Mg^{2+} ions on the surface of TNTs which had a negative impact on cell interactions [58] while the modification of TiO_2 NPs (25 nm, 80 % anatase+ 20 % rutile) surface with PEG reduced their toxicity and their induction of stress-related genes by preventing aggregation [126].

Surface charge is also one of the most important properties that could play a significant role determining the toxicity of NPs. Chalot et al. reported that all the examined SiO_2 NPs caused inflammatory effect and increased the production of TNF-α but only those with positive charge caused loss of cell membrane integrity at high doses (300 and 600 μg/ml) [69].

In case of ZnO NPs, adverse effects could be attributed to mitochondria sequestering zinc ions into cells, leading to elevation of zinc-ion concentration which can activate ROS generation, induce mitochondrial dysfunction, and initiate apoptosis in human neuroblastoma SHSY5Y cell line [121]. For this reason, PEGylation was one of numerous attempts that have been made to reduce toxicity by modifying surface properties. This modification presented a lower level of intracellular Zn ions due to minimizing protein corona formation which might reduce cellular uptake. Interestingly, another type of surface modification using 3-aminopropyltriethoxysilane (APTES) with more protein binding ability (due to the positively charged aminated surface) did not increase cellular uptake in comparison to uncoated NPs and similar cytotoxicity was observed (oxidative stress and cell death by apoptosis and necrosis) at all exposure concentrations [127]. Another study reported that silica coating significantly reduced the cytotoxicity caused by bare ZnO NPs (which released Zn^{2+} ions in the gastric fluid) on human colon adenocarcinoma cell line (SW480) and human colorectal adenocarcinoma epithelial cell lines (DLD-1) through prevention of their dissolution in neutral and acidic conditions. It is worth noticing that this coating is not totally benign as high concentrations of silica-coated ZnO NPs caused significant cytotoxicity to colorectal epithelial cells [122]. However, in contrast to the idea that toxicity of ZnO NPs may be attributed to their dissolution and ions release, Moos et al. concluded that ZnO NPs have a low potential for cytotoxicity by consumption because they are likely to dissolve in the highly acidic medium of stomach while their cytotoxic effects are produced upon their direct contact with cells. Their adverse effects could be summarized by decreased viability, activation of apoptosis pathway, disruption of mitochondrial function, and increased superoxide production [120].

As previously discussed, manipulating surface properties could be a proper strategy for producing safer NPs. For example, lipid-coating of iron oxide NPs (14 nm) presented the highest stability against acidic conditions that could lead to their degradation resulting in releasing ferric iron, inducing ROS generation and affecting cell function. On the other hand, the maximum number of ferric ions was released by citrate-coated NPs (4 nm), disrupting iron homeostasis and thus inducing the maximal ROS levels [118]. Vaudagna et al. functionalized the surface of TiO_2 NPs with vitamin B2 which led to significant reduction in the amount of produced ROS attributed to V·B2 antioxidant property that appeared to be higher than the oxidation damage induced by the bare NPs [48].

3.1.3. *Size & type of cell lines*

The effect of size on toxicity was also widely studied. Size factor is not only dependent on original particle size but also on agglomeration/aggregation state which could happen upon interaction with biological fluid resulting in negative impact on safety profile [6]. Regarding this aspect, Murugadoss et al. reported that large agglomerates (LA) of TiO_2 NPs induced stronger effects than smaller ones (SA) contrary to the common concept, and this effect was dependent on cell type and primary particle size. In vivo studies in mice confirmed these in vitro results, and indicated that large agglomerates (117 nm) caused stronger pulmonary effects (higher number of lymphocytes and higher retention of Ti). They also concluded that the effect of TiO_2 agglomeration state could also induce systemic responses as it was not limited to the site of particle deposition evidenced by the observed DNA damage [114]. Interestingly, the type of used cell line plays a critical role in explaining these results due to the differences in their sensitivity and uptake ability/mechanism. For instance, the agglomerates of TiO_2 induce response in monocytic (THP-1) cells but not in human bronchial epithelial (HBE) and colon epithelial (Caco-2) cell cultures. As THP-1 are phagocytic cells, their

response was stronger with LA of 17 nm TiO_2 than with SA because micron-sized agglomerates are more appropriate for phagocytosis than nano-sized ones. However, in case of 117 nm TiO_2, the size of SA and LA was already appropriate for phagocytosis, so they were equally cell internalized [114].

The size of agglomerates does not only depend on the primary size of NPs but could also be affected by the route of exposure. Interestingly, one study simulated the digestion process to evaluate the toxic effects of three different TiO_2 nanomaterials (anatase, rutile and mixture of anatase/rutile with 22, 28 and 30 nm diameter, respectively) on the cells of gastrointestinal tract after being modified in the organism and resulted in neither significant differences between digested/undigested nanomaterials nor cytotoxic effect to Caco-2 cells at all tested concentrations except for NM105 (mix of anatase/rutile, 30 nm, 46.18 m^2/g) where more distinct adverse effect with digested ones was observed on HT29-MTX-E12 intestinal cells, and this could be explained by the lower size of its agglomerates upon ingestion which makes them easier to uptake [108].

Regarding SiO_2 NPs, Kim et al. observed a greater decrease in cell viability with larger SiO_2 NPs in comparison to smaller ones [111] while Lojk et al. reported that large size related to intensive aggregation of SiO_2 NPs (1–10 μm) could lead to a lack of significant internalization, and to their deposition only on cell surface hence no observed effects will be detected unless the effects are related to the released ions not NPs themselves as in the case of Ag NPs [117]. The problematic issue regarding aggregation and its expected in vivo toxicity could be solved by surface modifications with proper molecules. Saker et al. have functionalized the surface of TNTs with acrylic acid-PEG copolymer which prevented their agglomeration and enhanced their stability and dispersibility in aqueous media in purpose of simulating what would happen after in vivo application [128].

It is worth to mention that even the mechanisms of toxicity (not just the effects) could vary between different cell lines. For example, membrane disruption was the main cytotoxicity mechanism of SiO_2 NPs (>60 nm) especially in NIH/3T3 cells which were the most sensitive while HepG2 cells were more resistant and the least sensitive to this exposure. A549 cells showed the highest ROS generation and the least LDH leakage demonstrating that in current case the main mechanism of the toxicity of SiO_2 NPs was mitochondrial-mediated ROS generation rather than membrane disruption [111].

The cytotoxicity of ZnO NPs was also size-dependent where the smaller ZnO NPs (18 nm) showed higher ROS generation than bigger ones (47 nm) suggesting that ROS generation mainly depends on particle size [121] which is in agreement with the results of Moos et al. who also reported that nano-sized ZnO was twice as toxic as micro-sized ones [120], and with the results of Li et al. who demonstrated that NPs produced more ROS than their bulk materials displaying greater toxic effects which was explained by their larger surface area which offers higher number of UV absorption sites [129]. This toxicity of ZnO NPs upon UV irradiation was further investigated by Chen et al. who explained it by the ability of ZnO NPs to activate NLRP3 pathway leading to pyroptosis, a fast type of lytic programmed cell death. This mechanism underlying toxicity could be explained by multiple effects: mitochondrial damage, increased ROS production, cellular autophagy dysfunction and increased release of exosome, which were translated in the treated mice into thickened and damaged skin with transepidermal water loss [49]. However, the toxicity of ZnO NPs (50 nm) in vivo was also reported by other routes such as inhalation, inducing significant changes in nasal respiratory epithelium (NRE) at *Mus musculus* such as vascular congestion, loss of cilia and granulation of mast cells, which were explained by the induction of acute inflammatory response upon exposure to the highest dose (40 mg/m^3) [130].

3.1.4. Concentration/time of exposure

It should be noticed that the used concentration/time of exposure would have a huge influence on the results of the toxicity study. For example, low reachable concentrations in vivo may cause only minor effects in vitro. However, continued accumulation in vivo could adversely influence cells and this was confirmed by the decrease in cell viability with Food Grade TiO_2 NPs, which were only apparent after 72 h of exposure, underlining the importance of long exposure experiments [117].

In the same context, toxicity of TiO_2 nanotubes was minimal with the injected dose (5 mg/kg) in male albino rats. However, histopathological examination of liver revealed that increased concentration would increase the severity of the toxic effects [74]. ZnO NPs also appeared to induce enormous toxicity in the studied cell lines (human tumoral cell lines A549, NCI–H460, SK-MES-1 and HeLa) after 24/48 h and appeared to increase the number of dead cells with increased concentrations/time of exposure [123]. This result was in agreement with many other studies like the study of Sahu et al. showing that ZnO NPs (50 nm) significantly induced ROS formation, decreased intracellular GSH level, induced apoptosis, and reduced cell viability in a concentration-dependent manner in human lung epithelial cell lines (L-132), in addition to almost complete destruction of the exposed cells with shrunken morphology, fragmented/rougher nuclei, and condensed nuclear material [110]. It is also in agreement with the results of Liu et al. who reported important oxidative stress-related gene changes in a concentration-dependent manner including a significant decrease in antioxidant genes expression levels such as SOD2, CAT, and GPX1 and an elevation in the expression of three apoptosis-related genes (BAX, BCL2, CYTC) [121].

3.1.5. Crystal structure

Several studies were dedicated to clarifying the influence of crystal structure on the toxicity of inorganic nanoparticles among them TiO_2 NPs attracted the majority of focus. TiO_2 could exist in three different crystalline structures: anatase, rutile and brookite which would subsequently affect the toxicity of the corresponding NPs. For example, by comparing their effects, anatase induced dendritic cells (DC) maturation to a higher extent and led to a higher production of interleukins, tumor necrosis factor (TNF-α) and IgE/IgG1. On the other hand, rutile induced neutrophils more strongly while the response of other allergic markers was similar with both of them [124]. In A549 human lung epithelial cells, IL-8 production was more induced by anatase NPs which were 100 times more toxic than rutile NPs [131]. Anatase had a higher ability to generate ROS [132], to induce glutathione depletion and to reduce superoxide dismutase in PC12 neuronal cells [133]. Shimizu et al. also indicated that maternal exposure of mice to anatase TiO_2 NPs may alter the expression of genes associated with apoptosis, brain development, neurotransmitters, and psychiatric diseases which would affect the development and function of CNS [134]. In contrast to the previous studies, rutile NPs induced ROS production more than anatase NPs in HEL30 keratinocytes and initiated cell death by apoptosis while anatase NPs induced it by necrosis [135]. Although the studies investigating the correlation between toxicity and crystal structure are rare, but they are not limited to TiO_2 NPs. Aluminium oxide could also exist in several crystalline phases: α, β, γ, δ, η, θ, κ and χ which are possibly different in their toxicity profile. Nogueira et al. investigated the impact of two of them (α and η) on the toxicity toward Daphnia magna (model for ecotoxicity studies) and concluded that η-Al_2O_3 NPs appeared to be more toxic [136]. This toxicity-crystalline phase relationship dependency was previously reported by the same research group but with human bronchial epithelial (BEAS-2B) and mouse neuroblastoma (N2A) cell lines. According to this study, η-Al_2O_3 NPs also proved to have the most harmful effects probably due to their high cellular uptake [137]. Moreover, This dependency was further confirmed with another type of NPs by Demir et al. who reported gamma-iron oxide (γ -Fe_2O_3) NPs being more toxic than alpha-iron oxide (α -Fe_2O_3) NPs using two types of marine microalgae species [138]. In contrast, Lei et al. demonstrated opposite opinion and reported higher toxicity of α -Fe_2O_3 NPs, explained by their stronger ability to produce free radicals and hence to initiate

more pronounced oxidative stress in comparison to γ -Fe_2O_3 NPs in green algae [139]. Briefly, establishing a solid and reliable estimation of toxicological effect based on the crystal structure is still controversial as multiple parameters should also be considered in this estimation such as other physicochemical properties of the tested NPs.

3.2. Metallic nanoparticles

3.2.1. Morphology

Opposite to Kamal's study regarding morphology impact on the toxicity of TiO_2 NPs, morphology did not have the same importance with Au nanorods where toxicity has shape-independent effect [65]. In contrast, Steckiewicz et al. argued that cytotoxicity of AuNPs is shape-dependent as AuNPs stars (≈215 nm) were more toxic than AuNPs rods (≈39 nm length, 18 nm width) and AuNPs spheres (≈6.3 nm) which appeared to be the least toxic ones. In this study, AuNPs (stars and rods) had the ability to permeate through the cell membrane causing structural changes and inducing apoptosis by increasing the expression of proapoptotic protein (Bax) and decreasing the expression of anti-apoptotic one (Bcl-2) [140]. This suggested apoptotic-initiated mechanism correlates well with the results of Selim et al. [141] and Choudhury et al. [142] who reported upregulation and downregulation of mRNA expression of Bax and Bcl-2, respectively, with the same type of NPs (AuNPs). It is worth to mention that this effect is not exclusive to AuNPs but it has been reported recently with other inorganic NPs such as SeNPs. According to Keshtmand et al. SeNPs could cause toxicity in a way similar to AuNPs by initiating cell death through disturbing the normal regulation of gene-expression that is responsible of apoptosis. For instance, increasing the expression of proapoptotic proteins (caspase- 3, caspase 9, Bax) while decreasing the expression of antiapoptotic ones (Bcl-2) This effect is of significant importance when applied to intiate the death of cancerous cells [143].

3.2.2. Surface properties (chemistry, coating, charge)

In some cases, the toxicity of inorganic nanoparticles could be linked to some impurities or chemicals on their surfaces that remain from the synthesis procedure [65,144] like cetyltrimethylammonium bromide (CTAB), a toxic cationic surfactant commonly used in the preparation process of Au nanorods, showing highly toxic effect with decreased cell viability, mitochondrial depolarization and swelling, increased ROS production, and increased apoptosis [65]. In contrast, another study demonstrated that toxicity is related to Au nanorods themselves (width 25 nm, length 52 nm) in concentrations ranging from 2.5 to 15 μg/ml, causing dose-dependent toxicity. This toxicity was indicated by decreased cell viability, induced LDH leakage as a sign of membrane damage, increased ROS generation in addition to swollen mitochondria [115].

As the case with PEGylated TiO_2 NPs, PEG-coated AuNPs showed negligible cytotoxicity [65] while other study suggested that these surface-modified NPs are not totally safe as they have long blood circulation time so they are able to accumulate in the spleen and liver for up to 7 days after injection inducing acute inflammation and apoptosis [145].

3.2.3. Size

Moderate pulmonary toxicity was induced in rats after 24 h of nose exposure to AgNPs (15 nm) while no signs of toxicity were observed with larger size (410 nm). The difference in the internal alveolar dose between the two sizes in addition to the difference in the release rate of silver ions could be the reason behind these different outcomes [146]. These results correlate well with the study of Gliga et al. who suggested size-dependent cytotoxicity of AgNPs as only the 10 nm AgNPs induced cytotoxicity in Human lung cells (BEAS-2B) while larger particles did not. According to this study, this effect is not related to differences in cellular internalization but it is probably associated with the ability of these NPs to release the highest amount of Ag^+ ions in what it is called "Trojan horse" effect. Interestingly, all the tested sizes (10, 40, 75 nm) caused DNA damage evidenced by comet assay which suggests that the mechanisms of AgNPs cytotoxicity and genotoxicity are probably different [147]. ElYamani et al. agreed with the previous findings and reported the genotoxicity AgNPs in addition to three metal oxide NPs (TiO_2 NPs, ZnO NPs, CeO_2 NPs) even with their non-cytotoxic concentrations which suggest the independency of these two concepts (genotoxicity and cytotoxicity) [148].

Although Liu et al. have agreed with the study of Gliga et al. and reported size-dependent toxicity of AgNPs in four human cell lines derived from different organs (A549, SGC-7901, HepG2 and MCF-7) with the smallest ones (5 nm) causing the highest toxic effects, they attributed these stronger impact to easier cell penetration of smaller NPs in comparison to larger ones (20 and 50 nm). Moreover, according to them, the release of Ag^+ ions could be one of the factors involved in toxicity but not the major one as the released amount was less than 1 % with all tested samples [149]. Carlson et al. have also reported size-dependent toxicity of AgNPs (15 nm in comparison to 55 nm) in alveolar macrophages. According to them, this toxicity is attributed to the triggered oxidative stress and inflammatory response evidenced by the increase of ROS levels and the release of inflammatory mediators such as tumor necrosis factor (TNF-α), macrophage inhibitory protein (MIP-2), and interleukin-1β (IL-1β) [150]. Liu et al. also agreed that the toxicity of AgNPs was mediated by oxidative stress and by boosting the production of ROS which resulted in damaged cell membrane, disturbed cell cycle progression and its arrest at S phase ending with apoptosis [149] while other studies reported that AgNPs induced cytotoxicity and DNA damage without any elevation in the production of ROS which opens the door for further studies to explain their toxicity mechanism [147].

It is worth to mention that the size-toxicity relationship was not limited to AgNPs but it was deeply investigated with numerous types of NPs. For example, Pan et al. have reported that larger AuNPs (15 nm) were not cytotoxic even when they were used at 60-fold concentration compared to the smaller NPs (1.4 nm). According to their results, even the toxicity mechanism could vary depending on the size of the applied NPs (apoptosis with 1.2 nm and necrosis with 1.4 nm) [151].

3.2.4. Released ions

Till now it is controversial whether the toxicity of some metallic nanoparticles could be attributed to NPs themselves or the ions releasing from them. Several kinds of research have been conducted to obtain a better insight to this unresolved question. One of these studies concluded that treatment with both forms of silver, nano and ionic, resulted in decreased viability and malfunction of hepatic cells with AgNPs displaying the weaker toxic effect. Although surface oxidation of AgNPs, as a result of contacting with cell culture medium or proteins in the cytoplasm may occur hence releasing Ag^+ ions, and increasing toxicity [113]. Changes in human hepatoma cell morphology like cellular shrinkage and pseudopodic irregular shape were also reported in addition to highly damaged chromosomes, induced stress genes coding metallothionein (MT1H, NT1X, MT2A) and heat shock protein (HSPA4L and HSPH1) resulting in reduced cell viability. This study suggested that both ionic Ag^+ and AgNPs (7–10 nm) contribute to these adverse outcomes [116].

Similar results were indicated by Lojk et al. with AgNPs (10–30 nm) causing a significant drop in the number of living cells and minor changes in the cell cycle, but in contrast to Vrček study, AgNPs were not internalized into the cells nor deposited on their surfaces due to their high stability and low sedimentation suggesting that toxicity may be caused by the release of Ag^+ ions [117].

3.3. Quantum dots (QDs)

QDs represent a special type of inorganic NPs thus they require special attention and precise investigation arising from their diverse

structures and unique properties. QDs are nano-sized, semiconductor crystals with excellent optical properties. They could be divided into 12 different types based on their comprised elements and their position in the periodic table. Basically, they are consisting of heavy metal core (CdSe, CdS, ZnSe, PbSe, etc.) with surrounding shell (ZnS, SiO_2, etc.) in purpose of decreasing toxicity or enhancing their characteristics [47,152]. These remarkable features (small size, optical properties, diversity in chemical structure) introduce them as attractive candidates with exceptional performance when being employed for biomedical purposes such as fluorescent probes in bioimaging [153,154], photosensitizers in photodynamic therapy (PDT) for cancer treatment [154,155], biosensors [154,156,157], targeted therapy and drug delivery [158,159].

3.3.1. Surface properties (chemistry, coating, charge)

Cytotoxicity of inorganic NPs correlates with intracellular levels, rather than extracellular ones which depend on many factors like surface coating. Non-PEG-substituted CdSe/CdS QDs showed the strongest toxic effects while PEGylated QDs led to decreased cellular uptake and thus decreased cell death. In this case, most studies would have suggested that the PEGylated QDs were the safest option. However, intracellular-exposure studies suggested that the bare and the PEGylated QDs are equal in cytotoxicity when the exposure concentrations led to equivalent cellular uptake of QDs [119].

Surface coating could affect intracellular levels and control the release of ions from NPs. On the other hand, it could be affected by the route of exposure as oral administration will expose NPs to an acidic environment in stomach. Increased cytotoxicity of CdSe QDs with ZnS shell and hydrophilic coating after being treated with simulated gastric fluid (SGF) was observed in a concentration ranging from 0.84 to 4.2 nmol while untreated QDs (0.84–105 nmol) did not cause the same effect due to the presence of coating which prevents the leakage of toxic Cd^{2+} ions. These same protective shell/coating could not withstand gastric fluid leaving the CdSe core exposed, allowing Cd^{2+} ions to be released and to increase toxicity (The relative viability of Caco-2 cells decreased from 90 % to 53 % when incubating with QDs which were not treated and QDs treated with SGF, respectively [109]). Furthermore, Sukhanova et al. investigated the impact of surface charge on the toxicity of QDs on WI-38 normal human fibroblasts and SK-BR-3 human breast cancer cells, after modifying the surface with different ligands with different charges. Low negatively-charged QDs were the most toxic among others while the positively-charged ones appeared to be the safest although they were able to penetrate cells and accumulate inside [160].

3.3.2. Size

Similar to other types of NPs, size is one of the most significant factors affecting the toxicity of QDs. In addition to surface charge, Sukhanova et al. have also investigated the impact of size on the toxicity of QDs on WI-38 normal human fibroblasts and SK-BR-3 human breast cancer cells, concluding that the smaller QDs showed higher toxicity for both cell lines. This was explained by their higher ability to penetrate cells compared to the larger ones, inducing death by oxidizing the internal medium components [160]. André et al. also confirmed the importance of size factor determining toxicity. As NPs usually tend to aggregate within biological media, they investigated the toxicity of QDs and their aggregates toward human and trout hepatocytes demonstrating that QDs were more toxic than their large aggregates which presented decreased toxicity when their size was increasing [161]. This size-dependent toxic effect was also reported by Zhang et al. using same type of QDs and with the same cell lines (HepG2 cell line) [162] and by Hassan et al. with E. coli suggesting that this toxicity could be invested in a useful way in the development of antimicrobial agents for several industries (food, textiles, wound dressings, etc.) [163].

4. Limitations, concerns and future perspectives

Formulating safe inorganic nanoparticles as a new discipline in drug delivery systems should consider several aspects of different specialties including pharmaceutical technology, toxicology and biopharmacy. Physicochemical properties are among these aspects that should be considered during formulation due to their direct impact on toxicological profile (Fig. 4).

The same properties could display different (positive or negative) effects on NPs toxicity due to the differences in the applied experimental condition like:

- The used cell line in vitro which could be totally variant in their sensitivity/uptake mechanism and this uptake could be affected by the size of NPs and their agglomerates/aggregates (for example, large aggregates of TiO_2 NPs were more toxic due to their size that was more appropriate for cell uptake [114] while large aggregates of SiO_2 NPs were safer because their size led to a lack of significant internalization and deposition of them only on the cell surface [117]).
- The used concentrations/time of exposure which differ between studies and could be the responsible reason of different outcomes (for example, some NPs could display the toxic effect only after chronic exposure and/or at high concentrations). This could explain why acute exposure/low concentrations studies may classified them as safe [117].
- The used route of administration/exposure that could affect toxicity indirectly in many different ways (for example, by affecting the size of agglomerates upon ingestion [108] or by disturbing the surface coating which has a direct impact on cellular uptake, intracellular levels and ions leakage [109]).
- The diversity of used methods/assays which reflect different indicators of toxicity like cell viability, oxidative stress, apoptosis, inflammatory effects, genotoxicity, etc. (Table 3)
- The difficulty to establish a good and trusted correlation between in vivo/in vitro study (for example, some in vitro studies confirm toxicity after using high concentrations that do not reflect what cells in the living organism could be really exposed to Ref. [69]. On the other hand, in vitro studies could dismiss toxicological effects of some NPs that appear only after accumulation in the body [117]). We should also mention that some inorganic NPs could be considered as safe in vitro without considering the modifications they could expose to in vivo (for example, after digestion) that may give them secondary characteristics different from the original ones turning them into toxic materials [108,109].

Regarding these conflicting results, it is of crucial importance to establish a unified procedure to investigate the toxicity of inorganic nanoparticles. This will make comparison between the toxicity of different types of NPs (or even same type with different characteristics) more logical and will enable researchers to build a stronger background with profound knowledge regarding formulation of inorganic nanoparticles with maximum benefits and minimal toxicity.

Finally, it is worth to highlight a fundamental concern regarding these nanomaterials which is ecotoxicity. Undoubtedly, the increased worldwide use of inorganic NPs, and their commercial marketing in almost every domain are affecting the surrounding environment as they are affecting the public health. The fact that the current knowledge is suffering a serious lack of sufficient studies discussing the ecological impact of these emerging materials are creating a major obstacle to design safe nanomaterials not just to human but also to the eco-system. However, several attempts have been made to clear this uncertainty regarding the environmental effects of these NPs. In this context, Nogueira et al. reported that Al_2O_3 NPs could be the suitable and harmless replacement for several materials (with similar properties) as these NPs do not pose a serious environmental risk especially toward

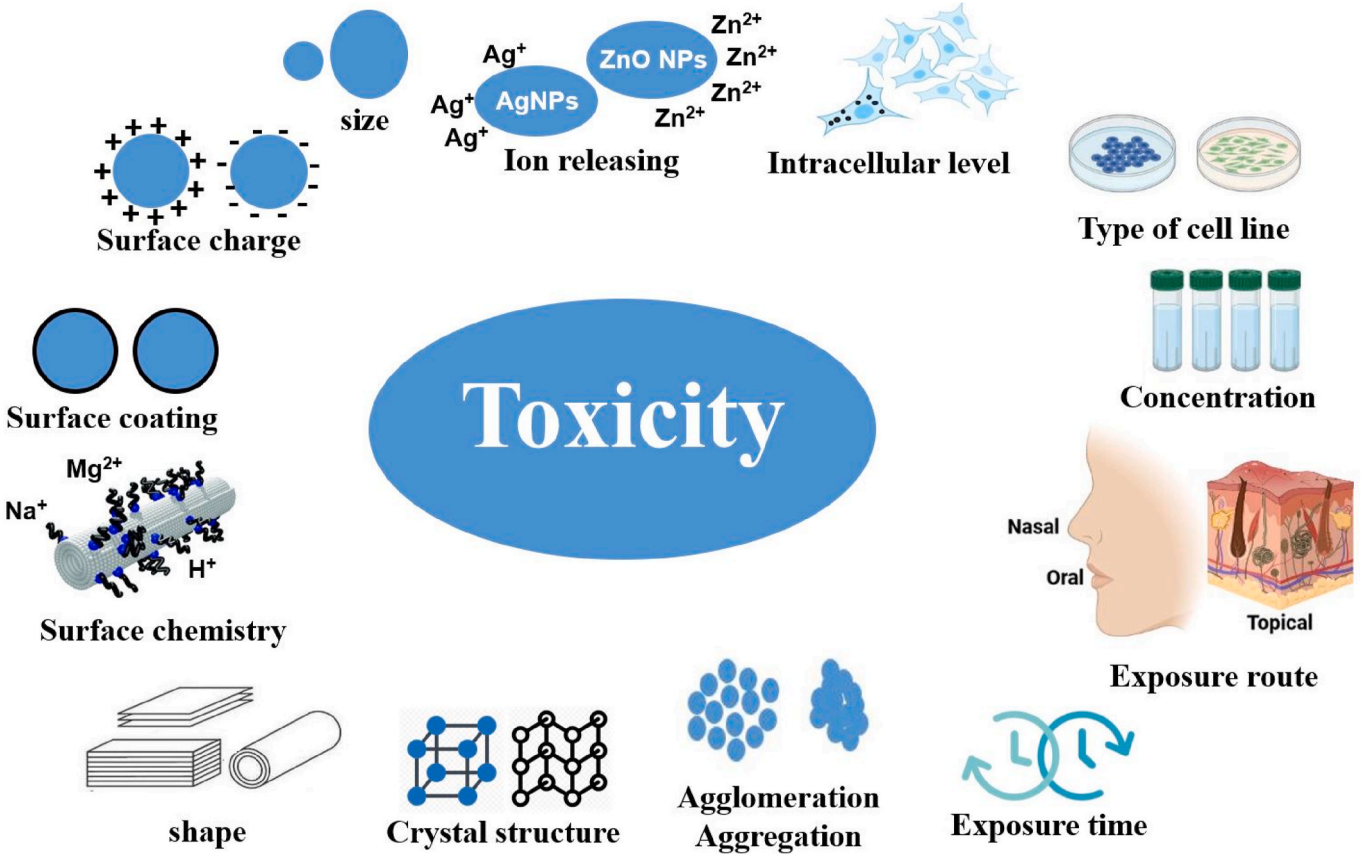

Fig. 4. The most important physicochemical properties and factors affecting toxicity of inorganic nanoparticles.
This figure represents the most significant factors affecting the toxicity of inorganic NPs which are: morphology (shape), surface properties (chemistry, coating, charge), size, released ions, intracellular level, type of cell line, concentration/time of exposure, route of entry, crystal structure and agglomeration/aggregation state.

aquatic organisms [136]. On the other hand, Demir et al. examined ecotoxicity of Fe_2O_3 NPs on two types of marine algae species, and reported their toxic impact evidenced by the occurred growth suppression even with the lowest applied concentrations. This toxic effect on such important organisms in the food chain is presenting a serious environmental issue regarding marine media [138]. Lei et al. demonstrated that this ecotoxicity of iron-based NPs depends on several factors such as particle size, crystal structure, etc. This toxicity was mainly attributed to oxidative stress induction and physical NPs-cells interaction while NPs dissolution had no significant effect. Surprisingly, according to this study, environmental aging weakened the toxicity effect of these NPs toward green algae [139]. Furthermore, several studies suggested environmentally-friendly method to reduce the hazards accompanying the preparation of inorganic NPs. Velidandi et al. proposed an eco-friendly method for fabricating of bimetallic NPs (Ag–Cu and Ag–Zn) and employed *Artemia nauplii* as animal model for assessing their toxicological impact. Ag–Zn appeared to be more toxic, causing 100 % mortality after 36 h of exposure with concentration of 100 μg/ml [164]. These contracted results, once again, confirm the urgent need for additional investigations to understand the behavior of these NPs toward different environmental aspects in order to produce hazard-free and eco-friendly materials.

5. Conclusion

The tremendous progress in the field of nanotechnology with the accelerated spread of investing it in many aspects of human life pose a significant need to establish a clear guideline regarding safety. Toxicity of inorganic NPs can be influenced by numerous factors including particle size, routes of exposure, crystal structure, surface chemistry, surface coating, morphology, etc., hence controlling these factors could offer a perfect approach to design safer nano carriers.

One of the most recommended method to reduce toxicity is manipulating surface properties by controlling the ions type on the surface (for example, TiO_2 nanotubes with Na^+ ions on their surface appeared to be less toxic than TNTs with H^+ or Mg^{2+}). Another possible way is surface functionalization such as PEGylation which minimizes the formation of protein corona in purpose of reducing cellular internalization and thus toxic effects. Surface coating using other materials like lipids could be also a good choice to reduce the toxicity related to ions releasing from NPs like Zn^{2+}, Ag^+, Fe^{3+} and Cd^{2+} especially if the route of exposure (for example, digestion) is affecting NPs original characteristics and increasing their possibility to dissolve, release ions and induce toxicity.

Smaller particles are considered to be more toxic than larger ones due to their easier uptake unless larger size is more appropriate for cell internalization (which is strongly associated with the type of targeted cell lines). Researchers should also give more attention to purification procedures after manufacturing as toxicity could sometimes be attributed to synthesis impurities rather than NPs themselves. Moreover, the determination of different crystalline structures (if existing) to compare their toxicity (for example anatase TiO_2 NPs appeared to be more toxic than other two crystal structures) seems to be important. Morphology is also one of the significant factors affecting toxicity (for example, TiO_2 nanotubes appeared to be more toxic than other shapes like rods, ribbons and wires, AuNPs stars showed higher toxicity than rods and spheres).

Finally, the desired formulation could not be completed and the targeted mission could not be achieved without establishing a comprehensive understanding of NPs pharmacokinetics as a fundamental step in their safety/toxicity assessment. This task requires serious

collaboration between scientists from several academic disciplines, regulatory bodies and manufacturers to transfer these novel NPs from laboratories to existing market.

Funding

This research was funded by Project no. TKP2021-EGA-32 and has been implemented with the support provided by the Ministry of Innovation and Technology of Hungary from the National Research, Development and Innovation Fund, financed under the TKP2021-EGA funding scheme. The publication was supported by University of Szeged Open Access Fund. Grant ID: 6913.

CRediT authorship contribution statement

Ranim Saker: Writing – original draft, Methodology, Formal analysis, Conceptualization. **Géza Regdon:** Writing – review & editing, Supervision, Conceptualization. **Tamás Sovány:** Writing – review & editing, Supervision, Methodology, Funding acquisition, Conceptualization.

Declaration of competing interest

The authors declare no conflict of interest. The funding party had no influence ont he content of the manuscript.

Data availability

No data was used for the research described in the article.

References

[1] S. Bayda, M. Adeel, T. Tuccinardi, M. Cordani, F. Rizzolio, The history of nanoscience and nanotechnology: from chemical–physical applications to nanomedicine, Molecules 25 (2019) 112, 10.3390%2Fmolecules25010112.
[2] J. Potočnik, Commission recommendation of 18 October 2011 on the definition of nanomaterial (2011/696/EU), Off. J. Eur. Union 275 (2011) 38–40.
[3] J. Lan, Overview of application of nanomaterials in medical domain, Contrast Media Mol. Imaging 2022 (2022) 3507383, https://doi.org/10.1155/2022/3507383.
[4] M.K. Greene, M.C. Johnston, C.J. Scott, Nanomedicine in pancreatic cancer: current status and future opportunities for overcoming therapy resistance, Cancers 13 (2021) 6175, https://doi.org/10.3390/cancers13246175.
[5] V. De Matteis, Exposure to inorganic nanoparticles: routes of entry, immune response, biodistribution and in vitro/in vivo toxicity evaluation, Toxics 5 (2017) 29, https://doi.org/10.3390/toxics5040029.
[6] G. Unnikrishnan, A. Joy, M. Megha, E. Kolanthai, M. Senthilkumar, Exploration of inorganic nanoparticles for revolutionary drug delivery applications: a critical review, Discov Nano 18 (2023) 157, https://doi.org/10.1186/s11671-023-03943-0.
[7] B.H. Alshammari, M.M.A. Lashin, M.A. Mahmood, F.S. Al-Mubaddel, N. Ilyas, N. Rahman, M. Sohail, A. Khan, S.S. Abdullaev, R. Khan, Organic and inorganic nanomaterials: fabrication, properties and applications, RSC Adv. 13 (2023) 13735–13785, https://doi.org/10.1039/d3ra01421e.
[8] V. Natesan, S.J. Kim, The trend of organic based nanoparticles in the treatment of diabetes and its perspectives, Biomol Ther (Seoul) 31 (2023) 16–26, https://doi.org/10.4062/biomolther.2022.080.
[9] G. Vargas-Nadal, M. Kober, A. Nsamela, F. Terenziani, C. Sissa, S. Pescina, F. Sonvico, A.M. Gazzali, H.A. Wahab, L. Grisanti, et al., Fluorescent multifunctional organic nanoparticles for drug delivery and bioimaging: a tutorial review, Pharmaceutics 14 (2022) 2498, https://doi.org/10.3390/pharmaceutics14112498.
[10] M. Hussein Kamareddine, Y. Ghosn, A. Tawk, C. Elia, W. Alam, J. Makdessi, Farhat, S.J.T.i.C.R.; Treatment, Organic nanoparticles as drug delivery systems and their potential role in the treatment of chronic myeloid leukemia, Technol. Cancer Res. Treat. 18 (2019) 1533033819879902, 10.1177%2F1533033819879902.
[11] L. Salvioni, L. Morelli, E. Ochoa, M. Labra, L. Fiandra, L. Palugan, D. Prosperi, M. Colombo, The emerging role of nanotechnology in skincare, Adv. Colloid Interface Sci. 293 (2021) 102437, https://doi.org/10.1016/j.cis.2021.102437.
[12] H. Akel, I. Csoka, R. Ambrus, A. Bocsik, I. Grof, M. Meszaros, A. Szecsko, G. Kozma, S. Veszelka, M.A. Deli, et al., In vitro comparative study of solid lipid and PLGA nanoparticles designed to facilitate nose-to-brain delivery of insulin, Int. J. Mol. Sci. 22 (2021) 13258, https://doi.org/10.3390/ijms222413258.
[13] H. Akel, R. Ismail, G. Katona, F. Sabir, R. Ambrus, I. Csoka, A comparison study of lipid and polymeric nanoparticles in the nasal delivery of meloxicam: formulation, characterization, and in vitro evaluation, Int. J. Pharm. 604 (2021) 120724, https://doi.org/10.1016/j.ijpharm.2021.120724.
[14] M. Kalbacova, J. Macak, F. Schmidt-Stein, C. Mierke, P. Schmuki, TiO2 nanotubes: photocatalyst for cancer cell killing, Phys. Status Solidi Rapid Res. Lett. 2 (2008) 194–196, https://doi.org/10.1002/pssr.200802080.
[15] C. Mirjolet, A. Papa, G. Créhange, O. Raguin, C. Seignez, C. Paul, G. Truc, P. Maingon, N. Millot, The radiosensitization effect of titanate nanotubes as a new tool in radiation therapy for glioblastoma: a proof-of-concept, Radiother. Oncol. 108 (2013) 136–142, https://doi.org/10.1016/j.radonc.2013.04.004.
[16] Y. Wang, L. Yuan, C. Yao, J. Fang, M. Wu, Cytotoxicity evaluation of pH-controlled antitumor drug release system of titanium dioxide nanotubes, J. Nanosci. Nanotechnol. 15 (2015) 4143–4148, https://doi.org/10.1166/jnn.2015.9792.
[17] A. Loiseau, J. Boudon, A. Oudot, M. Moreau, R. Boidot, R. Chassagnon, N.M. Said, S. Roux, C. Mirjolet, N. Millot, Titanate nanotubes engineered with gold nanoparticles and docetaxel to enhance radiotherapy on xenografted prostate tumors, Cancers 11 (2019) 1962, https://doi.org/10.3390/cancers11121962.
[18] M.S. Wason, J. Colon, S. Das, S. Seal, J. Turkson, J. Zhao, C.H. Baker, Sensitization of pancreatic cancer cells to radiation by cerium oxide nanoparticle-induced ROS production, Nanomedicine 9 (2013) 558–569, https://doi.org/10.1016/j.nano.2012.10.010.
[19] M.S. Wason, H. Lu, L. Yu, S.K. Lahiri, D. Mukherjee, C. Shen, S. Das, S. Seal, J. Zhao, Cerium oxide nanoparticles sensitize pancreatic cancer to radiation therapy through oxidative activation of the JNK apoptotic pathway, Cancers 10 (2018) 303, https://doi.org/10.3390/cancers10090303.
[20] T. Jiang, B. Zhang, S. Shen, Y. Tuo, Z. Luo, Y. Hu, Z. Pang, X. Jiang, Tumor microenvironment modulation by cyclopamine improved photothermal therapy of biomimetic gold nanorods for pancreatic ductal adenocarcinomas, ACS Appl. Mater. Interfaces 9 (2017) 31497–31508, https://doi.org/10.1021/acsami.7b09458.
[21] S.X. Ren, B. Zhan, Y. Lin, D.S. Ma, H. Yan, Selenium nanoparticles dispersed in phytochemical exert anti-inflammatory activity by modulating catalase, GPx1, and COX-2 gene expression in a rheumatoid arthritis rat model, Med. Sci. Mon. Int. Med. J. Exp. Clin. Res. 25 (2019) 991–1000, https://doi.org/10.12659/MSM.912545.
[22] H. Rizwana, R.M. Aljowaie, F. Al Otibi, M.S. Alwahibi, S.A. Alharbi, S.A. Al Asmari, N.S. Aldosari, H.A. Aldehaish, Antimicrobial and antioxidant potential of the silver nanoparticles synthesized using aqueous extracts of coconut meat (Cocos nucifera L), Sci. Rep. 13 (2023) 16270, https://doi.org/10.1038/s41598-023-43384-4.
[23] H.J. Nelagadarnahalli, G.K. Jacob, D. Prakash, R.R. Iska, V.B.R. Iska, F. Ameen, U. M. Rajadurai, N. Polachi, J.A. Jacob, Optimization and fabrication of silver nanoparticles to assess the beneficial biological effects besides the inhibition of pathogenic microbes and their biofilms, Inorg. Chem. Commun. 156 (2023) 111140, https://doi.org/10.1016/j.inoche.2023.111140.
[24] F.M. Aldakheel, M.M.E. Sayed, D. Mohsen, M.H. Fagir, D.K. El Dein, Green synthesis of silver nanoparticles loaded hydrogel for wound healing; systematic review, Gels 9 (2023) 530, https://doi.org/10.3390/gels9070530.
[25] R. Saker, H. Shammout, G. Regdon Jr, T. Sovány, An overview of hydrothermally synthesized titanate nanotubes: the factors affecting preparation and their promising pharmaceutical applications, Pharmaceutics 16 (2024) 635, https://doi.org/10.3390/pharmaceutics16050635.
[26] B. Sipos, K. Pintye-Hódi, Z. Kónya, A. Kelemen, G. Regdon Jr, T. Sovány, Physicochemical characterisation and investigation of the bonding mechanisms of API-titanate nanotube composites as new drug carrier systems, Int. J. Pharm. 518 (2017) 119–129, https://doi.org/10.1016/j.ijpharm.2016.12.053.
[27] B. Sipos, K. Pintye-Hodi, G. Regdon Jr., Z. Konya, M. Viana, T. Sovany, Investigation of the compressibility and compactibility of titanate nanotube-API composites, Materials 11 (2018) 2582, https://doi.org/10.3390/ma11122582.
[28] B. Sipos, G. Regdon Jr, Z. Kónya, K. Pintye-Hódi, T. Sovány, Comparative study on the rheological properties and tablettability of various APIs and their composites with titanate nanotubes, Powder Technol. 321 (2017) 419–427, https://doi.org/10.1016/j.powtec.2017.08.012.
[29] S. Vidya, S. Mutalik, K.U. Bhat, P. Huilgol, K. Avadhani, Preparation of gold nanoparticles by novel bacterial exopolysaccharide for antibiotic delivery, Life Sci. 153 (2016) 171–179, https://doi.org/10.1016/j.lfs.2016.04.022.
[30] A.K. Kodoth, V.M. Ghate, S.A. Lewis, B. Prakash, V. Badalamoole, Pectin-based silver nanocomposite film for transdermal delivery of Donepezil, Int. J. Biol. Macromol. 134 (2019) 269–279, https://doi.org/10.1016/j.ijbiomac.2019.04.191.
[31] Y. Ranjous, G. Regdon Jr, K. Pintye-Hódi, T. Varga, I. Szenti, Z. Kónya, T. Sovány, Optimization of the production process and product quality of titanate nanotube–drug composites, Nanomaterials 9 (2019) 1406, https://doi.org/10.3390/nano9101406.
[32] Q. Guo, L. Jia, R. Zhang, X. Yang, In vitro and in vivo evaluation of ketotifen-gold nanoparticles laden contact lens for controlled drug delivery to manage conjunctivitis, J. Drug Deliv. Sci. Technol. 64 (2021) 102538, https://doi.org/10.1016/j.jddst.2021.102538.
[33] A.S. Silva, A.M. Sousa, R.P. Cabral, M.C. Silva, C. Costa, S.P. Miguel, V.D. B. Bonifacio, T. Casimiro, I.J. Correia, A. Aguiar-Ricardo, Aerosolizable gold nano-in-micro dry powder formulations for theragnosis and lung delivery, Int. J. Pharm. 519 (2017) 240–249, https://doi.org/10.1016/j.ijpharm.2017.01.032.
[34] X. Shan, X. Gong, J. Li, J. Wen, Y. Li, Z. Zhang, Current approaches of nanomedicines in the market and various stage of clinical translation, Acta Pharm. Sin. B 12 (2022) 3028–3048, https://doi.org/10.1016/j.apsb.2022.02.025.

[35] R.K. Thapa, J.O. Kim, Nanomedicine-based commercial formulations: current developments and future prospects, J Pharm Investig 53 (2023) 19–33, https://doi.org/10.1007/s40005-022-00607-6.
[36] F. Aflakian, F. Mirzavi, H.T. Aiyelabegan, A. Soleimani, J. Gholizadeh Navashenaq, I. Karimi-Sani, A. Rafati Zomorodi, R. Vakili-Ghartavol, Nanoparticles-based therapeutics for the management of bacterial infections: a special emphasis on FDA approved products and clinical trials, Eur. J. Pharmaceut. Sci. 188 (2023) 106515, https://doi.org/10.1016/j.ejps.2023.106515.
[37] F. Paladini, M. Pollini, Antimicrobial silver nanoparticles for wound healing application: progress and future trends, Materials 12 (2019) 2540, https://doi.org/10.3390/ma12162540.
[38] S.S. Mandal, D. Jose, A. Bhattacharyya, Role of surface chemistry in modulating drug release kinetics in titania nanotubes, Mater. Chem. Phys. 147 (2014) 247–253, https://doi.org/10.1016/j.matchemphys.2014.04.036.
[39] N. Khoshnood, A. Zamanian, A. Massoudi, Mussel-inspired surface modification of titania nanotubes as a novel drug delivery system, Mater. Sci. Eng. C 77 (2017) 748–754, https://doi.org/10.1016/j.msec.2017.03.293.
[40] C.C. Torres, C.H. Campos, C. Díáz, V.A. Jiménez, F. Vidal, L. Guzmán, J. B. Alderete, PAMAM-grafted TiO2 nanotubes as novel versatile materials for drug delivery applications, Mater. Sci. Eng. C 65 (2016) 164–171, https://doi.org/10.1016/j.msec.2016.03.104.
[41] Z. Wang, C. Xie, F. Luo, P. Li, X. Xiao, P25 nanoparticles decorated on titania nanotubes arrays as effective drug delivery system for ibuprofen, Appl. Surf. Sci. 324 (2015) 621–626, https://doi.org/10.1016/j.apsusc.2014.10.147.
[42] S.C. Coelho, D.P. Reis, M.C. Pereira, M.A.N. Coelho, Gold nanoparticles for targeting varlitinib to human pancreatic cancer cells, Pharmaceutics 10 (2018) 91, https://doi.org/10.3390/pharmaceutics10030091.
[43] S. Banihashem, M.N. Nezhati, H.A. Panahi, Synthesis of chitosan-grafted-poly(N-vinylcaprolactam) coated on the thiolated gold nanoparticles surface for controlled release of cisplatin, Carbohydr. Polym. 227 (2020) 115333, https://doi.org/10.1016/j.carbpol.2019.115333.
[44] C. Xu, Y. Yan, J. Tan, D. Yang, X. Jia, L. Wang, Y. Xu, S. Cao, S. Sun, Biodegradable nanoparticles of polyacrylic acid–stabilized amorphous CaCO3 for tunable pH-responsive drug delivery and enhanced tumor inhibition, Adv. Funct. Mater. 29 (2019) 1808146, https://doi.org/10.1002/adfm.201808146.
[45] S.P.H. Moghaddam, M. Yazdimamaghani, H. Ghandehari, Glutathione-sensitive hollow mesoporous silica nanoparticles for controlled drug delivery, J. Contr. Release 282 (2018) 62–75, https://doi.org/10.1016/j.jconrel.2018.04.032.
[46] S. Naz, M. Wang, Y. Han, B. Hu, L. Teng, J. Zhou, H. Zhang, J. Chen, Enzyme-responsive mesoporous silica nanoparticles for tumor cells and mitochondria multistage-targeted drug delivery, Int. J. Nanomed. 14 (2019) 2533–2542, https://doi.org/10.2147/IJN.S202210.
[47] K. Khalid, X. Tan, H.F. Mohd Zaid, Y. Tao, C. Lye Chew, D.T. Chu, M.K. Lam, Y. C. Ho, J.W. Lim, L. Chin Wei, Advanced in developmental organic and inorganic nanomaterial: a review, Bioengineered 11 (2020) 328–355, https://doi.org/10.1080/21655979.2020.1736240.
[48] M.V. Vaudagna, V. Aiassa, A. Marcotti, M.F.P. Beti, M.F. Constantín, M.F. Pérez, A. Zoppi, M.C. Becerra, Titanium Dioxide Nanoparticles in sunscreens and skin photo-damage. Development, synthesis and characterization of a novel biocompatible alternative based on their in vitro and in vivo study, J. Photochem. Photobiol., A 15 (2023) 100173, https://doi.org/10.1016/j.jpap.2023.100173.
[49] Y.-Y. Chen, Y.-H. Lee, B.-J. Wang, R.-J. Chen, Y.-J. Wang, Skin damage induced by zinc oxide nanoparticles combined with UVB is mediated by activating cell pyroptosis via the NLRP3 inflammasome–autophagy–exosomal pathway, Part. Fibre Toxicol. 19 (2022) 1–22, https://doi.org/10.1186/s12989-021-00443-w.
[50] H. Shi, R. Magaye, V. Castranova, J. Zhao, Titanium dioxide nanoparticles: a review of current toxicological data, Part. Fibre Toxicol. 10 (2013) 15, https://doi.org/10.1186/1743-8977-10-15.
[51] N. Sadrieh, A.M. Wokovich, N.V. Gopee, J. Zheng, D. Haines, D. Parmiter, P. H. Siitonen, C.R. Cozart, A.K. Patri, S.E. McNeil, et al., Lack of significant dermal penetration of titanium dioxide from sunscreen formulations containing nano- and submicron-size TiO2 particles, Toxicol. Sci. 115 (2010) 156–166, https://doi.org/10.1093/toxsci/kfq041.
[52] M. Senzui, T. Tamura, K. Miura, Y. Ikarashi, Y. Watanabe, M. Fujii, Study on penetration of titanium dioxide (TiO2) nanoparticles into intact and damaged skin in vitro, J. Toxicol. Sci. 35 (2010) 107–113, https://doi.org/10.2131/jts.35.107.
[53] P. Filipe, J. Silva, R. Silva, J.C. De Castro, M.M. Gomes, L. Alves, R. Santus, T. Pinheiro, Stratum corneum is an effective barrier to TiO2 and ZnO nanoparticle percutaneous absorption, Skin Pharmacol. Physiol. 22 (2009) 266–275, https://doi.org/10.1159/000235554.
[54] F. Rancan, Q. Gao, C. Graf, S. Troppens, S. Hadam, S. Hackbarth, C. Kembuan, U. Blume-Peytavi, E. Ruhl, J. Lademann, et al., Skin penetration and cellular uptake of amorphous silica nanoparticles with variable size, surface functionalization, and colloidal stability, ACS Nano 6 (2012) 6829–6842, https://doi.org/10.1021/nn301622h.
[55] C. Bennat, C. Müller-Goymann, Skin penetration and stabilization of formulations containing microfine titanium dioxide as physical UV filter, Int. J. Cosmet. Sci. 22 (2000) 271–283, https://doi.org/10.1046/j.1467-2494.2000.00009.x.
[56] P.U. Jani, D.E. McCarthy, A.T. Florence, Titanium dioxide (rutile) particle uptake from the rat GI tract and translocation to systemic organs after oral administration, Int. J. Pharm. 105 (1994) 157–168, https://doi.org/10.1016/0378-5173(94)90461-8.
[57] C. Schleh, M. Semmler-Behnke, J. Lipka, A. Wenk, S. Hirn, M. Schaffler, G. Schmid, U. Simon, W.G. Kreyling, Size and surface charge of gold nanoparticles determine absorption across intestinal barriers and accumulation in secondary target organs after oral administration, Nanotoxicology 6 (2012) 36–46, https://doi.org/10.3109/17435390.2011.552811.
[58] Y. Ranjous, D. Kósa, Z. Ujhelyi, G. Regdon jr, K.A. Nagy, I. Szenti, Z. Kónya, I. Bácskay, T. Sovány, Evaluation of the permeability and in vitro cytotoxicity of functionalized titanate nanotubes on Caco-2 cell line, Acta Pharm. Hung. 91 (2021) 31–39, https://doi.org/10.33892/aph.2021.91.31-39.
[59] H.S. Choi, Y. Ashitate, J.H. Lee, S.H. Kim, A. Matsui, N. Insin, M.G. Bawendi, M. Semmler-Behnke, J.V. Frangioni, A. Tsuda, Rapid translocation of nanoparticles from the lung airspaces to the body, Nat. Biotechnol. 28 (2010) 1300–1303, https://doi.org/10.1038/nbt.1696.
[60] J. Wang, Y. Liu, F. Jiao, F. Lao, W. Li, Y. Gu, Y. Li, C. Ge, G. Zhou, B. Li, et al., Time-dependent translocation and potential impairment on central nervous system by intranasally instilled TiO(2) nanoparticles, Toxicology 254 (2008) 82–90, https://doi.org/10.1016/j.tox.2008.09.014.
[61] J. Wang, C. Chen, Y. Liu, F. Jiao, W. Li, F. Lao, Y. Li, B. Li, C. Ge, G. Zhou, et al., Potential neurological lesion after nasal instillation of TiO(2) nanoparticles in the anatase and rutile crystal phases, Toxicol. Lett. 183 (2008) 72–80, https://doi.org/10.1016/j.toxlet.2008.10.001.
[62] S. Md, R.A. Khan, G. Mustafa, K. Chuttani, S. Baboota, J.K. Sahni, J. Ali, Bromocriptine loaded chitosan nanoparticles intended for direct nose to brain delivery: pharmacodynamic, pharmacokinetic and scintigraphy study in mice model, Eur. J. Pharmaceut. Sci. 48 (2013) 393–405, https://doi.org/10.1016/j.ejps.2012.12.007.
[63] T. Cedervall, I. Lynch, S. Lindman, T. Berggård, E. Thulin, H. Nilsson, K. A. Dawson, S. Linse, Understanding the nanoparticle–protein corona using methods to quantify exchange rates and affinities of proteins for nanoparticles, Proc. Natl. Acad. Sci. USA 104 (2007) 2050–2055, https://doi.org/10.1073/pnas.0608582104.
[64] H.J. Yen, S.H. Hsu, C.L. Tsai, Cytotoxicity and immunological response of gold and silver nanoparticles of different sizes, Small 5 (2009) 1553–1561, https://doi.org/10.1002/smll.200900126.
[65] Y. Qiu, Y. Liu, L. Wang, L. Xu, R. Bai, Y. Ji, X. Wu, Y. Zhao, Y. Li, C. Chen, Surface chemistry and aspect ratio mediated cellular uptake of Au nanorods, Biomaterials 31 (2010) 7606–7619, https://doi.org/10.1016/j.biomaterials.2010.06.051.
[66] A. Lesniak, F. Fenaroli, M.P. Monopoli, C. Aberg, K.A. Dawson, A. Salvati, Effects of the presence or absence of a protein corona on silica nanoparticle uptake and impact on cells, ACS Nano 6 (2012) 5845–5857, https://doi.org/10.1021/nn300223w.
[67] A. Lesniak, A. Campbell, M.P. Monopoli, I. Lynch, A. Salvati, K.A. Dawson, Serum heat inactivation affects protein corona composition and nanoparticle uptake, Biomaterials 31 (2010) 9511–9518, https://doi.org/10.1016/j.biomaterials.2010.09.049.
[68] C. Cruje, D. Chithrani, Polyethylene glycol density and length affects nanoparticle uptake by cancer cells, J. Nano Res. 1 (2014), https://doi.org/10.15406/jnmr.2014.01.00006.
[69] A. Kurtz-Chalot, C. Villiers, J. Pourchez, D. Boudard, M. Martini, P.N. Marche, M. Cottier, V. Forest, Impact of silica nanoparticle surface chemistry on protein corona formation and consequential interactions with biological cells, Mater. Sci. Eng., C 75 (2017) 16–24, https://doi.org/10.1016/j.msec.2017.02.028.
[70] D. Simberg, J.-H. Park, P.P. Karmali, W.-M. Zhang, S. Merkulov, K. McCrae, S. N. Bhatia, M. Sailor, E. Ruoslahti, Differential proteomics analysis of the surface heterogeneity of dextran iron oxide nanoparticles and the implications for their in vivo clearance, Biomaterials 30 (2009) 3926–3933, https://doi.org/10.1016/j.biomaterials.2009.03.056.
[71] J. Lipka, M. Semmler-Behnke, R.A. Sperling, A. Wenk, S. Takenaka, C. Schleh, T. Kissel, W.J. Parak, W.G. Kreyling, Biodistribution of PEG-modified gold nanoparticles following intratracheal instillation and intravenous injection, Biomaterials 31 (2010) 6574–6581, https://doi.org/10.1016/j.biomaterials.2010.05.009.
[72] E. Fabian, R. Landsiedel, L. Ma-Hock, K. Wiench, W. Wohlleben, B. van Ravenzwaay, Tissue distribution and toxicity of intravenously administered titanium dioxide nanoparticles in rats, Arch. Toxicol. 82 (2008) 151–157, https://doi.org/10.1007/s00204-007-0253-y.
[73] J. Chen, X. Dong, J. Zhao, G. Tang, In vivo acute toxicity of titanium dioxide nanoparticles to mice after intraperitoneal injection, J. Appl. Toxicol. 29 (2009) 330–337, https://doi.org/10.1002/jat.1414.
[74] N. Kamal, A.H. Zaki, A.A. El-Shahawy, O.M. Sayed, S.I. El-Dek, Changing the morphology of one-dimensional titanate nanostructures affects its tissue distribution and toxicity, Toxicol. Ind. Health 36 (2020) 272–286, https://doi.org/10.1177/0748233720921693.
[75] R. Kumar, I. Roy, T.Y. Ohulchanskky, L.A. Vathy, E.J. Bergey, M. Sajjad, P. N. Prasad, In vivo biodistribution and clearance studies using multimodal organically modified silica nanoparticles, ACS Nano 4 (2010) 699–708, https://doi.org/10.1021/nn901146y.
[76] Q. He, Z. Zhang, F. Gao, Y. Li, J. Shi, In vivo biodistribution and urinary excretion of mesoporous silica nanoparticles: effects of particle size and PEGylation, Small 7 (2011) 271–280, https://doi.org/10.1002/smll.201001459.
[77] Y. Xue, S. Zhang, Y. Huang, T. Zhang, X. Liu, Y. Hu, Z. Zhang, M. Tang, Acute toxic effects and gender-related biokinetics of silver nanoparticles following an intravenous injection in mice, J. Appl. Toxicol. 32 (2012) 890–899, https://doi.org/10.1002/jat.2742.
[78] K. Dziendzikowska, J. Gromadzka-Ostrowska, A. Lankoff, M. Oczkowski, A. Krawczynska, J. Chwastowska, M. Sadowska-Bratek, E. Chajduk, M. Wojewodzka, M. Dusinska, et al., Time-dependent biodistribution and

excretion of silver nanoparticles in male Wistar rats, J. Appl. Toxicol. 32 (2012) 920–928, https://doi.org/10.1002/jat.2758.
[79] I. Takeuchi, S. Nobata, N. Oiri, K. Tomoda, K. Makino, Biodistribution and excretion of colloidal gold nanoparticles after intravenous injection: effects of particle size, Bio Med. Mater. Eng. 28 (2017) 315–323, https://doi.org/10.3233/BME-171677.
[80] W.H. De Jong, W.I. Hagens, P. Krystek, M.C. Burger, A.J. Sips, R.E. Geertsma, Particle size-dependent organ distribution of gold nanoparticles after intravenous administration, Biomaterials 29 (2008) 1912–1919, https://doi.org/10.1016/j.biomaterials.2007.12.037.
[81] G. Sonavane, K. Tomoda, K. Makino, Biodistribution of colloidal gold nanoparticles after intravenous administration: effect of particle size, Colloids Surf. B Biointerfaces 66 (2008) 274–280, https://doi.org/10.1016/j.colsurfb.2008.07.004.
[82] C.H. Li, C.C. Shen, Y.W. Cheng, S.H. Huang, C.C. Wu, C.C. Kao, J.W. Liao, J. J. Kang, Organ biodistribution, clearance, and genotoxicity of orally administered zinc oxide nanoparticles in mice, Nanotoxicology 6 (2012) 746–756, https://doi.org/10.3109/17435390.2011.620717.
[83] A. De, S. Ghosh, M. Chakrabarti, I. Ghosh, R. Banerjee, A. Mukherjee, Effect of low-dose exposure of aluminium oxide nanoparticles in Swiss albino mice: histopathological changes and oxidative damage, Toxicol. Ind. Health 36 (2020) 567–579, https://doi.org/10.1177/0748233720936828.
[84] W.H. Organization, Titanium-Environmental Health Criteria 24, 1982.
[85] B. Borak, P. Biernat, A. Prescha, A. Baszczuk, J. Pluta, In vivo study on the biodistribution of silica particles in the bodies of rats, Adv. Clin. Exp. Med. 21 (2012) 13–18.
[86] H. Tang, S.T. Yang, Y.F. Yang, D.M. Ke, J.H. Liu, X. Chen, H. Wang, Y. Liu, Blood clearance, distribution, transformation, excretion, and toxicity of near-infrared quantum dots Ag2Se in mice, ACS Appl. Mater. Interfaces 8 (2016) 17859–17869, https://doi.org/10.1021/acsami.6b05057.
[87] H.S. Choi, W. Liu, P. Misra, E. Tanaka, J.P. Zimmer, B. Itty Ipe, M.G. Bawendi, J. V. Frangioni, Renal clearance of quantum dots, Nat. Biotechnol. 25 (2007) 1165–1170, https://doi.org/10.1038/nbt1340.
[88] J.H. Lee, Y.S. Kim, K.S. Song, H.R. Ryu, J.H. Sung, J.D. Park, H.M. Park, N. W. Song, B.S. Shin, D. Marshak, Biopersistence of silver nanoparticles in tissues from Sprague–Dawley rats, Part. Fibre Toxicol. 10 (2013) 1–14, https://doi.org/10.1186/1743-8977-10-36.
[89] J.Y. Wang, J. Chen, J. Yang, H. Wang, X. Shen, Y.M. Sun, M. Guo, X.D. Zhang, Effects of surface charges of gold nanoclusters on long-term in vivo biodistribution, toxicity, and cancer radiation therapy, Int. J. Nanomed. 11 (2016) 3475–3485, https://doi.org/10.2147/IJN.S106073.
[90] Y. Li, J. Li, J. Yin, W. Li, C. Kang, Q. Huang, Q. Li, Systematic influence induced by 3 nm titanium dioxide following intratracheal instillation of mice, J. Nanosci. Nanotechnol. 10 (2010) 8544–8549, https://doi.org/10.1166/jnn.2010.2690.
[91] D. Liu, B. Lin, W. Shao, Z. Zhu, T. Ji, C. Yang, In vitro and in vivo studies on the transport of PEGylated silica nanoparticles across the blood–brain barrier, ACS Appl. Mater. Interfaces 6 (2014) 2131–2136, https://doi.org/10.1021/am405219u.
[92] L. Chen, R.A. Yokel, B. Hennig, M. Toborek, Manufactured aluminum oxide nanoparticles decrease expression of tight junction proteins in brain vasculature, J. Neuroimmune Pharmacol. 3 (2008) 286–295, https://doi.org/10.1007/s11481-008-9131-5.
[93] Y. Morishita, Y. Yoshioka, H. Satoh, N. Nojiri, K. Nagano, Y. Abe, H. Kamada, S. Tsunoda, H. Nabeshi, T. Yoshikawa, et al., Distribution and histologic effects of intravenously administered amorphous nanosilica particles in the testes of mice, Biochem. Biophys. Res. Commun. 420 (2012) 297–301, https://doi.org/10.1016/j.bbrc.2012.02.153.
[94] T.X. Garcia, G.M. Costa, L.R. Franca, M.C. Hofmann, Sub-acute intravenous administration of silver nanoparticles in male mice alters Leydig cell function and testosterone levels, Reprod. Toxicol. 45 (2014) 59–70, https://doi.org/10.1016/j.reprotox.2014.01.006.
[95] P. Wick, A. Malek, P. Manser, D. Meili, X. Maeder-Althaus, L. Diener, P.A. Diener, A. Zisch, H.F. Krug, U. von Mandach, Barrier capacity of human placenta for nanosized materials, Environ. Health Perspect. 118 (2010) 432–436, https://doi.org/10.1289/ehp.0901200.
[96] K. Takeda, K.-i. Suzuki, A. Ishihara, M. Kubo-Irie, R. Fujimoto, M. Tabata, S. Oshio, Y. Nihei, T. Ihara, M. Sugamata, Nanoparticles transferred from pregnant mice to their offspring can damage the genital and cranial nerve systems, J. Health Sci. 55 (2009) 95–102, https://doi.org/10.1248/jhs.55.95.
[97] K. Yamashita, Y. Yoshioka, K. Higashisaka, K. Mimura, Y. Morishita, M. Nozaki, T. Yoshida, T. Ogura, H. Nabeshi, K. Nagano, et al., Silica and titanium dioxide nanoparticles cause pregnancy complications in mice, Nat. Nanotechnol. 6 (2011) 321–328, https://doi.org/10.1038/nnano.2011.41.
[98] E. Feschet-Chassot, V. Raspal, Y. Sibaud, O. Awitor, F. Bonnemoy, J. Bonnet, J. Bohatier, Tunable functionality and toxicity studies of titanium dioxide nanotube layers, Thin Solid Films 519 (2011) 2564–2568, https://doi.org/10.1016/j.tsf.2010.12.184.
[99] M.G. Ammendolia, F. Iosi, F. Maranghi, R. Tassinari, F. Cubadda, F. Aureli, A. Raggi, F. Superti, A. Mantovani, B. De Berardis, Short-term oral exposure to low doses of nano-sized TiO(2) and potential modulatory effects on intestinal cells, Food Chem. Toxicol. 102 (2017) 63–75, https://doi.org/10.1016/j.fct.2017.01.031.
[100] F. Fenyvesi, Z. Konya, Z. Razga, M. Vecsernyes, P. Kasa Jr., K. Pintye-Hodi, I. Bacskay, Investigation of the cytotoxic effects of titanate nanotubes on Caco-2 cells, AAPS PharmSciTech 15 (2014) 858–861, https://doi.org/10.1208/s12249-014-0115-x.
[101] F. Brandao, N. Fernandez-Bertolez, F. Rosario, M.J. Bessa, S. Fraga, E. Pasaro, J. P. Teixeira, B. Laffon, V. Valdiglesias, C. Costa, Genotoxicity of TiO(2) nanoparticles in four different human cell lines (A549, HEPG2, A172 and SH-SY5Y), Nanomaterials 10 (2020) 412, https://doi.org/10.3390/nano10030412.
[102] M.J. Bessa, C. Costa, J. Reinosa, C. Pereira, S. Fraga, J. Fernández, M.A. Bañares, J.P. Teixeira, Moving into advanced nanomaterials. Toxicity of rutile TiO2 nanoparticles immobilized in nanokaolin nanocomposites on HepG2 cell line, Toxicol. Appl. Pharmacol. 316 (2017) 114–122, https://doi.org/10.1016/j.taap.2016.12.018.
[103] S. Wadhwa, C. Rea, P. O'Hare, A. Mathur, S.S. Roy, P.S. Dunlop, J.A. Byrne, G. Burke, B. Meenan, J.A. McLaughlin, Comparative in vitro cytotoxicity study of carbon nanotubes and titania nanostructures on human lung epithelial cells, J. Hazard Mater. 191 (2011) 56–61, https://doi.org/10.1016/j.jhazmat.2011.04.035.
[104] K.C. Popat, L. Leoni, C.A. Grimes, T.A. Desai, Influence of engineered titania nanotubular surfaces on bone cells, Biomaterials 28 (2007) 3188–3197, https://doi.org/10.1016/j.biomaterials.2007.03.020.
[105] L.M. Bjursten, L. Rasmusson, S. Oh, G.C. Smith, K.S. Brammer, S. Jin, Titanium dioxide nanotubes enhance bone bonding in vivo, J. Biomed. Mater. Res. 92 (2010) 1218–1224, https://doi.org/10.1002/jbm.a.32463.
[106] X. Li, S. Xu, Z. Zhang, H.J. Schluesener, Apoptosis induced by titanium dioxide nanoparticles in cultured murine microglia N9 cells, Chin. Sci. Bull. 54 (2009) 3830–3836, https://doi.org/10.1007/s11434-009-0548-x.
[107] Z. Guo, N.J. Martucci, F. Moreno-Olivas, E. Tako, G.J. Mahler, Titanium dioxide nanoparticle ingestion alters nutrient absorption in an in vitro model of the small intestine, NanoImpact 5 (2017) 70–82, https://doi.org/10.1016/j.impact.2017.01.002.
[108] A. Bettencourt, L.M. Goncalves, A.C. Gramacho, A. Vieira, D. Rolo, C. Martins, R. Assuncao, P. Alvito, M.J. Silva, H. Louro, Analysis of the characteristics and cytotoxicity of titanium dioxide nanomaterials following simulated in vitro digestion, Nanomaterials 10 (2020) 1516, https://doi.org/10.3390/nano10081516.
[109] L. Wang, D.K. Nagesha, S. Selvarasah, M.R. Dokmeci, R.L. Carrier, Toxicity of CdSe nanoparticles in caco-2 cell cultures, J. Nanobiotechnol. 6 (2008) 11, https://doi.org/10.1186/1477-3155-6-11.
[110] D. Sahu, G.M. Kannan, R. Vijayaraghavan, T. Anand, F. Khanum, Nanosized zinc oxide induces toxicity in human lung cells, ISRN Toxicol 2013 (2013) 316075, https://doi.org/10.1155/2013/316075.
[111] I.Y. Kim, E. Joachim, H. Choi, K. Kim, Toxicity of silica nanoparticles depends on size, dose, and cell type, Nanomedicine 11 (2015) 1407–1416, https://doi.org/10.1016/j.nano.2015.03.004.
[112] L. Dong, S. Tang, F. Deng, Y. Gong, K. Zhao, J. Zhou, D. Liang, J. Fang, M. Hecker, J.P. Giesy, et al., Shape-dependent toxicity of alumina nanoparticles in rat astrocytes, Sci. Total Environ. 690 (2019) 158–166, https://doi.org/10.1016/j.scitotenv.2019.06.532.
[113] I.V. Vrček, I. Žuntar, R. Petlevski, I. Pavičić, M. Dutour Sikirić, M. Ćurlin, W. Goessler, Comparison of in vitro toxicity of silver ions and silver nanoparticles on human hepatoma cells, Environ. Toxicol. 31 (2016) 679–692, https://doi.org/10.1002/tox.22081.
[114] S. Murugadoss, F. Brassinne, N. Sebaihi, J. Petry, S.M. Cokic, K.L. Van Landuyt, L. Godderis, J. Mast, D. Lison, P.H. Hoet, et al., Agglomeration of titanium dioxide nanoparticles increases toxicological responses in vitro and in vivo, Part. Fibre Toxicol. 17 (2020) 10, https://doi.org/10.1186/s12989-020-00341-7.
[115] Y. Tang, Y. Shen, L. Huang, G. Lv, C. Lei, X. Fan, F. Lin, Y. Zhang, L. Wu, Y. Yang, In vitro cytotoxicity of gold nanorods in A549 cells, Environ. Toxicol. Pharmacol. 39 (2015) 871–878, https://doi.org/10.1016/j.etap.2015.02.003.
[116] K. Kawata, M. Osawa, S. Okabe, In vitro toxicity of silver nanoparticles at noncytotoxic doses to HepG2 human hepatoma cells, Environ. Sci. Technol. 43 (2009) 6046–6051, https://doi.org/10.1021/es900754q.
[117] J. Lojk, J. Repas, P. Veranic, V.B. Bregar, M. Pavlin, Toxicity mechanisms of selected engineered nanoparticles on human neural cells in vitro, Toxicology 432 (2020) 152364, https://doi.org/10.1016/j.tox.2020.152364.
[118] S.J. Soenen, U. Himmelreich, N. Nuytten, T.R. Pisanic 2nd, A. Ferrari, M. De Cuyper, Intracellular nanoparticle coating stability determines nanoparticle diagnostics efficacy and cell functionality, Small 6 (2010) 2136–2145, https://doi.org/10.1002/smll.201000763.
[119] E. Chang, N. Thekkek, W.W. Yu, V.L. Colvin, R. Drezek, Evaluation of quantum dot cytotoxicity based on intracellular uptake, Small 2 (2006) 1412–1417, https://doi.org/10.1002/smll.200600218.
[120] P.J. Moos, K. Chung, D. Woessner, M. Honeggar, N.S. Cutler, J.M. Veranth, ZnO particulate matter requires cell contact for toxicity in human colon cancer cells, Chem. Res. Toxicol. 23 (2010) 733–739, https://doi.org/10.1021/tx900203v.
[121] J. Liu, Y. Kang, S. Yin, B. Song, L. Wei, L. Chen, L. Shao, Zinc oxide nanoparticles induce toxic responses in human neuroblastoma SHSY5Y cells in a size-dependent manner, Int. J. Nanomed. 12 (2017) 8085–8099, https://doi.org/10.2147/IJN.S149070.
[122] S.L. Chia, D.T. Leong, Reducing ZnO nanoparticles toxicity through silica coating, Heliyon 2 (2016) e00177, https://doi.org/10.1016/j.heliyon.2016.e00177.
[123] T. Lozano, M. Rey, E. Rojas, S. Moya, J. Fleddermann, I. Estrela-Lopis, E. Donath, B. Wang, Z. Mao, C. Gao, Cytotoxicity effects of metal oxide nanoparticles in human tumor cell lines, in: Proceedings of the Journal of Physics: Conference Series, 2011 012046.
[124] R.J. Vandebriel, J.P. Vermeulen, L.B. van Engelen, B. de Jong, L.M. Verhagen, L. J. de la Fonteyne-Blankestijn, M.E. Hoonakker, W.H. de Jong, The crystal structure of titanium dioxide nanoparticles influences immune activity in vitro

and in vivo, Part. Fibre Toxicol. 15 (2018) 9, https://doi.org/10.1186/s12989-018-0245-5.
[125] A. Magrez, L. Horvath, R. Smajda, V. Salicio, N. Pasquier, L. Forro, B. Schwaller, Cellular toxicity of TiO2-based nanofilaments, ACS Nano 3 (2009) 2274–2280, https://doi.org/10.1021/nn9002067.
[126] S.S. Mano, K. Kanehira, S. Sonezaki, A. Taniguchi, Effect of polyethylene glycol modification of TiO(2)nanoparticles on cytotoxicity and gene expressions in human cell lines, Int. J. Mol. Sci. 13 (2012) 3703–3717, https://doi.org/10.3390/ijms13033703.
[127] M. Luo, C. Shen, B.N. Feltis, L.L. Martin, A.E. Hughes, P.F. Wright, T.W. Turney, Reducing ZnO nanoparticle cytotoxicity by surface modification, Nanoscale 6 (2014) 5791–5798, https://doi.org/10.1039/c4nr00458b.
[128] R. Saker, O. Jójárt-Laczkovich, G. Regdon Jr, T. Takács, I. Szenti, N. Bózsity-Faragó, I. Zupkó, T. Sovány, Surface modification of titanate nanotubes with a carboxylic arm for further functionalization intended to pharmaceutical applications, Pharmaceutics 15 (2023) 2780, https://doi.org/10.3390/pharmaceutics15122780.
[129] Y. Li, W. Zhang, J. Niu, Y. Chen, Mechanism of photogenerated reactive oxygen species and correlation with the antibacterial properties of engineered metal-oxide nanoparticles, ACS Nano 6 (2012) 5164–5173, https://doi.org/10.1021/nn300934k.
[130] K. Mosquera-Murillo, A. Castañeda-Manquillo, K. Ángel-Camilo, P. Arciniegas-Grijalba, M.R. de Valdenebro, L. Mosquera-Sanchez, I. Meza-Cabrera, J. Rodriguez-Paez, Evaluation of the toxicity of ZnO nanoparticles obtained by a chemical route on the nasal respiratory epithelium of the biomodel Mus musculus, J. Nanoparticle Res. 25 (2023) 258, https://doi.org/10.1007/s11051-023-05902-3.
[131] C.M. Sayes, R. Wahi, P.A. Kurian, Y. Liu, J.L. West, K.D. Ausman, D.B. Warheit, V. L. Colvin, Correlating nanoscale titania structure with toxicity: a cytotoxicity and inflammatory response study with human dermal fibroblasts and human lung epithelial cells, Toxicol. Sci. 92 (2006) 174–185, https://doi.org/10.1093/toxsci/kfj197.
[132] J. Jiang, G. Oberdorster, A. Elder, R. Gelein, P. Mercer, P. Biswas, Does nanoparticle activity depend upon size and crystal phase? Nanotoxicology 2 (2008) 33–42, https://doi.org/10.1080/17435390701882478.
[133] J. Wu, J. Sun, Y. Xue, Involvement of JNK and P53 activation in G2/M cell cycle arrest and apoptosis induced by titanium dioxide nanoparticles in neuron cells, Toxicol. Lett. 199 (2010) 269–276, https://doi.org/10.1016/j.toxlet.2010.09.009.
[134] M. Shimizu, H. Tainaka, T. Oba, K. Mizuo, M. Umezawa, K. Takeda, Maternal exposure to nanoparticulate titanium dioxide during the prenatal period alters gene expression related to brain development in the mouse, Part. Fibre Toxicol. 6 (2009) 20, https://doi.org/10.1186/1743-8977-6-20.
[135] L.K. Braydich-Stolle, N.M. Schaeublin, R.C. Murdock, J. Jiang, P. Biswas, J. J. Schlager, S.M. Hussain, Crystal structure mediates mode of cell death in TiO2 nanotoxicity, J. Nanoparticle Res. 11 (2009) 1361–1374, https://doi.org/10.1007/s11051-008-9523-8.
[136] D.J. Nogueira, V.P. Vaz, O.S. Neto, M. Silva, C. Simioni, L.C. Ouriques, D. S. Vicentini, W.G. Matias, Crystalline phase-dependent toxicity of aluminum oxide nanoparticles toward Daphnia magna and ecological risk assessment, Environ. Res. 182 (2020) 108987, https://doi.org/10.1016/j.envres.2019.108987.
[137] D.J. Nogueira, M. Arl, J.S. Köerich, C. Simioni, L.C. Ouriques, D.S. Vicentini, W. G. Matias, Comparison of cytotoxicity of α-Al2O3 and η-Al2O3 nanoparticles toward neuronal and bronchial cells, Toxicol. Vitro 61 (2019) 104596, https://doi.org/10.1016/j.tiv.2019.104596.
[138] V. Demir, M. Ates, Z. Arslan, M. Camas, F. Celik, C. Bogatu, S.S. Can, Influence of alpha and gamma-iron oxide nanoparticles on marine microalgae species, Bull. Environ. Contam. Toxicol. 95 (2015) 752–757, https://doi.org/10.1007/s00128-015-1633-2.
[139] C. Lei, L. Zhang, K. Yang, L. Zhu, D. Lin, Toxicity of iron-based nanoparticles to green algae: effects of particle size, crystal phase, oxidation state and environmental aging, Environ. Pollut. 218 (2016) 505–512, https://doi.org/10.1016/j.envpol.2016.07.030.
[140] K.P. Steckiewicz, E. Barcinska, A. Malankowska, A. Zauszkiewicz-Pawlak, G. Nowaczyk, A. Zaleska-Medynska, I. Inkielewicz-Stepniak, Impact of gold nanoparticles shape on their cytotoxicity against human osteoblast and osteosarcoma in in vitro model. Evaluation of the safety of use and anti-cancer potential, J. Mater. Sci. Mater. Med. 30 (2019) 1–15, https://doi.org/10.1007/s10856-019-6221-2.
[141] M.E. Selim, A.A. Hendi, Gold nanoparticles induce apoptosis in MCF-7 human breast cancer cells, Asian Pac. J. Cancer Prev. APJCP 13 (2012) 1617–1620, https://doi.org/10.7314/apjcp.2012.13.4.1617.
[142] D. Choudhury, P.L. Xavier, K. Chaudhari, R. John, A.K. Dasgupta, T. Pradeep, G. Chakrabarti, Unprecedented inhibition of tubulin polymerization directed by gold nanoparticles inducing cell cycle arrest and apoptosis, Nanoscale 5 (2013) 4476–4489, https://doi.org/10.1039/c3nr33891f.
[143] Z. Keshtmand, E. Khademian, P.P. Jafroodi, M.S. Abtahi, M.T. Yaraki, Green synthesis of selenium nanoparticles using Artemisia chamaemelifolia: toxicity effects through regulation of gene expression for cancer cells and bacteria, Nano-Structures & Nano-Objects 36 (2023) 101049, https://doi.org/10.1016/j.nanoso.2023.101049.
[144] C. Uboldi, D. Bonacchi, G. Lorenzi, M.I. Hermanns, C. Pohl, G. Baldi, R.E. Unger, C.J. Kirkpatrick, Gold nanoparticles induce cytotoxicity in the alveolar type-II cell lines A549 and NCIH441, Part. Fibre Toxicol. 6 (2009) 18, https://doi.org/10.1186/1743-8977-6-18.
[145] W.S. Cho, M. Cho, J. Jeong, M. Choi, H.Y. Cho, B.S. Han, S.H. Kim, H.O. Kim, Y. T. Lim, B.H. Chung, et al., Acute toxicity and pharmacokinetics of 13 nm-sized PEG-coated gold nanoparticles, Toxicol. Appl. Pharmacol. 236 (2009) 16–24, https://doi.org/10.1016/j.taap.2008.12.023.
[146] H.M. Braakhuis, I. Gosens, P. Krystek, J.A. Boere, F.R. Cassee, P.H. Fokkens, J. A. Post, H. van Loveren, M.V. Park, Particle size dependent deposition and pulmonary inflammation after short-term inhalation of silver nanoparticles, Part. Fibre Toxicol. 11 (2014) 49, https://doi.org/10.1186/s12989-014-0049-1.
[147] A.R. Gliga, S. Skoglund, I.O. Wallinder, B. Fadeel, H.L. Karlsson, Size-dependent cytotoxicity of silver nanoparticles in human lung cells: the role of cellular uptake, agglomeration and Ag release, Part. Fibre Toxicol. 11 (2014) 11, https://doi.org/10.1186/1743-8977-11-11.
[148] N. El Yamani, A.R. Collins, E. Runden-Pran, L.M. Fjellsbo, S. Shaposhnikov, S. Zienolddiny, M. Dusinska, In vitro genotoxicity testing of four reference metal nanomaterials, titanium dioxide, zinc oxide, cerium oxide and silver: towards reliable hazard assessment, Mutagenesis 32 (2017) 117–126, https://doi.org/10.1093/mutage/gew060.
[149] W. Liu, Y. Wu, C. Wang, H.C. Li, T. Wang, C.Y. Liao, L. Cui, Q.F. Zhou, B. Yan, G. B. Jiang, Impact of silver nanoparticles on human cells: effect of particle size, Nanotoxicology 4 (2010) 319–330, https://doi.org/10.3109/17435390.2010.483745.
[150] C. Carlson, S.M. Hussain, A.M. Schrand, L.K. Braydich-Stolle, K.L. Hess, R. L. Jones, J.J. Schlager, Unique cellular interaction of silver nanoparticles: size-dependent generation of reactive oxygen species, J. Phys. Chem. B 112 (2008) 13608–13619, https://doi.org/10.1021/jp712087m.
[151] Y. Pan, S. Neuss, A. Leifert, M. Fischler, F. Wen, U. Simon, G. Schmid, W. Brandau, W. Jahnen-Dechent, Size-dependent cytotoxicity of gold nanoparticles, Small 3 (2007) 1941–1949, https://doi.org/10.1002/smll.200700378.
[152] A.A.H. Abdellatif, M.A. Younis, M. Alsharidah, O. Al Rugaie, H.M. Tawfeek, Biomedical applications of quantum dots: overview, challenges, and clinical potential, Int. J. Nanomed. 17 (2022) 1951–1970, https://doi.org/10.2147/IJN.S357980.
[153] M.A. Walling, J.A. Novak, J.R.E. Shepard, Quantum dots for live cell and in vivo imaging, Int. J. Mol. Sci. 10 (2009) 441–491, https://doi.org/10.3390/ijms10020441.
[154] K.S. Aryamol, K. Kanagaraj, S. Nangan, J.T. Haponiuk, M. Okhawilai, S. Pandiaraj, M.B. Hanif, A.N. Alodhayb, S. Thomas, N. Thirumalaivasan, et al., Recent advances of carbon pathways for sustainable environment development, Environ. Res. 250 (2024) 118513, https://doi.org/10.1016/j.envres.2024.118513.
[155] S. Ahirwar, S. Mallick, D. Bahadur, Photodynamic therapy using graphene quantum dot derivatives, J. Solid State Chem. 282 (2020) 121107, https://doi.org/10.1016/j.jssc.2019.121107.
[156] T. Nideep, M. Ramya, U. Sony, M. Kailasnath, MSA capped CdTe quantum dots for pH sensing application, Mater. Res. Express 6 (2019) 105002, https://doi.org/10.1088/2053-1591/ab35a0.
[157] R. Ding, Y. Chen, Q. Wang, Z. Wu, X. Zhang, B. Li, L. Lin, Recent advances in quantum dots-based biosensors for antibiotics detection, J Pharm Anal 12 (2022) 355–364, https://doi.org/10.1016/j.jpha.2021.08.002.
[158] A.A.H. Abdellatif, H.A. Abou-Taleb, A.A. Abd El Ghany, I. Lutz, A. Bouazzaoui, Targeting of somatostatin receptors expressed in blood cells using quantum dots coated with vapreotide, Saudi Pharmaceut. J. 26 (2018) 1162–1169, https://doi.org/10.1016/j.jsps.2018.07.004.
[159] L. Liu, H. Jiang, J. Dong, W. Zhang, G. Dang, M. Yang, Y. Li, H. Chen, H. Ji, L. Dong, PEGylated MoS(2) quantum dots for traceable and pH-responsive chemotherapeutic drug delivery, Colloids Surf. B Biointerfaces 185 (2020) 110590, https://doi.org/10.1016/j.colsurfb.2019.110590.
[160] A. Sukhanova, S. Bozrova, E. Gerasimovich, M. Baryshnikova, Z. Sokolova, P. Samokhvalov, C. Guhrenz, N. Gaponik, A. Karaulov, I. Nabiev, Dependence of quantum dot toxicity in vitro on their size, chemical composition, and surface charge, Nanomaterials 12 (2022) 2734, https://doi.org/10.3390/nano12162734.
[161] C. André, B. Lachance, P. Turcotte, F. Gagné, C. Gagnon, C. Emond, Size-dependent toxicity of CdTe quantum dot aggregates in trout and human hepatocytes, Toxicology 16 (2020).
[162] Y. Zhang, W. Chen, J. Zhang, J. Liu, G. Chen, C. Pope, In vitro and in vivo toxicity of CdTe nanoparticles, J. Nanosci. Nanotechnol. 7 (2007) 497–503, https://doi.org/10.1166/jnn.2007.125.
[163] M.S. Hassan, R. Khan, T. Amna, J. Yang, I.-H. Lee, M.-Y. Sun, M.H. El-Newehy, S. S. Al-Deyab, M.-S. Khil, The influence of synthesis method on size and toxicity of CeO2 quantum dots: potential in the environmental remediation, Ceram. Int. 42 (2016) 576–582, https://doi.org/10.1016/j.ceramint.2015.08.149.
[164] A. Velidandi, N.P.P. Pabbathi, S. Dahariya, R.R. Baadhe, Green synthesis of novel Ag–Cu and Ag–Znbimetallic nanoparticles and their in vitro biological, eco-toxicity and catalytic studies, Nano-Structures & Nano-Objects 26 (2021) 100687, https://doi.org/10.1016/j.nanoso.2021.100687.

pharmaceutics

MDPI

Article

Quality by Design-Based Methodology for Development of Titanate Nanotubes Specified for Pharmaceutical Applications Based on Risk Assessment and Artificial Neural Network Modeling

Ranim Saker, Géza Regdon, Jr., Krisztina Ludasi and Tamás Sovány *

Institute of Pharmaceutical Technology and Regulatory Affairs, University of Szeged, Eötvös u 6, H-6720 Szeged, Hungary; rnmsaker@gmail.com (R.S.); geza.regdon@pharm.u-szeged.hu (G.R.J.); krisztina.ludasi@szte.hu (K.L.)

* Correspondence: sovany.tamas@szte.hu; Tel.: +36-62-545-576

Abstract: Background: Nanotechnology has been the main area of focus for research in different disciplines, such as medicine, engineering, and applied sciences. Therefore, enormous efforts have been made to insert the use of nanoparticles into the daily routines of different platforms due to their impressive performance and the huge potential they could offer. Among numerous types of nanomaterials, titanate nanotubes have been widely recognised as some of the most promising nanocarriers due to their outstanding profile and brilliant design. Their implementation in pharmaceutical applications is of huge interest nowadays as it could be of fundamental importance in the development of the pharmaceutical industry and therapeutic systems. Methods: In the present work, a risk assessment-based procedure was developed and completed using ANN-based modeling to enable the design and fabrication of titanate nanotube-based drug delivery systems with desired properties, based on the critical analysis and evaluation of data collected from published articles regarding titanate nanotube preparation using the hydrothermal treatment method. Results: This analysis is presented as an integrated pathway for titanate nanotube preparation and utilization in a proper way that meets the strict requirements of pharmaceutical systems (quality, safety, and efficacy). Furthermore, a reasonable estimation of the factors affecting titanate nanotube preparation and transformation from traditional uses to novel pharmaceutical ones was established with the aid of a quality by design approach and risk assessment tools, mainly an Ishikawa diagram, a risk estimation matrix, and Pareto analysis. Conclusions: To the best of our knowledge, this is the first article using the QbD approach to suggest a systematic method for the purpose of upgrading TNT use to the pharmaceutical domain.

Keywords: titanate nanotubes; hydrothermal treatment; quality by design; ANN; risk assessment; pharmaceutical applications

Academic Editor: Seong Hoon Jeong

Received: 2 December 2024
Revised: 27 December 2024
Accepted: 30 December 2024
Published: 1 January 2025

Citation: Saker, R.; Regdon, G., Jr.; Ludasi, K.; Sovány, T. Quality by Design-Based Methodology for Development of Titanate Nanotubes Specified for Pharmaceutical Applications Based on Risk Assessment and Artificial Neural Network Modeling. *Pharmaceutics* **2025**, *17*, 47. https://doi.org/10.3390/pharmaceutics17010047

1. Introduction

Titanate nanotubes (TNTs) have attracted considerable attention during the past three decades since they were first presented in 1996 [1]. Numerous research works have been published focusing on the usage of titanium dioxide (TiO_2)-derived substances, including TNTs, in several applications, such as chemical catalysis, water purification, energy saving, and solar cells, but a very limited number of works have focused on their potential use in the pharmaceutical field as drug carriers (Figure 1).

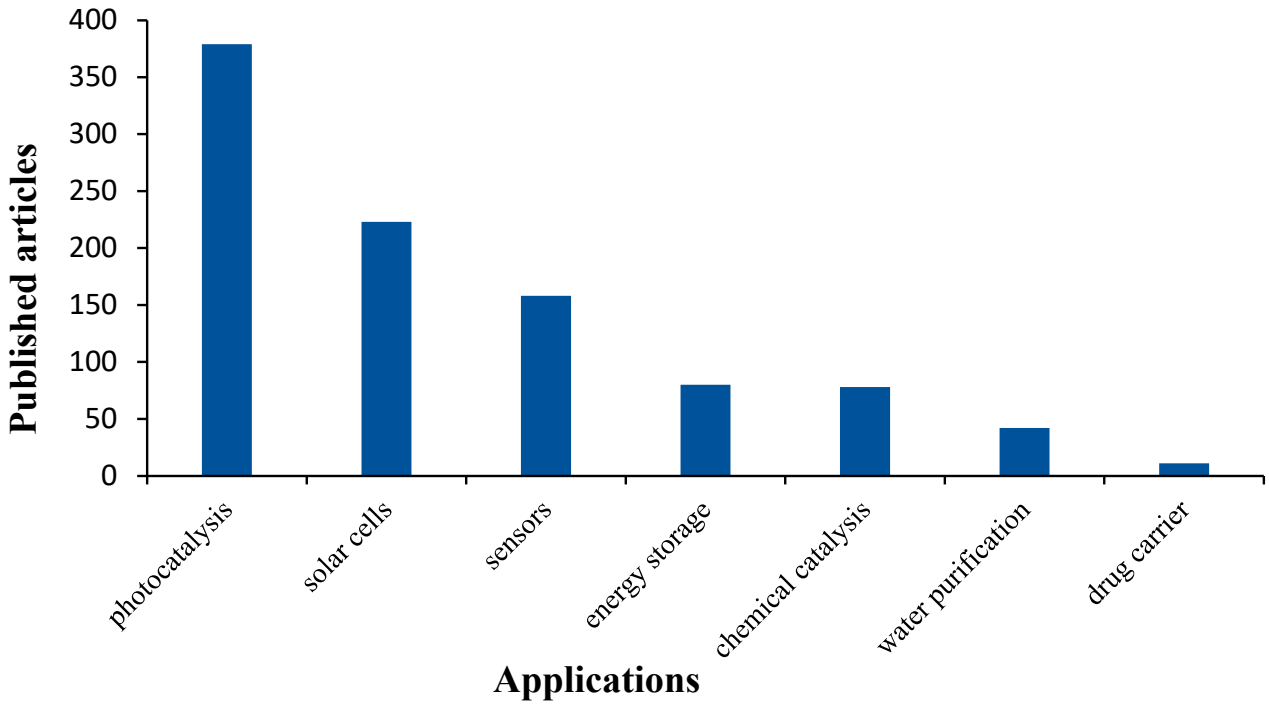

Figure 1. The number of publications regarding TNT usage in different applications (based on the Web of Science database. Available online: https://www.webofscience.com/wos/woscc/basic-search (accessed on 27 April 2023).

Their unique tubular morphology and higher surface area compared to their spherical precursors, in addition to the existence of hydroxyl groups on their vast surface, provide them with preferred features for medical/pharmaceutical applications. Furthermore, their surface properties may be tailored by functionalization or by grafting of specific molecules for diagnostic or therapeutic purposes [2,3]. Their tubular morphology also promotes cell internalization compared to their spherical counterparts [4]. Furthermore, their safety profile introduces them as an attractive candidate for drug delivery by loading them with therapeutic agents inside their tubular cavity or on their surface [5,6]. TNTs also present good processability in terms of flowability, compactibility, and compressibility, which has a huge, positive impact regarding manufacturing at the industrial level [7,8]. With these outstanding features, TNTs could be the key solution to overcoming the fundamental challenges of nanomedicines faced during pharmaceutical development, such as poor tabletting, solubility, and bioavailability. Therefore, they deserve more attention and a precise investigation so they can be introduced into therapeutic practice as efficient tools. However, this task is becoming more and more challenging due to the tremendous development happening around us in the modern world, which raises the bar, thus posing an urgent need to apply the innovative tools discovered recently (statistics software, computational systems, machine learning (ML), artificial intelligence (AI), etc.) to serve the evolution of the pharmaceutical domain as traditional ways are no longer sufficient to achieve this target. These intelligent tools should certainly consider the most important standards in the pharmaceutical industry: quality, safety, and efficacy.

Continuously, pharmaceutical authorities emphasize building these criteria into products by design rather than just testing them eventually. This concept was the essence of what is called today the quality by design (QbD) approach, which has been gaining more and more attention due to its fundamental contribution to pharmaceutical research. QbD tools revolutionized the formulation field with their potential to draw guidelines to obtain the requested specifications and design a workspace within which the quality of the final

product could be guaranteed [9,10]. The application of this novel approach is widespread and includes different types of drug delivery systems (polymeric microspheres, nanocrystals, pellets, nanostructured lipid carriers [11–14]) and several routes of administration (oral, dermal, parenteral, intranasal [13–16]).

This accelerated development in pharmaceutical research has not stopped with only the application of the QbD approach but is also supported by the application of artificial neural networks (ANNs), one of the most popular types of ML tools, as they can overcome the numerous limitations facing conventional methods, in addition to saving time, effort, and money, still with impressive outcomes. ANNs have been applied successfully in solid dosage forms for several purposes, such as modeling of tablet coatings [17], prediction of dissolution profiles and hardness [18], optimization of the spray-drying process [19], modeling of powder flow [20], and optimization of controlled/sustained release tablets [21,22]. Their application has also been extended to the formulation of other dosage forms/carriers (liposomes, hydrogels, emulsion, etc.) [23–25] and for multiple delivery routes (oral, transdermal, etc.) [21,22,26]. Based on the above discussion, the combination of the revolutionary concepts of QbD and AI—such as ANN—could write a new chapter in the development of pharmaceutical sciences and lead to a new era of research and industry [18,27].

For this reason, the main aim of this research is to propose a systematic procedure to shift the use of TNTs from their traditional applications to the pharmaceutical field using the tools of QbD and ANNs. In this context, this paper will suggest a multi-step procedure to achieve this goal and discuss in detail the appropriate parameters that could be implemented/adjusted to suit the special criteria of the therapeutic domain. This suggested methodology uses risk assessment tools based on the previous experience of the research group and the available data in the literature. The importance of the research team's previous experience with the evaluated topic should be emphasized as it will have a major impact on the selections/decisions made and the reliability of the evaluation produced. On the other hand, critical evaluation of previously reported information is also crucially important as it will help to build a solid background that enables a precise assessment of the risks associated with the utilization of TNTs as drug carriers in order to create applicable guidelines for the development of TNT-based drug delivery systems. It is worth mentioning that risk assessment is not a static analysis but can be modified and updated regularly based on upcoming research outcomes and continuously published articles [28–30].

In this paper, the hydrothermal treatment method, a chemical reaction that involves material crystallization from a highly concentrated alkaline solution at elevated temperature for a specific duration, was chosen for the preparation of TNTs due to its numerous advantages over other techniques (sol–gel process, electrochemical anodization, template-assisted method, vapor-liquid-solid growth) as it is simple, cost effective, environmentally friendly, scalable, and controllable [31–35]. In addition, the authors have experience with this method from their previously published research [7,8,36–38].

By using this method, the general characteristics of the obtained TNTs seem to be ideal for pharmaceutical applications. Furthermore, their characteristics (e.g., diameter, length, surface area, etc.) can be manipulated by varying the production conditions; thus, with an optimized process, TNTs may be obtained with specific properties preplanned for targeted application [32]. Regarding TNTs, their tubular morphology, nano-size, and crystal structure, in addition to their surface characteristics (area, chemistry, coating) and preparation yield would highly impact their use as potential drug carriers by affecting the selection of active pharmaceutical ingredient (API), dosage form, and route of administration, as well as their stability, safety profile, and drug release pattern.

To the best of our knowledge, no systematic approach was previously proposed to draw basic lines for the use of TNTs as nanocarriers for therapeutic agents starting from

the point of hydrothermal preparation and ending with a final dosage form that can be presented to the market/targeted patients. To achieve this goal, the QbD approach and risk assessment tools in combination with ANNs have been adopted for the first time to push the use of TNTs toward the pharmaceutical field, which is an innovative, under-explored application.

2. Materials and Methods

2.1. Risk Assessment

2.1.1. Definitions in QbD Methodology

The QbD approach is a multi-step procedure that starts from defining the quality target product profile (QTPP), which is a general abstraction of indicators of quality, safety, and efficiency of a product.

In the second step, the general QTPP indicators should be translated to measurable or calculable physical, chemical, biological, or microbiological parameters, called critical quality attributes (CQAs). Furthermore, the target values and acceptable tolerance ranges of CQAs should be determined and considered as the product design space (DS).

The third step is the identification of the material and process-related factors (critical material attributes (CMAs) and critical process parameters (CPPs), respectively) that may affect CQAs.

Finally, the interdependence between CPPs, CMAs, and CQAs should be determined, and the severity, probability, and detectability of the impacts caused by the changes in CPPs or CMAs should be estimated.

2.1.2. Methods of Literature Survey

CQAs, CMAs, and CPPs were selected using previous experience and literature data. Relevant scientific databases: Web of Science, Scopus, PubMed, etc., were searched using the keywords titanate nanotubes, synthesis, hydrothermal treatment, drug delivery, toxicity, etc. A database including the investigated CMAs, CPPs, and CQAs was created after critical evaluation of the gathered data, and this database was used for supporting the risk assessment and served as basis of the ANN modeling.

2.2. Quality Tools

Various quality tools were applied during the risk assessment. An Ishikawa diagram was used for the identification of CPPs and CMAs, a risk estimation matrix was used to determine their interdependence, while Pareto analysis was used to quantify the risk regarding various CQAs.

2.2.1. Ishikawa Diagram

The Ishikawa or fishbone diagram can be used to determine the root causes of a problem or the factors affecting a specific event. In this research, the factors affecting different steps and profiles (TNT preparation, API incorporation, functionalization, and safety profile) were identified. These factors should be seriously taken into consideration during the development process to achieve the desired results. This cause–effect diagram is very useful for preplanning the upcoming experimental work and highlighting the most prominent factors by visualization when a limited amount of quantitative data is available.

2.2.2. Risk Estimation Matrix and Pareto Analysis

The risk estimation matrix represents the correlations between QTPPs and CQAs or between CPPs/CMAs and CQAs. The interdependence rating, which describes the relationship between the parameters, was determined using a three-level scale, high (H),

medium (M), or low (L) dependence, and they appeared in the interdependence tables using the colors red, yellow, and green, respectively.

LeanQbD software (Version 1.3.6., 2014 QbD Works LLC, Fremont, CA, USA) was used for the evaluation. In the software, the qualitative three-level scale used for the estimation is linked to a selectable numeric scale which, at the end of estimation, gives the severity score of the evaluated risk factors based on mathematical calculations. After the categorization of the interdependence, the risk occurrence rating of the CPPs was made, applying the same three-grade scale (H/M/L) for the analysis. As the output of the initial RA evaluation, Pareto diagrams were generated by the software, presenting the numeric data and the rankings of CQAs and CPPs/CMAs according to their potential impact on the aimed final product. Pareto analysis is a statistical tool that enables effective data evaluation and facilitates a more reliable decision-making process by determining and prioritizing the factors having the greatest effect on the studied system. This method has crucial importance in the screening of numerous factors affecting the quality of the final desired product, and attention should be directed first toward the factors with the highest influence.

2.3. ANN Modeling

ANN modeling was performed using Statistica v.14.0.1.25 (Tibco Software Inc., Palo Alto, CA, USA). The full dataset collected from the literature is displayed in Table S1. It is easily visible that the range of the discussed data is very versatile among the various papers. After careful data curation, two outputs were identified in which the existing data enable suitable modeling. The morphology and the specific surface area of the obtained products were then handled as two different datasets for classification and regression-type modeling, and the corresponding datasets are displayed in Tables S2 and S3, respectively. The range of input variables was the same for both models. After setting the datasets, the minimum and maximum values of each input and the output parameters were identified manually, and these cases were included into the training subset to avoid the need for extrapolation during testing or validation of the model. The remaining data were then randomly distributed into the training, testing, and validation subsets, where the sizes of the training, testing, and validation subsets were 70%, 15%, and 15% of the full dataset, respectively.

Feed-forward, back-propagation multilayer perceptron networks were developed in both cases. The networks were trained with the BFGS algorithm. The possible range of the number of hidden neurons was set according to the following equation (Equation (1)):

$$1 \leq n \leq I + O + 1 \quad (1)$$

where I is the number of inputs, O is the number of outputs, and n is the number of hidden neurons; thus, the hidden neuron number varied from 1–20 for the classification and 1–12 for the regression network, respectively.

A multistart method including 10,000 networks was applied using the automated neural networks module of Statistica, including a training approach to screen the best performing network with different initialization patterns and activation functions for hidden and output neurons. The training was stopped when the root mean square error (RMSE) of the test dataset reached its minimum. The 10 best performing networks from each multistart run were retained for further analysis.

The prediction performance of the networks was evaluated based on network perfection, which is the mean R^2 of the observed vs. predicted data of each output neuron, and on the RMSE of predictions on the validation subset.

3. Results and Discussion

According to literature data, hydrothermally synthesized TNTs may be appropriate candidates for delivering APIs and for providing an efficient tool for use in healthcare systems thanks to their good biocompatibility and small size, which is hard to detect by the immune system [39]. However, the identification of QTPPs and related CQAs (Tables 1 and 2, respectively) is an essential step in the development procedure of a product as they are application-related parameters that are always different and unique for every case.

Table 1. QTPPs of titanate nanotubes prepared by the hydrothermal treatment method and intended for pharmaceutical applications.

QTPP	Details	Comments
Physical attributes	The most significant attribute is the tubular morphology	Provides unique characteristics compared to traditional spherical counterparts
Therapeutic effect	Based on the used API	Problems related to some APIs could be solved using TNTs as carriers, like poor tabletting or poor wettability, which would positively affect their therapeutic outcomes
Pharmacokinetics	Absorption, distribution, metabolism, and excretion	Could be optimized/enhanced by surface modification
Safety profile	Accumulation is the highest concern	Affected mainly by physical attributes and needs further investigation
Stability	During processing	TNTs need to be stable and preserve their original characteristics, especially their unique tubular structure and surface properties
Drug release	Depends on requested indication and type of surface modification	Immediate or sustained release could be achieved

Table 2. Critical quality attributes (CQAs) of hydrothermally synthesized titanate nanotubes as possible drug carriers.

CQA	Details	Comments
Type of TNT	Na-TNTs or H-TNTS	Affects several characteristics of TNTs, like morphology, surface area, stability, and safety
Size	Could be regulated by varying preparation conditions	Not large enough so they can be easily detected by the immune system
Surface characteristics	No modification	Aggregation problem, rapid elimination, poor pharmacokinetics profile, higher toxicity
	Functionalized surface	Prolonged circulation, better permeability and PK, less toxicity, targeting is a possibility
Morphology	Tubular	Self-organized or randomly distributed depending on the preparation method
Specific surface area (SSA)	Affect different applications and surface modification	Tubular morphology presents higher surface area compared to traditional nanoparticles
Crystal structure	Affect applications and safety profile	-
Yield	Affects cost efficiency	Critical for scaling up the process

The properties of manufactured nanotubes are dependent on the properties of the starting materials and on the operating conditions during the hydrothermal reaction. Furthermore, they are also dependent on the conducted post-treatment steps.

In the present investigation, QTPPs include appropriate physical properties and stability; therapeutic effects; and appropriate pharmacokinetics, including absorption followed by drug release and elimination, ensuring safe use for patients. Accordingly, morphology, which is unique in the case of nanotubes, size, type, crystal structure, specific surface area (SSA), surface characteristics, yield of preparation, and drug loading were chosen as CQAs.

To obtain TNTs with the required properties for a specific application, such as a pharmaceutical one, the hydrothermal synthesis method should be carefully optimized. As previously mentioned, in this chemical reaction, the starting precursor is subjected to high temperature in a concentrated alkaline medium for a specific duration, so the multiple parameters that are deeply involved in this procedure are highly responsible for the result.

For example, temperature was the most discussed factor affecting the success of the preparation process as it serves as an energy supply to help the intermediate nanosheets to curl up and form nanotubes. Therefore, it should be used in the appropriate range, as too low a temperature would not be enough to transform the starting nanoparticles/intermediate nanosheets to nanotubes. On the other hand, too high a temperature would also pose a problem, with several morphologies obtained other than the tubular one. This information could be of great importance if other morphologies are the morphologies of interest. In this case, the temperature can be raised up to create nanofibers (>150 °C) [40], nanorods or nanoribbons (>160 °C) [41–43], nanofibers or nanobelts (>170 °C) [44], and nanorods (>180 °C) [45]. According to the literature, the temperature range between 130 and 150 °C is the most repeated one in several research works, which represents a strong point of agreement and confirms the formation of complete nanotubes within this range. In addition, increasing the temperature within this range would increase the diameter, SSA, production yield, and enhance crystallinity without negatively affecting the requested tubular structure [40,42,45,46]. Together, these specifications could be an advantage to be invested for the benefit of drug delivery systems.

Besides high temperature, TNT preparation involves the usage of a highly concentrated alkaline medium, which supports the thermal energy to provide the required force for rolling up the sheet phase into a tubular one. Based on this, the concentration of this medium should also be within an appropriate range (10–15 M), as too low a concentration would result in unreacted powder/untransformed sheets, while too high a concentration would result in low yield [42,47,48]. It is worth mentioning that this treatment should take sufficient time to give the intermediate phase an opportunity to transform into nanotubes and then to give the obtained nanotubes enough time to grow and elongate their length. Fifteen hours is probably the optimal time for the formation of pure nanotubes, with the possibility of increasing their length by increasing the treatment time to 24 h. However, caution should be taken as longer duration could lead to the formation of other morphologies, such as nanoribbons [49,50]. Furthermore, after a specific point, no length increase occurs, so further treatment will be just a waste of energy, which would subsequently have a negative impact on the economic cost [51].

The pressure inside the sealed autoclave during the reaction is one of the variable preparation conditions, but its impact on nanotube formation was not sufficiently discussed [52,53]. Morgan et al. suggested that the pressure effect could be excluded from the significant factors affecting the formation of TNTs [43].

After the hydrothermal reaction is finished, the post-treatment processes (acid washing, calcination) take place and play a major role in preserving the desired morphology and

obtaining the targeted characteristics. According to several publications, washing with acid could affect the size of TNTs and enhance their crystallinity [54]. However, two critical factors were deeply discussed in literature regarding this process. Firstly, the pH of the washing solution was suggested to be kept between 2 and 4 to obtain a high yield and high SSA [55]. The second one is the concentration of the used acid, on which there is disagreement, as few studies recommended the use of low concentrations because high ones would destroy the tube-like morphology (>0.01 M) [56] and result in the formation of granules (>0.2 M) [57] or clumps (>2 M) [52,58], while others disagreed and indicated that high concentrations (0.5–1 M) were the optimal range to use [52].

Another post-treatment process (calcination) can be used to enhance the crystallinity of the resulted materials, but caution should be taken not to negatively affect the morphology and thus the SSA. The safest range to work in is between 200 and 400 °C, as increasing temperature within this range would enhance crystallinity without negatively affecting the tubular structure [42,49,59–61]. Higher temperature could lead to destroying the tubular structure (>450 °C) [61] and complete collapse of the nanotubes into irregular shapes (>500 °C) [60], nanorods (>540 °C) [42], nanoparticles (>600 °C) [49,59], or aggregates (>800 °C) [51,62].

It was noticed that the discussed results in the literature were not always comparable as different operating conditions would lead to different and conflicted results. These differences make it difficult to establish strict guidelines for TNT preparation with prespecified characteristics. This means that studying the effect of different preparation factors separately poses a research challenge because they act as a full combination rather than independent ones. For example, a lower alkaline medium concentration could be compensated by the utilization of higher temperature [43]. In the same context, lower temperature could be applied as long as prolonged treatment is used [50]. Moreover, numerous factors during the preparation reaction could shorten the required duration for TNT formation, such as stirring, smaller particle size of the starting material, or using less stable, higher energy anatase phase precursors [47,61,63]. For this reason, the required parameters should be modified together to achieve the appropriate balance. This could be performed according to the requested final specifications of the prepared TNTs and according to the available laboratory instruments/equipment and the ranges within which they can work.

Careful evaluation and curation of the existing data enables us to better understand and model how to manipulate the operating conditions to achieve a specific purpose or affect a specific property of the resulting TNTs. For instance, increasing the factors (temperature, alkaline concentration, acid concentration) within the previously specified limits and decreasing the particle size of the starting precursor would increase the SSA, but the opposite would happen by increasing the treatment time [42,46,47,64–66]. This conclusion is very important because high surface area is one of the most significant characteristics of TNTs due to its direct impact on their possible functionalization and drug loading, so it could serve as an advantage for pharmaceutical applications as it successfully served earlier in energy saving and chemical catalysis.

Starting from a crystalline precursor (anatase) that promotes the thermal stability of the resulting nanotubes [67], washing them with acid will reduce the sodium content and resistance to temperature, resulting in H-TNTs that are thermally less stable than Na-TNTs [55,58,65,66,68].

The concentration of the used precursor also has an impact on the specifications of TNTs. High concentration increases the length/aspect ratio and diameter of the prepared TNTs but negatively affects the SSA [40,69]. It could affect morphology; therefore, manipulating the Ti/Na molar ratio is an important step in shaping the structure of the resulting material into the desired direction (nanotubes, nanowires, nanofibers) [49].

After titanate nanotubes have been prepared properly according to the planned design and predetermined specifications, modifying their vast surface is a well-known technique for giving them secondary characteristics that differ from their original ones. Surface modification could be the key solution to overcoming several problems facing the upgrading of TNT use to the pharmaceutical field. For example, surface functionalization using hydrophobic moieties could be a suitable way for enhancing the poor permeability of TNTs, which originates from their hydrophilic properties and hydroxylated surface [38]. PEGylation could also present several advantages as it could be an appropriate solution for the aggregation problem in addition to making them undetectable by the immune system, prolonging their circulation time as well as reducing their toxicity [2,70,71]. Determining the purpose of surface functionalization is an unavoidable step, as it would affect the type of molecule that is going to be fixed on the surface of TNTs and the type of interaction that will be created. This interaction is highly dependent on the chemical structure of the functionalizing agent and the chemical bond that is going to be created, which is preferred to be a strong, long-lasting bond like covalent or ionic bonds rather than hydrogen ones [38,72]. Hydrogen bonds could be more favorable in some cases, such as during API incorporation, as weak interaction between TNTs and APIs would not strongly affect drug release unless the modification of drug release is the main target of incorporation [36].

Drug incorporation is also considered to be a challenging step during the development of nanocarrier drug delivery systems as multiple factors could affect the success of this procedure. Based on the authors' previous experience, the chemical properties of the used drug and solvents are essential during TNT-drug composite formation. Solvent polarity (protic/aprotic nature) and volatility would highly affect the success of composite formation as they would affect the possibility of drug solubilization, the strength of solvent–drug interactions, and the ability to remove solvent from the system. In the ideal state, the requested drug–carrier interaction should be stronger than the one created between the drug molecules themselves or between the drug and the solvent. However, the strength/type of TNT–drug interaction should be further investigated as it could be determined according to the desired release type (immediate or sustained) [36,37].

Finally, presenting titanate nanotubes as possible candidates for drug delivery systems is strongly dependent on their safety profile, which is still a matter of debate. However, several points have been thoroughly discussed in the literature and could be considered as a starting point to build safer nanocarriers for therapeutic use. Morphology is one of these critical points affecting toxicity. It is true that the high surface area related to the tubular morphology is considered an advantage, but it also promotes cell penetration and the subsequent toxic effects [73]. Surface chemistry/coating could also play a significant role in determining toxicity as changing the existing Na^+ ions on the surface of TNTs to H^+ or Mg^{2+} will increase their toxic effects [38,74], while applying a specific type of hydrophilic coating, such as PEGylation, could be a proper way to reduce aggregation and toxicity [70,72]. The applied concentration is also crucial as increasing the used dose of these nanotubes would increase the impact of their hazard [73]. In addition, the crystal structure could also affect the safety profile of TNTs as TiO_2 can exist as three different structures (anatase, rutile, and brookite), of which anatase appears to exert the highest toxic effects [75–78]. Understanding these elements and their direct impact on toxicity would help researchers to optimize the preparation procedure and the subsequent steps to obtain a safer final product.

The CMAs and CPPs identified to affect the development of TNTs as possible drug carriers for pharmaceutical applications are discussed in Table 2 and an Ishikawa diagram is proposed (Figure 2) to summarize the necessary materials and processes for the utilization of TNTs in drug carrier systems starting from the moment of preparation until adjusting the surface properties by functionalization, loading with therapeutic molecules, and finally

assessing the safety profile in order to incorporate these synthesized nanomaterials into final dosage form (oral, dermal, etc.).

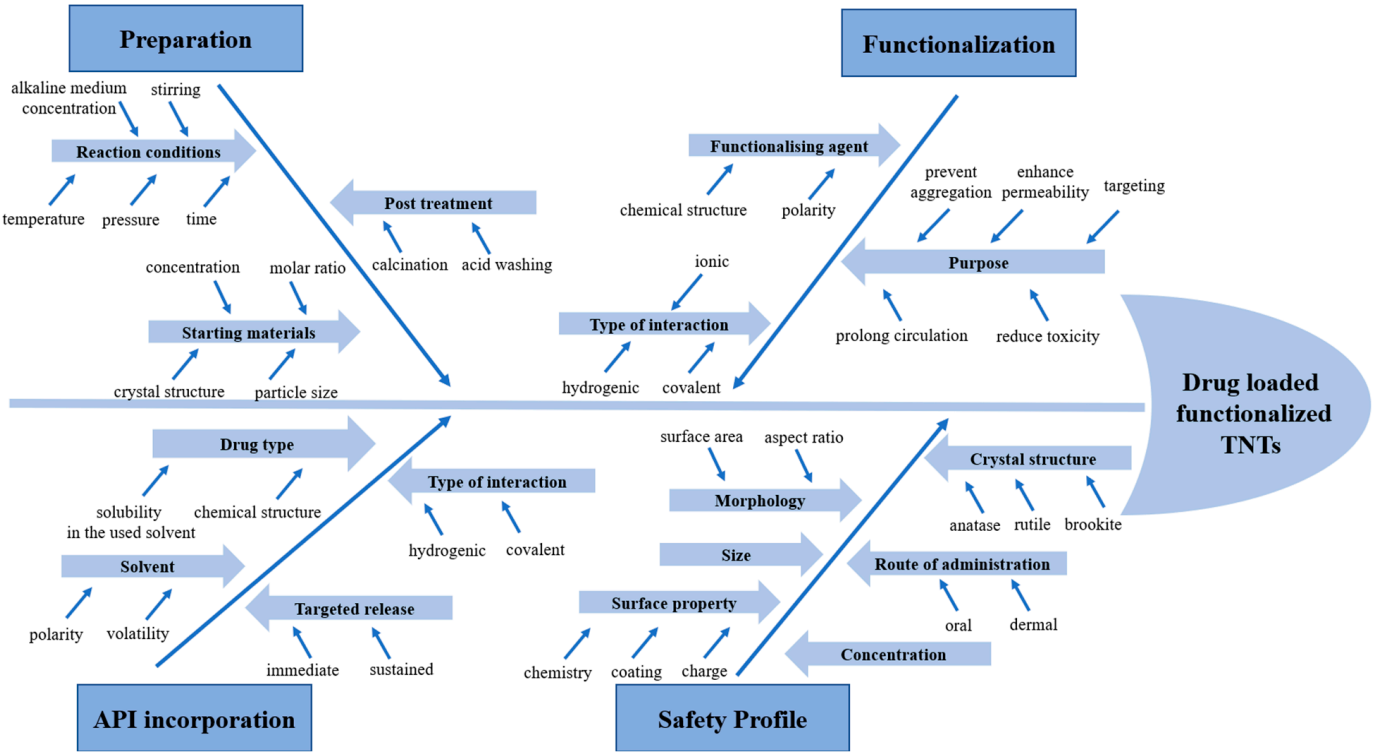

Figure 2. Ishikawa diagram of the factors affecting the procedure of TNT transformation into possible drug carriers. The arrows are representing the structure of the "Fishbone".

Most of the selected CQAs are attributed to multiple elements of QTPPs. Therefore, a risk estimation matrix (REM) was created (Table 3) with the aid of LeanQbD v1.3.6. software to estimate the interdependence ratings between the collected elements. Furthermore, Figure 3 visualizes the priority of CQAs of hydrothermally synthesized TNTs as drug carriers depending on the chosen QTPPs. According to Pareto analysis, the most significant CQAs were surface characteristics, morphology, SSA, size, type of TNT, crystal structure, drug loading, and yield.

Table 3. Interdependence between CQAs and QTPPs. (Red (H), Yellow (M) and Green (L) are associated with high, medium and low risk, respectively).

QTPP / CQA	Drug Release	Stability	Safety Profile	Therapeutic Effect	Pharmacokinetics	Physical Attributes
Size	M	M	H	H	H	H
Crystal structure	L	H	H	L	L	M
Morphology	M	H	H	H	H	H
Specific surface area	H	M	H	H	H	H
Yield	L	L	L	L	L	L
TNT type	L	H	H	L	M	H
Surface characteristics	H	H	H	H	H	M
Drug loading	L	L	L	H	L	M

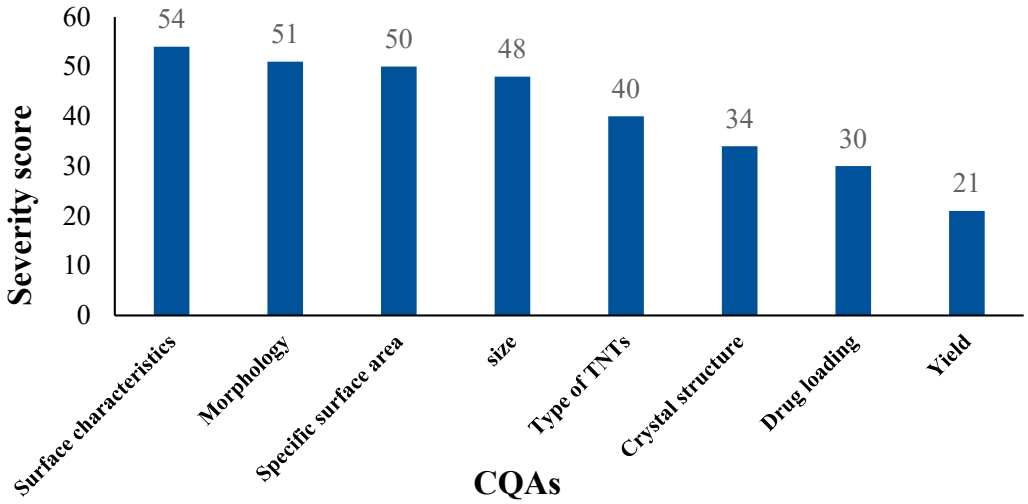

Figure 3. Ranking of CQAs of hydrothermally synthesized TNTs as possible drug carriers.

The results of REM and Pareto analysis correspond well with the available data in the literature, which repeatedly emphasized the importance of the tubular morphology and large surface area of TNTs in their possible usage as drug carriers due to the unique characteristics that come along with these two parameters, such as high cell internalization, as well as the ability to load APIs inside the tubular cavity or on their vast surface.

However, according to Pareto analysis, the properties of this vast surface, which can be controlled through modification with a proper molecule, is the most important as it can determine the success of the whole transformation procedure by its fundamental impact on the chosen QTPPs. For example, surface modification could be used to control/enhance the release rate of loaded drugs [79–81] and to enhance the pharmacokinetic properties (for example, absorption), which would have a huge influence on determining the used dosage form/route of administration and a high positive impact on the therapeutic effect [38]. It could also be used to improve the safety profile and decrease toxicity [81].

The same evaluation was performed again by creating a risk estimation matrix (Table 4), as well as conducting Pareto analysis (Figure 4), to study the importance and ranking of CPPs and CMAs during the transformation of hydrothermally synthesized TNTs into possible drug carriers. The most important CPPs were the pH of the washing solution, reaction temperature, reaction time, calcination temperature, and stirring, while the important CMAs were precursor concentration, functionalizing agent, alkaline medium concentration, precursor particle size, precursor crystal structure, drug type, and used solvent.

The results of this evaluation agreed well with the literature data as most of the performed studies reported that the washing step is an unavoidable phase in the preparation of TNTs [54,62,82], along with selection of the appropriate set of temperature [40–46], time [49–51], and precursor concentration [40,49,69].

The pH of the washing solution is a significant factor in the washing process, which serves as the complementary step to obtain the desired tubular morphology of TNTs if the reaction conditions are not sufficient to achieve this. It would also have a major impact on most selected CQAs, such as the size of the resulting nanotubes, their type, SSA, and the preparation yield. For these reasons, it is justified why the pH of the washing solution is in the top ranking of CPPs, followed by reaction temperature and time, which also have a high impact on the majority of CQAs, like morphology, size, SSA, and yield. Moreover, these previously mentioned CQAs were influenced in the same way by the top-ranked CMA, which was precursor concentration. Again, these findings correlated well with the

data presented in the literature, as the resulting top-ranked factors were the most discussed factors in the literature, which supports their priority classification according to the results of Pareto analysis.

Table 4. Interdependence between CQAs, CMAs, and CPPs. (Red (H), Yellow (M) and Green (L) are associated with high, medium and low risk, respectively).

Process	Preparation Reaction						
CPP/CMA / CQA	Temperature	Alkaline Medium Concentration	Time	Stirring	Precursor Particle Size	Precursor Crystal Structure	Precursor Concentration
Size	H	L	H	M	L	L	H
Crystal structure	H	L	M	L	L	H	L
Morphology	H	H	H	M	H	H	H
Specific surface area	H	H	H	L	H	L	H
Yield	H	H	H	H	L	L	H
TNT type	L	L	L	L	L	L	L
Surface characteristics	L	L	L	L	L	L	L
Drug loading	L	L	L	L	L	L	L

Process	Post Treatment		Surface Modification	API Incorporation	
CPP/CMA / CQA	pH of Washing Solution	Calcination Temperature	Functionalizing Agent	Drug Type	Solvent
Size	H	L	M	L	L
Crystal structure	M	H	L	L	L
Morphology	H	H	L	L	L
Specific surface area	H	H	L	L	L
Yield	H	H	L	L	L
TNT type	H	L	L	L	L
Surface modification	L	L	H	M	L
Drug loading	L	L	M	H	H

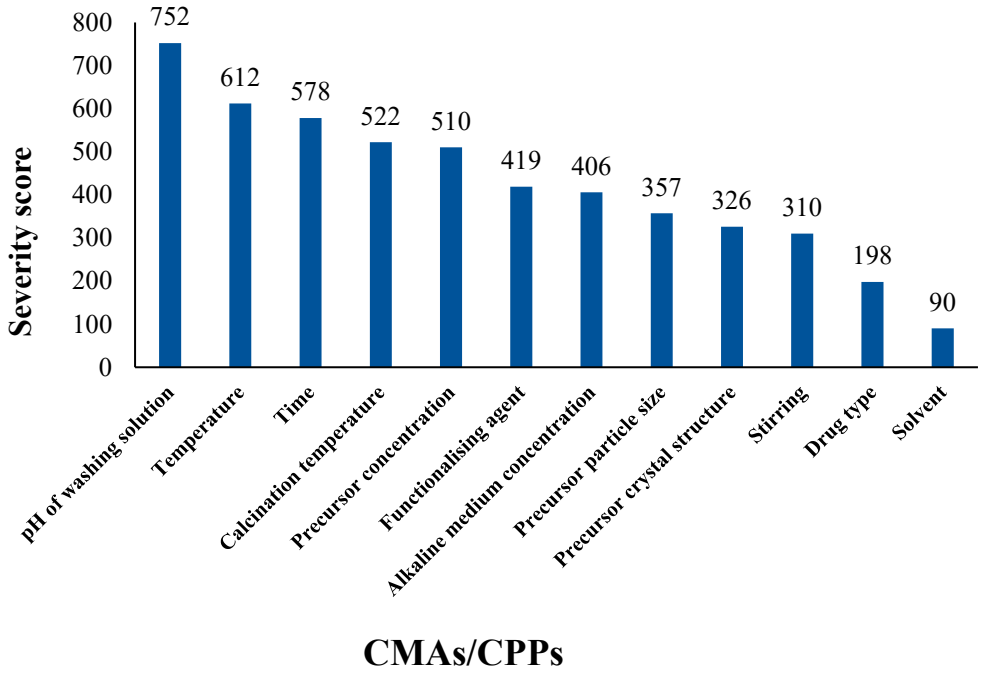

Figure 4. Ranking of CMAs and CPPs during transformation of hydrothermally synthesized TNTs into possible drug carriers.

As discussed above, a dataset (Table S1) was created based on the existing literature [4,5,41,47,48,50–53,55,57–65,67–69,73,74,79–134] to perform ANN modeling on possible CQAs. The most discussed CQAs in the literature were the morphology and SSA of the obtained product, which enabled the gathering of data sufficient to build an ANN-based model for the prediction of the possible outcome of a synthesis and post-treatment process. Furthermore, the global sensitivity analysis also enabled us the check the validity of the results obtained during the risk assessment procedure.

The structure (e.g., the percentages of rutile, anatase, and amorphous phases), surface area, and particle size of the starting precursor were considered as input CMAs, while the temperature and NaOH concentration of the reaction medium, the reaction time, the acid concentration of the washing liquid, and calcination temperature were selected as input CPPs. Most researchers used HCl in the washing step, but in some cases HNO_3 was applied. This meant a considerable difficulty in that the morphology of the obtained product was described in the literature with high versatility, which necessitated intensive data curation regarding this aspect. Besides the nanotubular morphology (1), the terms nanorods (2), nanofibers (3), and nanowires (4) were given to those products where one direction of particle growth was featured, such that products with structures with an increasing length to diameter ratio were named nanorods, nanofibers, and nanowires, respectively. The classification of those particles where growth was featured in two directions were unified under the term nanoribbons (5), while spherical products were classified as nanoparticles (6) or spherical agglomerates (7). Two additional classes were made for those cases where no conversion (8) of the starting material was observed, or the product obtained was a mixture (9) of particles with different morphologies.

The best performing network for the classification of morphology had 10 input, 10 hidden, and 9 output neurons, where the activation of the hidden and output neurons were based on identity and softmax functions, respectively. The network structure (e.g., the weights between various neurons) is displayed in Table S4. The perfection of the classification for the training, testing, and validation subsets was 85.71%, 61.9%, and 76.19%, respectively. The results of the classification on the validation dataset are displayed in Figure 5. Most of the misclassified cases predicted the formation of nanotubes, which may have been due to over-representation of this class in the training subset, and a considerable increase in classification accuracy may be expected with a more balanced dataset. The results of the other retained networks showed high consistency with these results.

The results of the global sensitivity analysis partially supported the results of the risk assessment, but the highest impact was exhibited by the calcination temperature, which was followed by particle size and the structure of the precursor material (mostly by the amorphous content), with approximately equal contributions, while the NaOH content and the temperature of the reaction medium took third place, again with approximately equal contributions.

In the case of modeling of SSA, the best performing network had 10 input, 10 hidden, and 1 output neurons, where the activation of the hidden and output neurons was based on tanh and logistic functions, respectively. The perfection of the classification for the training, testing, and validation subsets was 0.8924, 0.7834, and 0.9213, respectively. The network structure (e.g., the weights between various neurons) is displayed in Table S5. The target vs. output predictions on the validation subset are displayed in Figure 6.

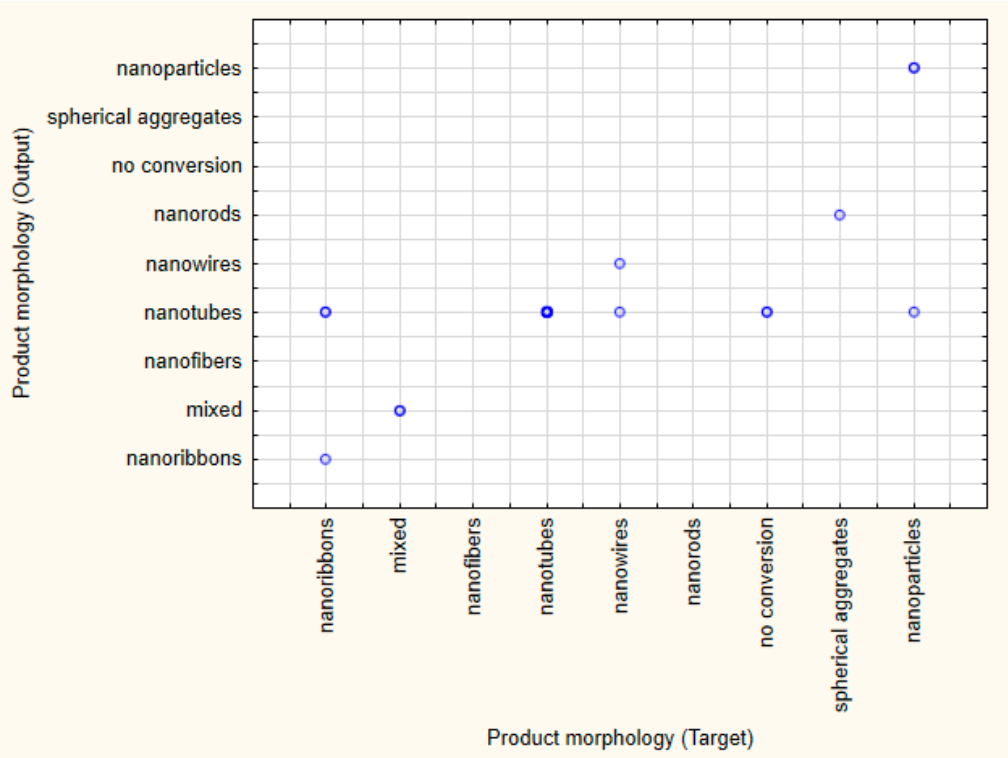

Figure 5. Target vs. output results of the classification of particle morphology on the validation subset. (light and dark blue dots represents one single case and multiple cases, respectively).

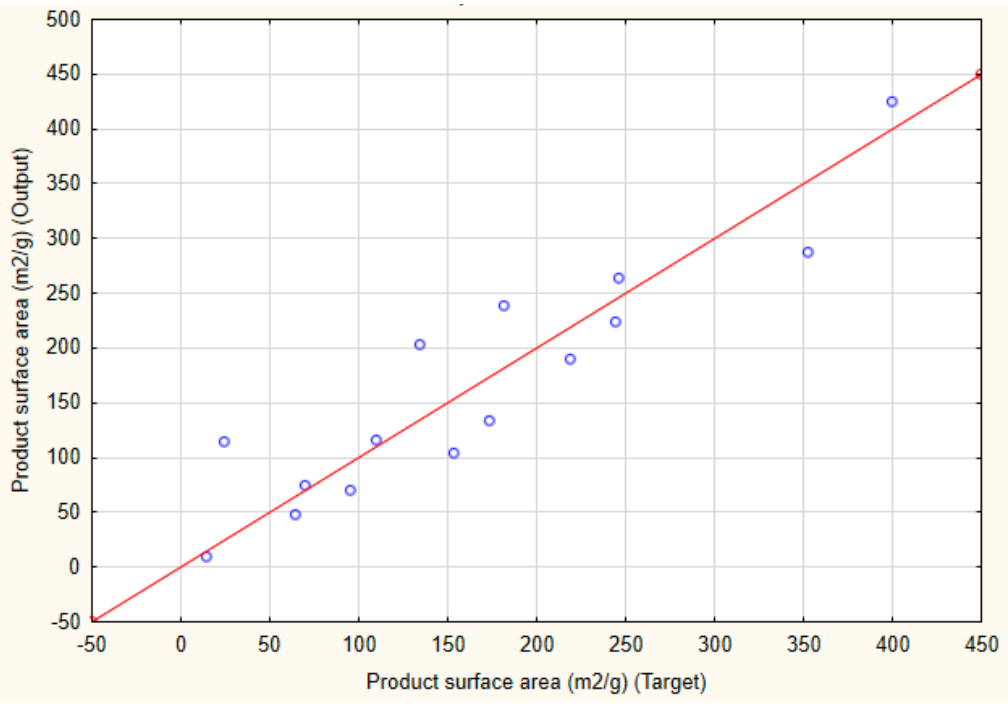

Figure 6. Target vs. output results of the specific surface area on the validation subset. (red line represents the ideal target vs. output relation while blue dots represent the individual predictions).

The global sensitivity analysis showed a similar picture as in case of the classification of morphology. The most important factor affecting the SSA was found to be the calcination temperature, followed by the structure of the precursor materials (where also the amorphous content was the most predominant), the reaction temperature, and acid content of

the washing liquid, respectively. The SSA of the starting precursor also plays a considerable role in the SSA of the product but, regarding the size of this effect, the different models exhibited some inconsistencies, which may be due to that fact that most of the available papers discussed limited information on the physical properties of the starting materials or the available data showed high versatility. One of the most used precursors was TiO_2 P25 (Degussa AG or Evonik AG, Essen, Germany), but its reported properties highly varied in the literature. The specification datasheet refers to a unique anatase/rutile ratio, which varied between 80.21 ± 5.59% anatase and 17.40 ± 5.39% rutile contents, respectively, while some publications also reported 4.75 ± 5.72% amorphous content. Similarly, the average particle size of the anatase and rutile components varied between 10–48 nm and 14.4–51 nm, respectively. The SSA of the product was found to be 52.9 ± 12.08 m^2/g [135–137].

According to the discussed findings, a detailed flow chart (Figure 7) is presented as a systematic pathway for TNT transformation into possible drug carriers, indicating the CMAs and CPPs that could affect this procedure and its multiple steps according to the authors' previous experience and precise screening of the published articles discussing this topic.

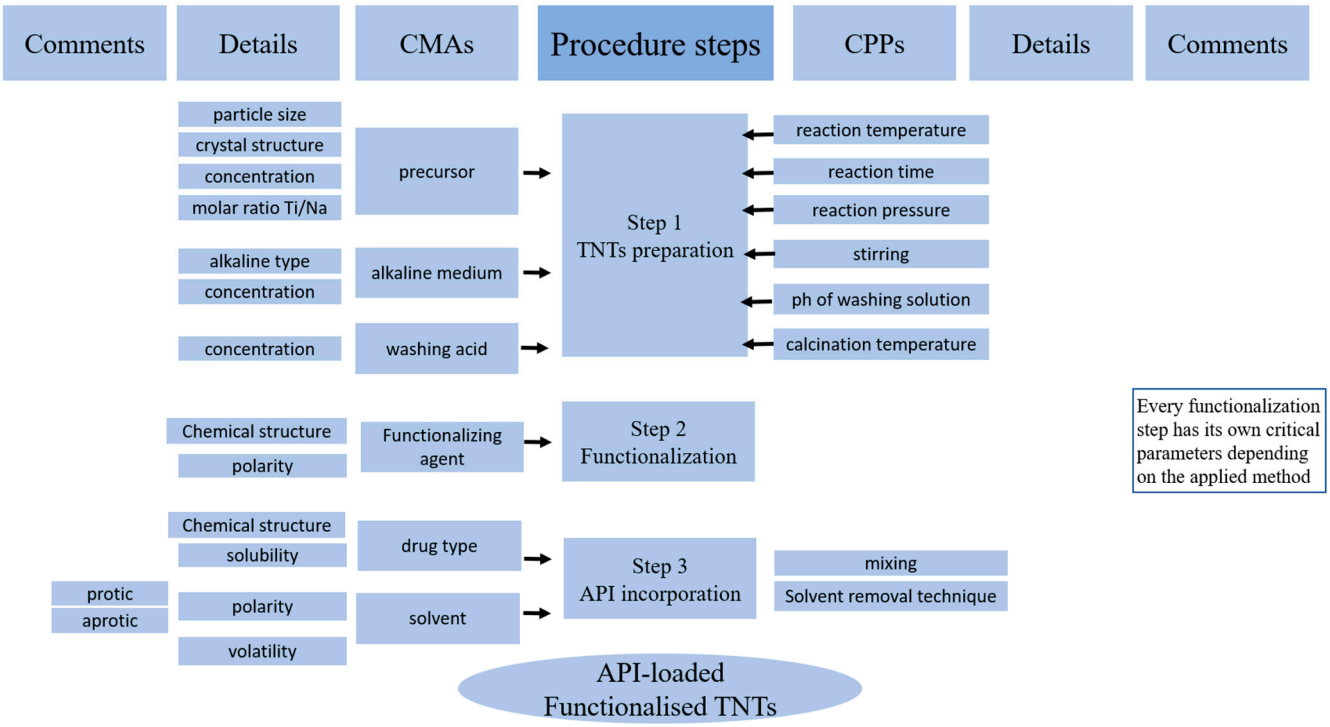

Figure 7. Critical material attributes and critical process parameters that affect TNT transformation into possible drug carriers.

4. Conclusions

The hydrothermal treatment method holds huge promise for the future development of titanate nanotubes with tailored specifications intended for therapeutic purposes. Therefore, suggesting a systematic approach for transforming hydrothermally synthesized TNTs for pharmaceutical applications should be adopted. This could be achieved through the QbD approach and risk assessment tools, which have recently created a new chapter in the development of the pharmaceutical industry. Moreover, creating clear guidelines for TNT preparation using the QbD approach could open the door for accelerating the scale-up process and transferring their manufacture/use to the next level, especially with the existence of too many factors affecting this complicated procedure. This would have a huge positive impact on the effort needed, time, and cost.

In this study, the most important QTPP elements of hydrothermally synthesized TNTs were identified. Then, the CQAs of nanotubes, CMAs, and CPPs that could have an impact on hydrothermal treatment during titanate nanotube preparation and subsequent steps for their functionalization and loading with APIs were also collected and evaluated.

The CQAs, CMAs, and CPPs with the highest influence and most important impact were identified using Pareto analysis. Surface characteristics, morphology, and SSA were the most significant CQAs. The pH of the washing solution, reaction temperature, and reaction time were the most important CPPs, while precursor concentration, functionalizing agent, and alkaline medium concentration were the highest influencing factors among CMAs.

One of the main targets of this work was to collect and analyze all of the available data into a single paper, thus establishing a solid base that could be of great importance to other researchers as it could be used as a starting point for deeper investigation and further development, and to establish an ANN-based model for the prediction of the most important CQAs. In conclusion, the available literature contains numerous inconsistencies, especially regarding the physical properties of the precursor materials and the parameters of the washing step, which would enable the building of more robust models for the prediction of the expected research outcome. Nevertheless, it was possible to build models for the prediction of product morphology and SSA with acceptable prediction performance.

Supplementary Materials: The following supporting information can be downloaded at: https://www.mdpi.com/article/10.3390/pharmaceutics17010047/s1, Table S1: Full dataset extracted from the literature; Table S2: Curated dataset for morphology classification model; Table S3: Curated dataset for modelling of SSA; Table S4: Weight structure of the ANN for morphology classification; Table S5: Weight structure of ANN for SSA modeling

Author Contributions: Conceptualization, T.S.; methodology, R.S. and T.S.; formal analysis, R.S. and K.L.; investigation, R.S.; data curation, R.S.; writing—original draft preparation, R.S.; writing—review and editing, T.S. and K.L.; supervision, T.S. and G.R.J.; project administration, T.S.; funding acquisition, T.S. All authors have read and agreed to the published version of the manuscript.

Funding: This research was funded by project no. TKP2021-EGA-32 and has been implemented with the support provided by the Ministry of Innovation and Technology of Hungary from the National Research, Development and Innovation Fund, financed under the TKP2021-EGA funding scheme. The first author was supported by the EKOP-24-3-The University Research Scholarship Program of the Ministry of Culture and Innovation, financed from the National Research, Development and Innovation Fund (EKOP-24-3-SZTE-226).

Institutional Review Board Statement: Not applicable.

Informed Consent Statement: Not applicable.

Data Availability Statement: Data used in risk assessment and ANN modeling are available in public databases, while the exact dataset used for training, testing, and validating the ANNs are displayed in the Supplementary Material.

Conflicts of Interest: The authors declare no conflicts of interest.

References

1. Hoyer, P. Semiconductor nanotube formation by a two-step template process. *Adv. Mater.* **1996**, *8*, 857–859. [CrossRef]
2. Boudon, J.; Papa, A.-L.; Paris, J.; Millot, N. Titanate nanotubes as a versatile platform for nanomedicine. In *Nanomedicine*; One Central Press: Paris, France, 2014; pp. 403–428.
3. Ranjous, Y.; Regdon, G., Jr.; Pintye-Hodi, K.; Sovany, T. Standpoint on the priority of TNTs and CNTs as targeted drug delivery systems. *Drug Discov. Today* **2019**, *24*, 1704–1709. [CrossRef] [PubMed]
4. Papa, A.L.; Dumont, L.; Vandroux, D.; Millot, N. Titanate nanotubes: Towards a novel and safer nanovector for cardiomyocytes. *Nanotoxicology* **2013**, *7*, 1131–1142. [CrossRef] [PubMed]

5. Fenyvesi, F.; Konya, Z.; Razga, Z.; Vecsernyes, M.; Kasa, P., Jr.; Pintye-Hodi, K.; Bacskay, I. Investigation of the cytotoxic effects of titanate nanotubes on Caco-2 cells. *AAPS PharmSciTech* **2014**, *15*, 858–861. [CrossRef]
6. Feschet-Chassot, E.; Raspal, V.; Sibaud, Y.; Awitor, O.K.; Bonnemoy, F.; Bonnet, J.L.; Bohatier, J. Tunable functionality and toxicity studies of titanium dioxide nanotube layers. *Thin Solid Film.* **2011**, *519*, 2564–2568. [CrossRef]
7. Sipos, B.; Regdon, G.; Konya, Z.; Pintye-Hodi, K.; Sovany, T. Comparative study on the rheological properties and tablettability of various APIs and their composites with titanate nanotubes. *Powder Technol.* **2017**, *321*, 419–427. [CrossRef]
8. Sipos, B.; Pintye-Hodi, K.; Regdon, G., Jr.; Konya, Z.; Viana, M.; Sovany, T. Investigation of the Compressibility and Compactibility of Titanate Nanotube-API Composites. *Materials* **2018**, *11*, 2582. [CrossRef]
9. Sahinovic, M.; Hassan, A.; Kristo, K.; Regdon, G., Jr.; Vranic, E.; Sovany, T. Quality by Design-Based Development of Solid Self-Emulsifying Drug Delivery System (SEDDS) as a Potential Carrier for Oral Delivery of Lysozyme. *Pharmaceutics* **2023**, *15*, 995. [CrossRef] [PubMed]
10. Pallagi, E.; Jojart-Laczkovich, O.; Nemeth, Z.; Szabo-Revesz, P.; Csoka, I. Application of the QbD-based approach in the early development of liposomes for nasal administration. *Int. J. Pharm.* **2019**, *562*, 11–22. [CrossRef]
11. Hales, D.; Vlase, L.; Porav, S.A.; Bodoki, A.; Barbu-Tudoran, L.; Achim, M.; Tomuta, I. A quality by design (QbD) study on enoxaparin sodium loaded polymeric microspheres for colon-specific delivery. *Eur. J. Pharm. Sci.* **2017**, *100*, 249–261. [CrossRef] [PubMed]
12. Iurian, S.; Bogdan, C.; Tomuta, I.; Szabo-Revesz, P.; Chvatal, A.; Leucuta, S.E.; Moldovan, M.; Ambrus, R. Development of oral lyophilisates containing meloxicam nanocrystals using QbD approach. *Eur. J. Pharm. Sci.* **2017**, *104*, 356–365. [CrossRef] [PubMed]
13. Wang, J.; Kan, S.; Chen, T.; Liu, J. Application of quality by design (QbD) to formulation and processing of naproxen pellets by extrusion-spheronization. *Pharm. Dev. Technol.* **2015**, *20*, 246–256. [CrossRef] [PubMed]
14. Kovacs, A.; Berko, S.; Csanyi, E.; Csoka, I. Development of nanostructured lipid carriers containing salicyclic acid for dermal use based on the Quality by Design method. *Eur. J. Pharm. Sci.* **2017**, *99*, 246–257. [CrossRef] [PubMed]
15. Mockus, L.N.; Paul, T.W.; Pease, N.A.; Harper, N.J.; Basu, P.K.; Oslos, E.A.; Sacha, G.A.; Kuu, W.Y.; Hardwick, L.M.; Karty, J.J.; et al. Quality by design in formulation and process development for a freeze-dried, small molecule parenteral product: A case study. *Pharm. Dev. Technol.* **2011**, *16*, 549–576. [CrossRef]
16. Pallagi, E.; Ambrus, R.; Szabo-Revesz, P.; Csoka, I. Adaptation of the quality by design concept in early pharmaceutical development of an intranasal nanosized formulation. *Int. J. Pharm.* **2015**, *491*, 384–392. [CrossRef] [PubMed]
17. Benayache, A.; Lamoudi, L.; Daoud, K. Artificial neural network modeling of tablet coating in a pan coater. *J. Coat. Technol. Res.* **2023**, *20*, 485–499. [CrossRef]
18. Nagy, B.; Szabados-Nacsa, Á.; Fülöp, G.; Nagyné, A.T.; Galata, D.L.; Farkas, A.; Mészáros, L.A.; Nagy, Z.K.; Marosi, G. Interpretable artificial neural networks for retrospective QbD of pharmaceutical tablet manufacturing based on a pilot-scale developmental dataset. *Int. J. Pharm.* **2023**, *633*, 122620. [CrossRef]
19. Mihajlovic, T.; Ibric, S.; Mladenovic, A. Application of design of experiments and multilayer perceptron neural network in optimization of the spray-drying process. *Dry Technol.* **2011**, *29*, 1638–1647. [CrossRef]
20. Kachrimanis, K.; Karamyan, V.; Malamataris, S. Artificial neural networks (ANNs) and modeling of powder flow. *Int. J. Pharm.* **2003**, *250*, 13–23. [CrossRef]
21. Barmpalexis, P.; Kanaze, F.I.; Kachrimanis, K.; Georgarakis, E. Artificial neural networks in the optimization of a nimodipine controlled release tablet formulation. *Eur. J. Pharm. Biopharm.* **2010**, *74*, 316–323. [CrossRef]
22. Chaibva, F.; Burton, M.; Walker, R.B. Optimization of salbutamol sulfate dissolution from sustained release matrix formulations using an artificial neural network. *Pharmaceutics* **2010**, *2*, 182–198. [CrossRef]
23. Cardoso-Daodu, I.M.; Ilomuanya, M.O.; Amenaghawon, A.N.; Azubuike, C.P. Artificial neural network for optimizing the formulation of curcumin-loaded liposomes from statistically designed experiments. *Prog. Biomater.* **2022**, *11*, 55–65. [CrossRef] [PubMed]
24. Brahima, S.; Boztepe, C.; Kunkul, A.; Yuceer, M. Modeling of drug release behavior of pH and temperature sensitive poly(NIPAAm-co-AAc) IPN hydrogels using response surface methodology and artificial neural networks. *Mater. Sci. Eng. C Mater. Biol. Appl.* **2017**, *75*, 425–432. [CrossRef] [PubMed]
25. Umaña, M.; Llull, L.; Bon, J.; Eim, V.S.; Simal, S. Artificial Neural Networks to Optimize Oil-in-Water Emulsion Stability with Orange By-Products. *Foods* **2022**, *11*, 3750. [CrossRef]
26. Kandimalla, K.K.; Kanikkannan, N.; Singh, M. Optimization of a vehicle mixture for the transdermal delivery of melatonin using artificial neural networks and response surface method. *J. Control Release* **1999**, *61*, 71–82. [CrossRef] [PubMed]
27. Benkő, E.; Ilič, I.G.; Kristó, K.; Regdon, G., Jr.; Csóka, I.; Pintye-Hódi, K.; Srčič, S.; Sovány, T. Predicting drug release rate of implantable matrices and better understanding of the underlying mechanisms through experimental design and artificial neural network-based modelling. *Pharmaceutics* **2022**, *14*, 228. [CrossRef]
28. Nemeth, Z.; Pallagi, E.; Dobo, D.G.; Csoka, I. A Proposed Methodology for a Risk Assessment-Based Liposome Development Process. *Pharmaceutics* **2020**, *12*, 1164. [CrossRef]

29. Nemeth, Z.; Pallagi, E.; Dobo, D.G.; Kozma, G.; Konya, Z.; Csoka, I. An Updated Risk Assessment as Part of the QbD-Based Liposome Design and Development. *Pharmaceutics* **2021**, *13*, 1071. [CrossRef] [PubMed]
30. ICH. Pharmaceutical Development Q8. In *ICH Harmonised Tripartite Guideline*; ICH: Geneva, Switzerland, 2009; pp. 1–28.
31. Batool, S.A.; Maqbool, M.S.S.; Javed, M.A.; Niaz, A.; Rehman, M.A.U. A Review on the Fabrication and Characterization of Titania Nanotubes Obtained via Electrochemical Anodization. *Surfaces* **2022**, *5*, 456–480. [CrossRef]
32. Adeleye, A.T.; John, K.I.; Adeleye, P.G.; Akande, A.A.; Banjoko, O.O. One-dimensional titanate nanotube materials: Heterogeneous solid catalysts for sustainable synthesis of biofuel precursors/value-added chemicals-a review. *J. Mater. Sci.* **2021**, *56*, 18391–18416. [CrossRef]
33. Tsvetkov, N.; Larina, L.; Ku Kang, J.; Shevaleevskiy, O. Sol-Gel Processed TiO_2 Nanotube Photoelectrodes for Dye-Sensitized Solar Cells with Enhanced Photovoltaic Performance. *Nanomaterials* **2020**, *10*, 296. [CrossRef]
34. Owens, G.J.; Singh, R.K.; Foroutan, F.; Alqaysi, M.; Han, C.M.; Mahapatra, C.; Kim, H.W.; Knowles, J.C. Sol-gel based materials for biomedical applications. *Prog. Mater. Sci.* **2016**, *77*, 1–79. [CrossRef]
35. Yue, L.; Gao, W.; Zhang, D.; Guo, X.; Ding, W.; Chen, Y. Colloids seeded deposition: Growth of titania nanotubes in solution. *J. Am. Chem. Soc.* **2006**, *128*, 11042–11043. [CrossRef] [PubMed]
36. Sipos, B.; Pintye-Hodi, K.; Konya, Z.; Kelemen, A.; Regdon, G., Jr.; Sovany, T. Physicochemical characterisation and investigation of the bonding mechanisms of API-titanate nanotube composites as new drug carrier systems. *Int. J. Pharm.* **2017**, *518*, 119–129. [CrossRef]
37. Ranjous, Y.; Regdon, G., Jr.; Pintye-Hodi, K.; Varga, T.; Szenti, I.; Konya, Z.; Sovany, T. Optimization of the Production Process and Product Quality of Titanate Nanotube-Drug Composites. *Nanomaterials* **2019**, *9*, 1406. [CrossRef] [PubMed]
38. Ranjous, Y.; Kósa, D.; Ujhelyi, Z.; Regdon, G.; Nagy, K.A.; Szenti, I.; Kónya, Z.; Bácskay, I.; Sovány, T. Evaluation of the permeability and in vitro cytotoxicity of functionalized titanate nanotubes on Caco-2 cell line. *Acta Pharm. Hung.* **2021**, *91*, 31–39. [CrossRef]
39. Saker, R.; Shammout, H.; Regdon, G., Jr.; Sovány, T. An Overview of Hydrothermally Synthesized Titanate Nanotubes: The Factors Affecting Preparation and Their Promising Pharmaceutical Applications. *Pharmaceutics* **2024**, *16*, 635. [CrossRef]
40. Bavykin, D.V.; Parmon, V.N.; Lapkin, A.A.; Walsh, F.C. The effect of hydrothermal conditions on the mesoporous structure of TiO_2 nanotubes. *J. Mater. Chem.* **2004**, *14*, 3370–3377. [CrossRef]
41. Lee, C.K.; Lyu, M.D.; Liu, S.S.; Chen, H.C. The synthetic parameters for the preparation of nanotubular titanate with highly photocatalytic activity. *J. Taiwan. Inst. Chem. Eng.* **2009**, *40*, 463–470. [CrossRef]
42. Yuan, Z.Y.; Su, B.L. Titanium oxide nanotubes, nanofibers and nanowires. *Colloid. Surf. A* **2004**, *241*, 173–183. [CrossRef]
43. Morgan, D.L.; Zhu, H.Y.; Frost, R.L.; Waclawik, E.R. Determination of a morphological phase diagram of titania/titanate nanostructures from alkaline hydrothermal treatment of Degussa P25. *Chem. Mater.* **2008**, *20*, 3800–3802. [CrossRef]
44. Ma, R.; Fukuda, K.; Sasaki, T.; Osada, M.; Bando, Y. Structural features of titanate nanotubes/nanobelts revealed by Raman, X-ray absorption fine structure and electron diffraction characterizations. *J. Phys. Chem. B* **2005**, *109*, 6210–6214. [CrossRef]
45. Lan, Y.; Gao, X.P.; Zhu, H.Y.; Zheng, Z.F.; Yan, T.Y.; Wu, F.; Ringer, S.P.; Song, D.Y. Titanate nanotubes and nanorods prepared from rutile powder. *Adv. Funct. Mater.* **2005**, *15*, 1310–1318. [CrossRef]
46. Lee, D.S.; Lee, S.Y.; Rhee, K.Y.; Park, S.J. Effect of hydrothermal temperature on photocatalytic properties of TiO_2 nanotubes. *Curr. Appl. Phys.* **2014**, *14*, 415–420. [CrossRef]
47. Vu, T.H.T.; Au, H.T.; Tran, L.T.; Nguyen, T.M.T.; Tran, T.T.T.; Pham, M.T.; Do, M.H.; Nguyen, D.L. Synthesis of titanium dioxide nanotubes via one-step dynamic hydrothermal process. *J. Mater. Sci.* **2014**, *49*, 5617–5625. [CrossRef]
48. Guo, Y.; Lee, N.H.; Oh, H.J.; Yoon, C.R.; Park, K.S.; Lee, H.G.; Lee, K.S.; Kim, S.J. Structure-tunable synthesis of titanate nanotube thin films via a simple hydrothermal process. *Nanotechnology* **2007**, *18*, 295608. [CrossRef]
49. Sreekantan, S.; Wei, L.C. Study on the formation and photocatalytic activity of titanate nanotubes synthesized via hydrothermal method. *J. Alloys Compd.* **2010**, *490*, 436–442. [CrossRef]
50. Elsanousi, A.; Elssfah, E.M.; Zhang, J.; Lin, J.; Song, H.S.; Tang, C.C. Hydrothermal treatment duration effect on the transformation of titanate nanotubes into nanoribbons. *J. Phys. Chem. C* **2007**, *111*, 14353–14357. [CrossRef]
51. Weng, L.Q.; Song, S.H.; Hodgson, S.; Baker, A.; Yu, J. Synthesis and characterisation of nanotubular titanates and titania. *J. Eur. Ceram. Soc.* **2006**, *26*, 1405–1409. [CrossRef]
52. Poudel, B.; Wang, W.Z.; Dames, C.; Huang, J.Y.; Kunwar, S.; Wang, D.Z.; Banerjee, D.; Chen, G.; Ren, Z.F. Formation of crystallized titania nanotubes and their transformation into nanowires. *Nanotechnology* **2005**, *16*, 1935–1940. [CrossRef]
53. Tsai, C.C.; Teng, H.S. Structural features of nanotubes synthesized from NaOH treatment on TiO_2 with different post-treatments. *Chem. Mater.* **2006**, *18*, 367–373. [CrossRef]
54. Viet, P.V.; Phan, B.T.; Hieule, V.; Thi, C.M. The Effect of Acid Treatment and Reactive Temperature on the Formation of TiO_2 Nanotubes. *J. Nanosci. Nanotechnol.* **2015**, *15*, 5202–5206. [CrossRef]
55. Nguyen, N.H.; Bai, H. Effect of washing pH on the properties of titanate nanotubes and its activity for photocatalytic oxidation of NO and NO_2. *Appl. Surf. Sci.* **2015**, *355*, 672–680. [CrossRef]

56. Lee, C.-K.; Wang, C.-C.; Juang, L.-C.; Lyu, M.-D.; Hung, S.-H.; Liu, S.-S. Effects of sodium content on the microstructures and basic dye cation exchange of titanate nanotubes. *Colloids Surf. A Physicochem. Eng. Asp.* **2008**, *317*, 164–173. [CrossRef]
57. Tsai, C.C.; Teng, H.S. Regulation of the physical characteristics of Titania nanotube aggregates synthesized from hydrothermal treatment. *Chem. Mater.* **2004**, *16*, 4352–4358. [CrossRef]
58. Turki, A.; Kochkar, H.; Guillard, C.; Berhault, G.; Ghorbel, A. Effect of Na content and thermal treatment of titanate nanotubes on the photocatalytic degradation of formic acid. *Appl. Catal. B Environ.* **2013**, *138*, 401–415. [CrossRef]
59. Lopez Zavala, M.A.; Lozano Morales, S.A.; Avila-Santos, M. Synthesis of stable TiO_2 nanotubes: Effect of hydrothermal treatment, acid washing and annealing temperature. *Heliyon* **2017**, *3*, e00456. [CrossRef] [PubMed]
60. Kiatkittipong, K.; Scott, J.; Amal, R. Hydrothermally synthesized titanate nanostructures: Impact of heat treatment on particle characteristics and photocatalytic properties. *ACS Appl. Mater. Interfaces* **2011**, *3*, 3988–3996. [CrossRef]
61. Ma, Y.T.; Lin, Y.; Xiao, X.R.; Zhou, X.W.; Li, X.P. Sonication-hydrothermal combination technique for the synthesis of titanate nanotubes from commercially available precursors. *Mater. Res. Bull.* **2006**, *41*, 237–243. [CrossRef]
62. Li, W.J.; Fu, T.; Xie, F.; Yu, S.F.; He, S.L. The multi-staged formation process of titanium oxide nanotubes and its thermal stability. *Mater. Lett.* **2007**, *61*, 730–735. [CrossRef]
63. Nakahira, A.; Kato, W.; Tamai, M.; Isshiki, T.; Nishio, K.; Aritani, H. Synthesis of nanotube from a layered $H_2Ti_4O_9 \cdot H_2O$ in a hydrothermal treatment using various titania sources. *J. Mater. Sci.* **2004**, *39*, 4239–4245. [CrossRef]
64. Qamar, M.; Zaidi, S.A.; Rafatullah, M.; Qutob, M.; Kim, S.J.; Drmosh, Q.A. Role of Post-Hydrothermal Treatment on the Microstructures and Photocatalytic Activity of TiO_2-Based Nanotubes. *Catalysts* **2022**, *12*, 702. [CrossRef]
65. Morgado, E.; de Abreu, M.A.S.; Pravia, O.R.C.; Marinkovic, B.A.; Jardim, P.M.; Rizzo, F.C.; Araújo, A.S. A study on the structure and thermal stability of titanate nanotubes as a function of sodium content. *Solid State Sci.* **2006**, *8*, 888–900. [CrossRef]
66. Ribbens, S.; Meynen, V.; Van Tendeloo, G.; Ke, X.; Mertens, M.; Maes, B.U.W.; Cool, P.; Vansant, E.F. Development of photocatalytic efficient Ti-based nanotubes and nanoribbons by conventional and microwave assisted synthesis strategies. *Microporous Mesoporous Mater.* **2008**, *114*, 401–409. [CrossRef]
67. Preda, S.; Teodorescu, V.S.; Musuc, A.M.; Andronescu, C.; Zaharescu, M. Influence of the TiO_2 precursors on the thermal and structural stability of titanate-based nanotubes. *J. Mater. Res.* **2013**, *28*, 294–303. [CrossRef]
68. Nakahira, A.; Kubo, T.; Numako, C. TiO_2-derived titanate nanotubes by hydrothermal process with acid treatments and their microstructural evaluation. *ACS Appl. Mater. Interfaces* **2010**, *2*, 2611–2616. [CrossRef] [PubMed]
69. Saponjic, Z.V.; Dimitrijevic, N.M.; Tiede, D.M.; Goshe, A.J.; Zuo, X.; Chen, L.X.; Barnard, A.S.; Zapol, P.; Curtiss, L.; Rajh, T. Shaping Nanometer-Scale Architecture Through Surface Chemistry. *Adv. Mater.* **2005**, *17*, 965–971. [CrossRef]
70. Mano, S.S.; Kanehira, K.; Sonezaki, S.; Taniguchi, A. Effect of polyethylene glycol modification of TiO_2 nanoparticles on cytotoxicity and gene expressions in human cell lines. *Int. J. Mol. Sci.* **2012**, *13*, 3703–3717. [CrossRef]
71. Lipka, J.; Semmler-Behnke, M.; Sperling, R.A.; Wenk, A.; Takenaka, S.; Schleh, C.; Kissel, T.; Parak, W.J.; Kreyling, W.G. Biodistribution of PEG-modified gold nanoparticles following intratracheal instillation and intravenous injection. *Biomaterials* **2010**, *31*, 6574–6581. [CrossRef]
72. Saker, R.; Jojárt-Laczkovich, O.; Regdon, G.J.r.; Takács, T.; Szenti, I.; Bózsity-Faragó, N.; Zupkó, I.; Sovány, T. Surface Modification of Titanate Nanotubes with a Carboxylic Arm for Further Functionalization Intended to Pharmaceutical Applications. *Pharmaceutics* **2023**, *15*, 2780. [CrossRef] [PubMed]
73. Kamal, N.; Zaki, A.; El-Shahawy, A.A.; Sayed, O.M.; El-Dek, S. Changing the morphology of one-dimensional titanate nanostructures affects its tissue distribution and toxicity. *Toxicol. Ind. Health* **2020**, *36*, 272–286. [CrossRef]
74. Magrez, A.; Horvath, L.; Smajda, R.; Salicio, V.; Pasquier, N.; Forro, L.; Schwaller, B. Cellular toxicity of TiO_2-based nanofilaments. *ACS Nano* **2009**, *3*, 2274–2280. [CrossRef]
75. Sayes, C.M.; Wahi, R.; Kurian, P.A.; Liu, Y.; West, J.L.; Ausman, K.D.; Warheit, D.B.; Colvin, V.L. Correlating nanoscale titania structure with toxicity: A cytotoxicity and inflammatory response study with human dermal fibroblasts and human lung epithelial cells. *Toxicol. Sci.* **2006**, *92*, 174–185. [CrossRef] [PubMed]
76. Jiang, J.; Oberdörster, G.; Elder, A.; Gelein, R.; Mercer, P.; Biswas, P. Does nanoparticle activity depend upon size and crystal phase? *Nanotoxicology* **2008**, *2*, 33–42. [CrossRef] [PubMed]
77. Wu, J.; Sun, J.; Xue, Y. Involvement of JNK and P53 activation in G2/M cell cycle arrest and apoptosis induced by titanium dioxide nanoparticles in neuron cells. *Toxicol. Lett.* **2010**, *199*, 269–276. [CrossRef] [PubMed]
78. Shimizu, M.; Tainaka, H.; Oba, T.; Mizuo, K.; Umezawa, M.; Takeda, K. Maternal exposure to nanoparticulate titanium dioxide during the prenatal period alters gene expression related to brain development in the mouse. *Part. Fibre Toxicol.* **2009**, *6*, 1–8. [CrossRef] [PubMed]
79. Mandal, S.S.; Jose, D.; Bhattacharyya, A.J. Role of surface chemistry in modulating drug release kinetics in titania nanotubes. *Mater. Chem. Phys.* **2014**, *147*, 247–253. [CrossRef]
80. Khoshnood, N.; Zamanian, A.; Massoudi, A. Mussel-inspired surface modification of titania nanotubes as a novel drug delivery system. *Mater. Sci. Eng. C Mater. Biol. Appl.* **2017**, *77*, 748–754. [CrossRef] [PubMed]

81. Torres, C.C.; Campos, C.H.; Diaz, C.; Jimenez, V.A.; Vidal, F.; Guzman, L.; Alderete, J.B. PAMAM-grafted TiO_2 nanotubes as novel versatile materials for drug delivery applications. *Mater. Sci. Eng. C Mater. Biol. Appl.* **2016**, *65*, 164–171. [CrossRef] [PubMed]
82. Arruda, L.B.; Santos, C.M.; Orlandi, M.O.; Schreiner, W.H.; Lisboa, P.N. Formation and evolution of TiO_2 nanotubes in alkaline synthesis. *Ceram. Int.* **2015**, *41*, 2884–2891. [CrossRef]
83. An, H.; Hu, X.; Zhu, B.; Song, J.; Zhao, W.; Zhang, S.; Huang, W. Preparation, characterization and photocatalytic performances of materials based on CS_2-modified titanate nanotubes. *Mater. Sci.* **2013**, *31*, 531–542. [CrossRef]
84. Aphairaj, D.; Wirunmongkol, T.; Niyomwas, S.; Pavasupree, S.; Limsuwan, P. Synthesis of anataseTiO_2 nanotubes derived from a natural leucoxene mineral by the hydrothermal method. *Ceram. Int.* **2014**, *40*, 9241–9247. [CrossRef]
85. Bavykin, D.V.; Friedrich, J.M.; Lapkin, A.A.; Walsh, F.C. Stability of Aqueous Suspensions of Titanate Nanotubes. *Chem. Mater.* **2006**, *18*, 1124–1129. [CrossRef]
86. Bavykin, D.V.; Kulak, A.N.; Walsh, F.C. Metastable Nature of Titanate Nanotubes in an Alkaline Environment. *Cryst. Growth Des.* **2010**, *10*, 4421–4427. [CrossRef]
87. Camposeco, R.; Castillo, S.; Mejia-Centeno, I.; Navarrete, J.; Gómez, R. Effect of the Ti/Na molar ratio on the acidity and the structure of TiO_2 nanostructures: Nanotubes, nanofibers and nanowires. *Mater. Charact.* **2014**, *90*, 113–120. [CrossRef]
88. Chen, Q.; Du, G.H.; Zhang, S.; Peng, L.-M. The structure of trititanate nanotubes. *Acta Crystallogr. Sect. B* **2002**, *58*, 587–593. [CrossRef]
89. Chen, Q.; Zhou, W.; Du, G.H.; Peng, L.-M. Trititanate nanotube made via a single alkali treatment. *Adv. Mater.* **2002**, *14*, 1208–1211. [CrossRef]
90. Chen, W.; Guo, X.; Zhang, S.; Jin, Z. TEM study on the formation mechanism of sodium titanate nanotubes. *J. Nanopart. Res.* **2007**, *9*, 1173–1180. [CrossRef]
91. Deng, Q.; Wei, M.; Ding, X.; Jiang, L.; Ye, B.; Wei, K. Brookite-type TiO_2 nanotubes. *Chem. Commun.* **2008**, *31*, 3657–3659. [CrossRef] [PubMed]
92. Du, G.H.; Chen, Q.; Che, R.C.; Yuan, Z.Y.; Peng, L.-M. Preparation and structure analysis of titanium oxide nanotubes. *Appl. Phys. Lett.* **2001**, *79*, 3702. [CrossRef]
93. Haro-González, P.; Pedroni, M.; Piccinelli, F.; Martín, L.L.; Polizzi, S.; Giarola, M.; Mariotto, G.; Speghini, A.; Bettinelli, M.; Martín, I.R. Synthesis, characterization and optical spectroscopy of Eu3þ doped titanate nanotubes. *J. Lumin.* **2011**, *131*, 2473–2477. [CrossRef]
94. Hodos, M.; Haspel, H.; Horváth, E.; Kukovecz, Á.; Kónya, Z.; Kiricsi, I. Vibrational Spectroscopic Studies on the Formation of Ion-exchangeable Titania Nanotubes. In *Electronic Properties of Novel Nanostructures*; Kuzmany, E., Fink, J., Mehring, M., Roth, S., Eds.; American Institute of Physics: College Park, MD, USA, 2005.
95. Jitputti, J.; Suzuki, Y.; Yoshikawa, S. Synthesis of TiO_2 nanowires and their photocatalytic activity for hydrogen evolution. *Catal. Commun.* **2008**, *9*, 1265–1271. [CrossRef]
96. Li, M.-J.; Chi, Z.-Y.; Wu, Y.-C. Morphology, Chemical Composition and Phase Transformation of Hydrothermal Derived Sodium Titanate. *J. Am. Ceram. Soc.* **2012**, *95*, 3297–3304. [CrossRef]
97. Kasuga, T.; Hiramatsu, M.; Hoson, A.; Sekino, T.; Niihara, K. Formation of Titanium Oxide Nanotube. *Langmuir* **1998**, *14*, 3160–3163. [CrossRef]
98. Kasuga, T.; Hiramatsu, M.; Hoson, A.; Sekino, T.; Niihara, K. Titania Nanotubes Prepared by Chemical Processing. *Adv. Mater.* **1999**, *11*, 1307–1311. [CrossRef]
99. Kukovecz, Á.; Hodos, M.; Horváth, E.; Radnóczi, G.; Kónya, Z.; Kiricsi, I. Oriented Crystal Growth Model Explains the Formation of Titania Nanotubes. *J. Phys. Chem. Lett. B* **2005**, *109*, 17781–17783. [CrossRef] [PubMed]
100. Lai, S.; Zhang, W.; Liu, F.; Wu, C.; Zeng, D.; Sun, X.; Xu, Y.; Fang, Y.; Zhou, W. TiO_2 Nanotubes as Animal Drug Delivery System and In Vitro Controlled Release. *J. Nanosci. Nanotechnol.* **2013**, *13*, 91–97. [CrossRef]
101. Lee, C.-K.; Lin, K.-S.; Wu, C.-F.; Lyu, M.-D.; Lo, C.-C. Effects of synthesis temperature on the microstructures and basic dyes adsorption of titanate nanotubes. *J. Hazard. Mater.* **2008**, *150*, 494–503. [CrossRef]
102. Li, K.; Li, M.; Xu, C.; Du, Z.; Chen, J.; Zou, F.; Zou, C.; Xu, S.; Li, G. A TiO_2 nanotubes film with excellent antireflective and near-perfect self-cleaning performances. *J. Mater. Sci. Technol.* **2021**, *88*, 11–20. [CrossRef]
103. Loiseau, A.; Boudon, J.; Oudot, A.; Moreau, M.; Boidot, R.; Chassagnon, R.; Saïd, N.M.; Roux, S.; Mirjolet, C.; Millot, N. Titanate Nanotubes Engineered with Gold Nanoparticles and Docetaxel to Enhance Radiotherapy on Xenografted Prostate Tumors. *Cancers* **2019**, *11*, 1962. [CrossRef]
104. Morgan, D.L.; Triani, G.; Blackford, M.G.; Raftery, N.A.; Frost, R.L.; Waclawik, E.R. Alkaline hydrothermal kinetics in titanate nanostructure formation. *J. Mater. Sci.* **2011**, *46*, 548–557. [CrossRef]
105. Morgan, D.L.; Liu, H.-W.; Frost, R.L.; Waclawik, E.R. Implications of Precursor Chemistry on the Alkaline Hydrothermal Synthesis of Titania/Titanate Nanostructures. *J. Phys. Chem. C* **2010**, *114*, 101–110. [CrossRef]
106. Nada, A.; Moustafa, Y.; Hamdy, A. Improvement of Titatnium Dioxide Nanotubes through Study Washing Effect on Hydrothermal. *Br. J. Environ. Sci.* **2014**, *2*, 29–40.

107. Nian, J.-N.; Chen, S.-A.; Tsai, C.-C.; Teng, H. Structural Feature and Catalytic Performance of Cu Species Distributed over TiO_2 Nanotubes. *J. Phys. Chem. B* **2006**, *110*, 25817–25824. [CrossRef]
108. Papa, A.-L.; Maurizi, L.; Vandroux, D.; Walker, P.; Millot, N. Synthesis of Titanate Nanotubes Directly Coated with USPIO in Hydrothermal Conditions: A New Detectable Nanocarrier. *J. Phys. Chem. C* **2011**, *115*, 19012–19017. [CrossRef]
109. Papa, A.-L.; Millot, N.; Saviot, L.; Chassagnon, R.; Heintz, O. Effect of Reaction Parameters on Composition and Morphology of Titanate Nanomaterials. *J. Phys. Chem. C* **2009**, *113*, 12682–12689. [CrossRef]
110. Peng, S.; Zeng, X.; Li, Y. Titanate nanotube modified with different nickel precursors for enhanced Eosin Y-sensitized photocatalytic hydrogen evolution. *Int. J. Hydrogen Energy* **2015**, *40*, 6038–6049. [CrossRef]
111. Ranjitha, A.; Muthukumarasamy, N.; Thambidurai, M.; Velauthapillai, D.; Agilan, S.; Balasundaraprabhu, R. Effect of reaction time on the formation of TiO_2 nanotubes prepared by hydrothermal method. *Optik* **2015**, *126*, 2491–2494. [CrossRef]
112. Ray, M.; Chatterjee, S.; Das, T.; Bhattacharyya, S.; Ayyub, P.; Mazumdar, S. Conjugation of cytochrome c with hydrogen titanate nanotubes: Novel conformational state with implications for apoptosis. *Nanotechnology* **2011**, *22*, 415705. [CrossRef]
113. Rendon-Rivera, A.; Toledo-Antonio, J.A.; Cortes-Jacome, M.A.; Angeles-Chavez, C. Generation of highly reactive OH groups at the surface of TiO_2 nanotubes. *Catal. Today* **2011**, *166*, 18–24. [CrossRef]
114. Samir, H.; Taha, M.; El-Dek, S.I.; Zaki, A.H. Electronic Structures and Electrical Properties of Cr^{2+}-, Cu^{2+}-, Ni^{2+}-, and Zn^{2+}-Doped Sodium Titanate Nanotubes. *ACS Omega* **2022**, *7*, 27587–27601. [CrossRef] [PubMed]
115. Seo, D.-S.; Lee, J.-K.; Kim, H. Preparation of nanotube-shaped TiO_2 powder. *J. Cryst. Growth* **2001**, *229*, 428–432. [CrossRef]
116. Sun, X.; Li, Y. Synthesis and Characterization of Ion-Exchangeable Titanate Nanotubes. *Chem. Eur. J.* **2003**, *9*, 2229–2238. [CrossRef] [PubMed]
117. Tang, Z.-R.; Zhang, Y.; Xu, Y.-J. Tuning the Optical Property and Photocatalytic Performance of Titanate Nanotube toward Selective Oxidation of Alcohols under Ambient Conditions. *ACS Appl. Mater. Interfaces* **2012**, *4*, 1512–1520. [CrossRef] [PubMed]
118. Thorne, A.; Kruth, A.; Tunstall, D.; Irvine, J.T.S.; Zhou, W. Formation, Structure, and Stability of Titanate Nanotubes and Their Proton Conductivity. *J. Phys. Chem. B* **2005**, *109*, 5439–5444. [CrossRef] [PubMed]
119. Tian, Z.R.; Voigt, J.A.; Liu, J.; Mckenzie, B.; Xu, H. Large Oriented Arrays and Continuous Films of TiO_2-Based Nanotubes. *J. Am. Chem. Soc.* **2003**, *125*, 12384–12385. [CrossRef]
120. Vuong, D.; Tram, D.; Pho, P.; Chien, N. Hydrothermal Synthesis and Photocatalytic Properties of TiO_2 Nanotubes. In *Physics and Engineering of New Materials. Springer Proceedings in Physics*; Cat, D.T., Pucci, A., Wandelt, K., Eds.; Springer: Berlin/Heidelberg, Germany, 2009; Volume 127. [CrossRef]
121. Wadhwa, S.; Rea, C.; O'Hare, P.; Mathur, A.; Roy, S.S.; Dunlop, P.S.M.; Byrne, J.A.; Burke, G.; Meenan, B.; McLaughlin, J.A. Comparative in vitro cytotoxicity study of carbon nanotubes and titania nanostructures on human lung epithelial cells. *J. Hazard. Mater.* **2011**, *191*, 56–61. [CrossRef]
122. Wang, Y.; Yuan, L.; Yao, C.; Fang, J.; Wu, M. Cytotoxicity Evaluation of pH-Controlled Antitumor Drug Release System of Titanium Dioxide Nanotubes. *J. Nanosci. Nanotechnol.* **2015**, *15*, 4143–4148. [CrossRef] [PubMed]
123. Wang, G.Y.Q.; Hu, Q.; Duan, X.F.; Sun, H.L.; Xue, Q.K. Microstructure and formation mechanism of titanium dioxide nanotubes. *Chem. Phys. Lett.* **2002**, *365*, 427–431. [CrossRef]
124. Wang, W.; Varghese, O.K.; Paulose, M.; Grime, C.A.; Wang, Q.; Dickey, E.C. A study on the growth and structure of titania nanotubes. *J. Mater. Res.* **2004**, *19*, 417–422. [CrossRef]
125. Xiao, N.; Li, Z.; Liu, J.; Gao, Y. Effects of calcination temperature on the morphology, structure and photocatalytic activity of titanate nanotube thin films. *Thin Solid Film.* **2010**, *519*, 541–548. [CrossRef]
126. Yao, B.D.; Chan, Y.F.; Zhang, X.Y.; Zhang, W.F.; Yang, Z.Y.; Wang, N. Formation mechanism of TiO_2 nanotubes. *Appl. Phys. Lett.* **2003**, *82*, 281. [CrossRef]
127. Yu, J.; Yu, H. Facile synthesis and characterization of novel nanocomposites of titanate nanotubes and rutile nanocrystals. *Mater. Chem. Phys.* **2006**, *100*, 507–512. [CrossRef]
128. Yu, J.; Yu, H.; Cheng, B.; Trapalis, C. Effects of calcination temperature on the microstructures and photocatalytic activity of titanate nanotubes. *J. Mol. Catal. A Chem.* **2006**, *249*, 135–142. [CrossRef]
129. Yuan, Z.-Y.; Zhou, W.; Su, B.-L. Hierarchical interlinked structure of titanium oxide nanofibers. *Chem. Commun.* **2002**, 1202–1203. [CrossRef]
130. Yuan, Z.-Y.; Zhang, X.-B.; Su, B.-L. Moderate hydrothermal synthesis of potassium titanate nanowires. *Appl. Phys. A* **2004**, *78*, 1063–1066. [CrossRef]
131. Zhang, Q.; Gao, L.; Sun, J.; Zheng, S. Preparation of Long TiO_2 Nanotubes from Ultrafine Rutile Nanocrystals. *Chem. Lett.* **2002**, *31*, 2226–2227. [CrossRef]
132. Zhang, S.; Peng, L.-M.; Chen, Q.; Du, G.H.; Dawson, G.; Zhou, W.Z. Formation Mechanism of $H_2Ti_3O_7$ Nanotubes. *Phys. Rev. Lett.* **2003**, *91*, 256103. [CrossRef] [PubMed]
133. Zhang, M.; Jin, Z.; Zhang, J.; Guo, X.; Yang, J.; Li, W.; Wang, X.; Zhang, Z. Effect of annealing temperature on morphology, structure and photocatalytic behavior of nanotubed $H_2Ti_2O_4(OH)_2$. *J. Mol. Catal. A Chem.* **2004**, *217*, 203–210. [CrossRef]

134. Zhang, S.; Chen, Q.; Peng, L.-M. Structure and formation of $H_2Ti_3O_7$ nanotubes in an alkali environment. *Phys. Rev. B* **2005**, *71*, 014104. [CrossRef]
135. Ohno, T.; Sarukawa, K.; Tokieda, K.; Matsumura, M. Morphology of a TiO_2 photocatalyst (Degussa, P-25) consisting of anatase and rutile crystalline phases. *J. Catal.* **2001**, *203*, 82–86. [CrossRef]
136. Ohtani, B.; Prieto-Mahaney, O.O.; Li, D.; Abe, R. What is Degussa (Evonik) P25? Crystalline composition analysis, reconstruction from isolated pure particles and photocatalytic activity test. *J. Photochem. Photobiol. A Chem.* **2010**, *216*, 179–182. [CrossRef]
137. Tobaldi, D.M.; Pullar, R.C.; Seabra, M.P.; Labrincha, J.A. Fully quantitative X-ray characterisation of evonik aeroxide TiO_2 P25®. *Mater. Lett.* **2014**, *122*, 345–347. [CrossRef]